Cationic Nanoparticles: Friend or Foe?

Deciphering the mechanisms of cell death induced by cationic nanoparticles

Mariana Godinho Bexiga

Dissertation presented to the Faculty of Sciences and Technology, University of Coimbra, in partial fulfilment of the requirements for obtaining a Doctoral degree in Molecular Biology.

Universidade de Coimbra
July 2011

Nanopartículas Catiónicas: Amigo ou Inimigo?
Decifrando os mecanismos de morte celular induzida por nanopartículas catiónicas

Mariana Godinho Bexiga

Dissertação apresentada à Faculdade de Ciências e Tecnologia da Universidade de Coimbra, para prestação de provas de Doutoramento em Bioquímica, na especialidade de Biologia Molecular.

Universidade de Coimbra
Julho 2011

Este trabalho foi efectuado sob a tutela do Centro de Neurociências e Biologia Celular de Coimbra ao abrigo do Programa Doutoral de Biologia Experimental e Biomedicina (2005), sob a orientação do Professor Luís Pereira de Almeida, Faculdade de Farmácia. O trabalho prático foi realizado sob a orientação do Professor Jeremy C. Simpson na escola – *School of Biology and Environmental Science* –, e do Professor Kenneth A. Dawson no centro – *Centre for BioNano Interactions* – ambos no University College Dublin, Dublin, Irlanda. Este trabalho foi financiado pela bolsa SFRH/BD/15892/2005 da Fundação para a Ciência e a Tecnologia, Lisboa, Portugal.

This work was carried out under the tutorage of the Center for Neuroscience and Cell Biology of Coimbra, in the context of the PhD programme for Experimental Biology and Biomedicine (2005), under the supervision of Professor Luís Pereira de Almeida, Faculty of Pharmacy. The practical work was performed under the supervision of Professor Jeremy C. Simpson in the School of Biology and Environmental Science and of Professor Kenneth A. Dawson in the Centre for BioNano Interactions, both in the University College Dublin, Dublin, Ireland. This work was supported by the grant SFRH/BD/15892/2005 from Fundação para a Ciência e a Tecnologia, Lisbon, Portugal.

ACKNOWLEDGEMENTS

No final de tamanha jornada, há que começar por agradecer a quem possibilitou a sua execução. Aos "carrascos" das entrevistas para o PDBEB4, o meu muito obrigada por me terem dado semelhante oportunidade de desenvolver as minhas competências. À *Susana Rocha*, obrigada pela sempre impecável eficiência e por nos ter aturado diariamente durante a nossa permanência em Coimbra. Aos meus colegas do PDBEB4, obrigada por terem feito com que as noites de trabalho não parecessem tão longas, bem como pelas gargalhadas e confidências que trocamos! Agradeço-vos também o apoio que me deram quando as coisas não corriam pelo melhor!

Jez, there aren't enough words to thank you for your mentorship, patience, support and friendship, but above all for rescuing my love for science and for the ever present encouraging words! I have learnt so much from you – more than you can imagine! – and I hope not to disappoint you in this final stage of the journey. I will always cherish the time spent in your lab and I am sure I will continue to learn from you in the future!

Kenneth, I must thank you for transforming a simple collaboration into a full time PhD project and for giving me the opportunity to express myself and communicate science. Things weren't always easy, but I think at the end it worked out nicely! *Iseult*, thank you so much for everything you had to deal with on my behalf.

Ao *Professor Luís Pereira de Almeida*, o meu muito obrigada pela sua incessável paciência ao longo destes anos todos e por todas as palavras de ânimo que sempre me dedicou. Agradeço também todos os conselhos que me tem oferecido. Espero tê-los aproveitado bem!

A todos os Professores que me incutiram o gosto pela ciência o meu mais profundo obrigada. À *Professora Conceição Pedroso de Lima* por me ter dado a conhecer o mundo fantástico da terapia génica, à *Professora Paula Veríssimo* pela sua amizade e estímulo durante o curso de Bioquímica e depois durante o meu doutoramento, ao *Professor João Ramalho Santos* pela sua amizade e carinho que sempre demonstrou por mim, por todas as palavras encorajadoras que sempre me dedicou e por ter organizado um dos meus cursos favoritos: Viva a fertilidade! ;)

To all my colleagues in Jez's group and in CBNI, thank you for all your support and help with my project and for all the fruitful discussions we had. *Vasanth*, thank you for the warm welcome and all the help you gave me throughout the years, and also for your infinite patience while discussing Indian culture. ;)

To *Paulo*, *Andrzej*, *Fiona*, *Francesca*, *Angela* and *George*, thank you from the bottom of my heart for your friendship and for all the good moments we shared! :) A special thanks to Andrzej for all his IT advice and help and to George for his magic hands with Photoshop.

A todos os meus amigos de aqui e dali, muito obrigada pelas palavras de ânimo e pelos momentos que partilhamos! Aos meus amigos de sempre, *Diana*, *João*, *Margarida* e *Lili*, o meu muito sincero obrigada. À *Diana*, mágica das artes, obrigada por mais uma vez me teres ajudado a embelezar os meus trabalhos! Normalmente sou mais apologista de demonstrar por gestos que por palavras, mas neste momento, há que gravar no papel um agradecimento por sempre terem estado presentes ao longo desta aventura! Um grande abraço do fundo do meu coração!

Gracias *Juan* por todo lo que hiciste por mi, no solo por la ayuda en el laboratorio e todas las discusiones científicas que tuvimos, pero sobretodo por tu amistad e por tu insistencia en transformarme en una persona mejor y mas optimista! :) ¡Tu eres uno de los mejores recuerdos que llevo de Dublín y espero que nuestros caminos siempre se crucen aunque que sea en el cyber espacio! Las guitarreadas y tu buen humor me van a acompañar para siempre. ¡Muchas gracias! :)

A toda a minha *família*, o meu sincero obrigada. Nem sempre as coisas foram fáceis, mas pude sempre contar convosco e com as vossas palavras de incentivo! Às minhas *avós*, obrigada por me terem compreendido e pelo sempre presente apoio e carinho! À minha irmã, *Joana*, e ao meu cunhado, *Nuno*, obrigada por tudo. Houve alturas em que teria sido difícil enfrentar as contrariedades sem a vossa presença, ainda que espiritual! :) À *Inês* e à *Mena*, minha família "postiça", o meu muito obrigada pelo ombro, pelas gargalhadas, pelo carinho e pelas conversas debaixo do nosso solzinho português! :)

À minha madrinha, *Rosa*, é tarde para agradecer... A vida às vezes coloca-nos obstáculos que julgamos inultrapassaveis, no entanto, sempre me incentivaste a não desistir perante a adversidade. A tua presença acompanhou-me sempre durante este longo percurso e a tua ausência é sentida com muita dor e saudade. Espero que esta tese seja um tributo a ti e àquilo que me ensinaste.

Tenho por fim que agradecer aos meus *pais*. Estes anos foram vividos sempre em conjunto embora separados. Obrigada por sempre terem estado no outro lado da linha, quer eu tivesse um sorriso nos lábios ou uma lágrima nos olhos. E quantas lágrimas foram derramadas ao longo desta dura jornada! Toda a angústia era calma e lentamente afastada durante as nossas longas conversas! Tenho dúvidas se algum dia teria conseguido chegar aqui sem o vosso apoio incondicional, por isso, esta tese não é só minha. É nossa! O meu mais sincero OBRIGADA!

Para os meus pais

TABLE OF CONTENTS

LIST OF ABBREVIATIONS

ADP	Adenosine diphosphate
AGO2	Argonaute 2
APAF1	Apoptosis protease associated factor-1
ATF4	Activating transcription factor 4
ATF6	Activating transcription factor 6
ATG	Autophagy-related gene
ATP	Adenosine triphosphate
BAD	BCL-2 associated agonist of cell death
BAK	BCL-2 antagonist/killer
BAX	BCL-2-associated X protein
BBC3/PUMA	BCL-2 binding component 3
BCA	Bicinchoninic acid
BCL-2	B-cell lymphoma protein 2
BCL2L11/BIM	BCL-2 like protein 11
BCL-xL	BCL-2 related gene, long isoform
BECN1	Beclin-1
BH	BCL-2 homology
BID	BH3 interacting domain death agonist
BIK	BCL-2 interacting killer
BIM/BCL2L11	BCL-2 like 11
BOK	BCL-2 related ovarian killer
CASP10	Caspase 10
CASP3	Caspase 3
CASP7	Caspase 7
CASP8	Caspase 8
CASP9	Caspase 9
cDNA	Complementary DNA
CHOP	C/EBP homologous protein

COOH-PS	Carboxylated polystyrene nanoparticles
C-terminal	Carboxyl-terminal
CTSL	Cathepsin L
DISC	Death-inducing signalling complex
DLS	Dynamic light scattering
DMEM	Dulbecco's modified Eagle medium
DNA	Deoxyribonucleic acid
DRP1	Dynamin related protein 1
dsRNA	Double-stranded RNA
EDEM1	ER degradation enhancing α-mannosidase-like protein
eIF2α	Eukaryotic translation initiation factor 2α
ER	Endoplasmic reticulum
ERAD	ER-associated protein degradation
ERdj4/DNAJB9	DnaJ homolog, superfamily B, member 9
F-actin	Filamentous actin
FADD	Fas-associated via death domain
FBS	Foetal bovine serum
FIS1	Fission 1 homolog
GAPDH	Glyceraldehyde 3-phosphate dehydrogenase
GFP	Green fluorescent protein
HERPUD1	Homocysteine-inducible, endoplasmic reticulum stress-inducible, ubiquitin-like domain member 1
IMM	Inner mitochondrial membrane
IMS	Intermembrane space
INCENP	Inner centromere protein
IRE1α	Inositol-requiring enzyme 1α
JNK	c-Jun N-terminal kinase
LC3	Microtubule-associated protein 1 light chain 3
LMP	Lysosomal membrane permeabilisation
MFN	Mitofusin

MLB	Multi lamellar body
MnSOD	Manganese superoxide dismutase
MOMP	Mitochondrial outer-membrane permeabilisation
mRNA	Messenger RNA
NH_2	Amine
NH_2-PS	Amine-modified polystyrene
NH_4Cl	Ammonium chloride
N-terminal	Amine-terminal
OMM	Outer mitochondrial membrane
OPA1	Optic atrophy 1
PACT	Protein activator of proteinkinase
PAGE	Polyacrylamide gel electrophoresis
PARP1	Poly (ADP)Ribose polymerase - 1
PBS	Phosphate buffered saline
PCR	Polymerase chain reaction
PDI	Polydispersity index
PERK	Protein kinase RNA-activated-like ER kinase
PFA	Paraformaldehyde
PI	Propidium iodide
PMAIP1/NOXA	Phorbol-12-myristate-13-acetate-induced protein 1
PtdIns3K	Phosphatidylinositol 3-kinase
RIP1	Receptor interacting protein-1
RISC	RNA induced silencing complex
RNA	Ribonucleic acid
RNAi	RNA interference
ROS	Reactive oxygen species
SDS	Sodium dodecyl sulphate
siRNA	Small interfering RNA
STS	Staurosporine
TBHP	*tert*-butyl hydroperoxide

tBID	Truncated BID
TEM	Transmission electron microscopy
TMRE	Tetramethyl rhodamine ethyl-ester
TMRM	Tetramethyl rhodamine methyl-ester
TRBP	Tar RNA binding protein
Ulk	Atg1/unc-51-like kinase
UPR	Unfolded protein response
XBP1	X-box binding protein 1

ABSTRACT

Humans come into contact with nanoparticles in all aspects of their daily lives: in food, clothing, cosmetics and pollution. Despite this, the knowledge of how nanoparticles interact with cells is still very scarce, and therefore there are genuine concerns surrounding the application of nanotechnology to humans. Many of the therapeutically appealing nanoparticles display a positive charge at their surface, as this increases their interactions with the negatively charged plasma membrane and with nucleic acids. In addition, studies carried out on people living in highly polluted areas have shown a high incidence of deposition of nanoparticles in the brain which in turn often displayed various inflammatory and neurodegenerative signs typical of Alzheimer's and Parkinson's diseases, thereby prompting questions over possible nanoparticle-induced pathologies.

In this work, the mechanisms by which cationic nanoparticles interact with cells, in particular with astrocytes, the most abundant cell type of the central nervous system, have been addressed. An array of molecular and biochemical tools have been applied in the context of a model system composed of 50 nm polystyrene amine-modified positively-charged nanoparticles and an astrocytoma cell line – 1321N1.

Investigation of various markers of apoptosis revealed that cells incubated with the amine-modified nanoparticles were dying by apoptosis in a concentration- and time-dependent manner. Studies with polystyrene nanoparticles of the same size but displaying a negative surface charge did not show any toxicity to the cells, indicating that the observed effect was due to the positive charge.

The signalling pathway of apoptosis that was being induced in the 1321N1 cells treated with the amine-modified nanoparticles was studied in

detail using classical biochemical techniques such as Western blotting, and modern molecular techniques such as RNA interference. Together these studies revealed that the intrinsic pathway of apoptosis was being activated upon incubation of cells with nanoparticles. This was mediated through the formation of the apoptosome by APAF1, caspase 9 and cytochrome c, and was regulated through proteins of the BCL-2 family, namely BAX and BAK, which were in turn activated by BIM, BID and PUMA. In cells treated with nanoparticles, an increase in the expression of several pro-apoptotic genes – PUMA, NOXA and BIM – was also observed.

Further analyses revealed that nanoparticles became concentrated in lysosomes, which in turn became susceptible to rupture, releasing their contents into the cytosol with potentially devastating effects to the cell. Mitochondria were also found to be severely damaged, with a loss of their normal architecture and function. Production of reactive oxygen species, a source of oxidative stress to the cell, was also detected, thus confirming the impairment of mitochondrial function.

This study also investigated the role of two cellular adaptive pathways, namely autophagy and the endoplasmic reticulum stress response, in response to nanoparticle internalisation. Both of these processes function to help the cell overcome a stressful event, but if they fail, the cell can be driven into apoptosis. In the system under study, both mechanisms were shown to occur, although further studies will be needed in order to fully understand their relevance to the death mechanism elicited by the amine-modified nanoparticles in 1321N1 cells.

A final objective of this work was to evaluate the use of RNA interference technology as an approach to the study of the interactions between nanoparticles and cells. The successful demonstration of this method, and its use in deciphering the apoptosis machinery molecules

relevant to nanoparticle-induced cell death, indicates that this methodology is likely to rapidly lead to a deeper understanding of the field.

The work presented here provides only the beginning of our understanding of how cationic nanoparticles interact with the cellular machinery and induce cytotoxicity, however, it marks one important step to the further development of nanotechnology as a safe technology for application in therapeutics.

RESUMO

O Ser Humano encontra-se em contacto com nanopartículas em todos os aspectos da sua rotina: na alimentação, vestuário, cosméticos e poluição. Apesar disto, o conhecimento sobre o modo como as nanopartículas interagem com as células ainda é bastante escasso havendo, por isso, preocupações genuínas em torno da aplicabilidade da nanotecnologia ao Ser Humano. Muitas das nanopartículas apelativas para aplicação terapêutica possuem uma carga de superfície positiva, pois tal aumenta a interação entre elas e a membrana plasmática que apresenta uma carga negativa, bem como com ácidos nucléicos. Adicionalmente, estudos realizados em habitantes de áreas extremamente poluídas demonstraram uma grande incidência na acumulação de nanopartículas no cérebro que, por sua vez, apresentavam vários sintomas de inflamação e de neurodegeneração típicos das doenças de Alzheimer e Parkinson, o que levantou questões sobre possíveis patologias induzidas pelas nanopartículas.

Neste trabalho foram abordados os mecanismos de interacção entre as nanopartículas e células, em particular com astrócitos que são o tipo celular mais abundante no sistema nervoso central. Uma série de técnicas bioquímicas e de biologia molecular foram aplicadas no contexto de um sistema modelo composto por nanopartículas de poliestireno de 50 nm modificadas com grupos amínicos à superficie que lhes conferiam carga positiva e uma linha celular de astrocitoma – 1321N1.

A investigação de vários marcadores da apoptose revelou que células incubadas com as nanopartículas aminadas morriam por apoptose de uma forma dependente tanto da concentração como do tempo de incubação. Estudos realizados com nanopartículas de poliestireno de tamanhos semelhantes mas com carga negativa não revelaram qualquer

toxicidade para as células, indicando por isso, que o efeito observado era devido à carga positiva das nanopartículas.

A via de sinalização de apoptose que estava a ser induzida nas células 1321N1 tratadas com as nanopartículas aminadas foi estudada em detalhe usando técnicas bioquímicas como Western blot, bem como técnicas de biologia molecular moderna como a interferência de RNA. Combinando os resultados destes estudos foi revelado que após incubação das células com as nanopartículas o mechanismo de apoptose era mediado pela activação da via de sinalização intrínseca. Esta ocorria com a formação do apoptosoma pelas proteínas APAF1, caspase 9 e citocromo c e era regulada por proteínas pertencentes à família da BCL-2, nomeadamente BAX e BAK, que eram por seu turno activadas por BIM, BID e PUMA. Em células tratadas com nanopartículas, também foi observado um aumento da expressão de vários genes pro-apoptóticos, em particular PUMA, NOXA e BIM.

Outras observações revelaram que as nanopartículas se concentravam nos lisossomas tornando-os susceptíceis a ruptura libertando, desse modo, o seu conteúdo para o citoplasma acarretando efeitos potencialmente devastadores para a célula. Danos severos foram também observados nas mitocôndrias, que perderam a morfologia e actividade normais. A produção de espécies reactivas de oxigénio, uma fonte de stress oxidativo para as células, foi também detectada confirmando deste modo a destruição da função mitocondrial.

Este estudo também investigou o papel de duas vias celulares de adaptação, nomeadamente autofagia e a resposta do stress do retículo endoplasmático, em resposta à internalização das nanopartículas. Ambos os processos funcionam de forma a que a célula ultrapasse um evento traumatizante, mas que se falham podem fazer com que a célula morra por apoptose. No sistema em estudo foi demonstrada a ocorrência de ambos

os mecanismos, no entanto, estudos mais detalhados têm de ser realizados de modo a compreender a sua relevância para o mecanismo de morte celular induzido pelas nanopartículas aminadas nas células 1321N1.

Um último objectivo deste trabalho era avaliar a utilização da tecnologia de interferência de RNA como abordagem ao estudo das interacções entre nanopartículas e células. A demonstração bem sucedida deste método e do seu uso na elucidação dos componentes da maquinaria apoptótica relevantes para a morte celular induzida por nanopartículas, indica que esta metodologia poderá levar rapidamente a uma maior compreensão desta área.

O trabalho aqui apresentado constitui apenas o início da compreensão de como nanopartículas catiónicas interagem com a maquinaria celular e como induzem citotoxicidade, marcando no entanto, um passo importante no desenvolvimento da nanotecnologia como uma tecnologia de aplicação terapêutica segura.

CHAPTER 1

INTRODUCTION

I. Nanotechnology

Nanotechnology refers to the engineering and manufacture of materials at the atomic and molecular scale (Farokhzad and Langer, 2009). Nanotechnology is being increasingly used in commercial applications and it is projected to become a one trillion dollar market by 2015 (Nel et al., 2006). Currently, nanomaterials are being used in a wide variety of applications such as engineering, food industry, cosmetics and medicine (Dekkers et al., 2010; Nel et al., 2006; Osmond and McCall, 2010). In medicine, nanoparticles are being used for improving diagnostic tests (Mailander and Landfester, 2009), but there are also big expectations on the use of nanotechnology to facilitate targeted drug delivery, as nanoparticles would be able to protect the drug, as well as specifically deliver it to the target cell overcoming all the barriers that it could encounter (Farokhzad and Langer, 2009; Pack et al., 2005; Peer et al., 2007).

The development of nanotechnology for human applications is still recent, therefore the knowledge of how nanoparticles interact with living systems and the environment is still lacking, which raises concerns about its safe application (Nel et al., 2006).

1. What is a nanoparticle?

Nanoparticles can either be man-made to intentionally comply with certain parameters, the so called engineered nanoparticles, or be unintentionally produced or derived from normal processes in nature, thus called nonengineered nanoparticles (Auffan et al., 2009). An example of the latter are the nanoparticles present in pollution.

Nanoparticles are usually defined according to their size, as measuring from 1 to 100 nm in at least one of their dimensions (Auffan et al., 2009). A very important characteristic is that, due to their small size, nanoparticles present physicochemical properties very different from those of the bulk material (Nel et al., 2009). Another consequence of their small size is that the relative surface area increases as the size decreases, which leads to an increase in the reactivity of the nanoparticle (Nel et al., 2006).

Nanoparticles can be composed of many different materials, such as metals (for example gold or zinc), carbon (such as fullerenes, or carbon nanotubes), silica, polymers (for example polystyrene) or biocompatible molecules (Lewinski et al., 2008; Nel et al., 2009; Pack et al., 2005). They can also present various shapes ranging from spheres to rods (Khanal and Zubarev, 2008) and indeed, this characteristic has been found to affect the capacity of the nanoparticle to enter the cell (Gratton et al., 2008). Other properties such as hydrophobicity, charge and magnetism can also be manipulated.

As nanoparticles are becoming increasingly more present in our daily lives and their characteristics influence the way they interact with living systems, it is of the utmost importance to fully understand their physicochemical characteristics before conducting a biological experiment. Apart from knowing the chemical composition, it is very important to define the size of the nanoparticle and the surface charge. These two parameters are usually measured while the nanoparticles are dispersed in a liquid, and provide a quality control measurement of the nanoparticle solution. This aspect will be further developed in Appendix I.

2. BioNano interactions

When nanoparticles are used in human applications, they will interact with the different biological systems in what has been termed 'Bionano interactions'.

Once nanoparticles come in contact with a biological fluid, such as blood or lymph, they immediately become coated with proteins which form the so-called 'protein corona' (Cedervall et al., 2007). The association between proteins and nanoparticles has been described to be highly dependent on the nanoparticle's physicochemical characteristics, such as size, charge and chemical composition (Lundqvist et al., 2008; Mahmoudi et al., 2011). Even though the protein corona underges dynamic changes as it interacts with the different biological and cellular environments (Nel et al., 2009), it still appears to have a long-lived component present directly at the nanoparticle surface, suggesting that it is the proteins at the nanoparticle surface that come in contact with the cells and not the bare nanoparticle (Walczyk et al., 2010). The protein coating of the nanoparticle might also promote a delay in the clearance of nanoparticles from circulation, as by being coated with endogenous proteins, the nanoparticle is hidden from the organism. Another advantage that this protein corona might provide is to promote a targeted biodistribution (Nel et al., 2009). Examples of these are proteins of the apolipoprotein family which are present at high levels at the surface of the nanoparticles (Lundqvist et al., 2008) and that have been used in the past to target the brain (Spencer and Verma, 2007).

An important aspect to consider is that as proteins adsorb into the nanoparticle surface their conformation might change which can result in exposure of previously hidden motifs, such as new antigenic epitopes, or protein loss of function, for example in the case of enzymes (Nel et al., 2009). Another consequence of the interaction between nanoparticles and

proteins is the induction of conformational changes in those proteins followed by promotion of protein fibrillation (Linse et al., 2007). In opposition to this, it has been reported that polymeric nanoparticles can also inhibit amyloid-β fibrillation (Cabaleiro-Lago et al., 2008). Protein fibrillation is a pathogenic process common to many diseases such as Alzheimer's disease or amyloidosis, so, although it remains to be confirmed in vivo, it is alarming that nanoparticles can replicate this process. Despite these contradictory reports, the presence of amyloid plaques in the brains of people living in highly polluted areas has been shown (Calderon-Garciduenas et al., 2008), thereby raising concerns about the safety of use of nanoparticles.

The use of nanoparticles as potential targeted drug delivery vectors is very appealing, but for that the biodistribution and biokinetics of those nanoparticles must be studied. The preferred administration routes for nanoparticles are intravenous and inhalation (Choi et al., 2010; Vergoni et al., 2009), introducing in this way many barriers until the nanoparticle reaches the target cell. In contrast to small molecules, nanoparticles are not allowed to freely diffuse across cellular barriers. Instead, they rely on active processes to enter cells and their ability to cross barriers like the blood-brain barrier is under study. However, nanoparticles have been shown to cross capillaries that are more permeable, such as those present in tumours (Li and Huang, 2008).

In biodistribution studies, it is not surprising to see that the majority of the nanoparticles are found in organs involved in detoxification and excretion of the organism such as the liver, kidneys and lungs (Choi et al., 2010; Vergoni et al., 2009). This poses an obstacle that must be circumvented, as clearance from the organism by those organs will prevent the nanoparticles from reaching their final target and also from remaining

in circulation for long enough. In this sense, attachment of targeting moieties to the nanoparticles could help delivery.

Apart from being appealing for targeted drug delivery, nanoparticles could also be helpful in reaching privileged places in the body, such as the central nervous system, as the majority of drugs developed against neurologic diseases are not in use due to their inability to cross the blood-brain barrier (Pardridge, 2007). Nanoparticles have also been shown to cross into the brain through the nasal epithelium following inhalation (Oberdorster et al., 2004).

Once nanoparticles are out of circulation, they interact with cells, but how this occurs, which subcellular compartments are targeted and what are the effects of internalisation is still not understood. The focus of research in this area has been on mechanisms of endocytosis and a very limited number of organelles, using as models fluorescently labelled or radiolabelled nanoparticles (Mailander and Landfester, 2009; Nel et al., 2009; Salvati et al., 2011). Depending on their physicochemical characteristics, intracellular nanoparticle concentration and distribution, as well as interaction with biological molecules, nanoparticles elicit different cellular responses (Nel et al., 2009). Endocytosis can occur via different pathways that depend on distinct protein components and mechanisms, including the formation of caveolae or of clathrin-coated pits, or mechanisms independent from both proteins (Mayor and Pagano, 2007). Cell type and differentiation status have been pointed as a determinant factor in the choice of the internalisation pathway, as there are cells that are more specialised in a certain type of mechanism, as occurs with macrophages which are phagocytic cells (Nel et al., 2009). Characteristics of the nanoparticles, such as size, shape or charge, have also been suggested to be involved in this choice (Gratton et al., 2008), however, detailed studies which integrate the cell and molecular biology knowledge with the physicochemical properties

of the nanoparticles are lacking. Presently, the consensus is that particles smaller that 120 nm enter the cell by endocytosis, while bigger ones enter either by pynocytosis or phagocytosis. However, adding targeting moieties can change both the cellular and subcellular fate of the nanoparticles (Peer et al., 2007).

Apart from entering the cells and accumulating in different organelles, nanoparticles can exert effects on them as well. A particular case that has been studied is the interaction of cationic nanoparticles with lysosomes (Bexiga et al., 2010; Nel et al., 2009), where nanoparticles induce lysosomal membrane rupture which can result in serious consequences to the cell.

3. Nanotoxicology

Despite all the potential to bring development to medicine, technology and different types of industry there are major concerns about the safety of nanotechnology to humans and to the environment. To address this, a new field within nanotechnology – nanotoxicology – has arisen which deals with the effects and potential risks of nanoparticles (Oberdorster et al., 2007).

The unusual physicochemical characteristics of nanoparticles which result from their small size, pose new challenges on how to deal with their interaction with biological systems which at the cellular level include structural arrangements that resemble those of nanoparticles (Nel et al., 2006). At the same time, many other characteristics relating to the way nanoparticles and cells interact are also very important for their possible toxic effects, among others biokinetics and nanoparticle dose (Oberdorster, 2010). As one would expect, unrelated to the type of nanoparticle, the

higher the concentration the more toxic it will be for cells (AshaRani et al., 2009; Bexiga et al., 2010; Lewinski et al., 2008), something that is also dependent on the incubation time.

Much of the research into the cellular mechanisms of toxicity has shown that different cell types react by different mechanisms to the same type of nanoparticle (Xia et al., 2008b). However, one common feature appears to be induction of oxidative stress in the cells (Bexiga et al., 2010; Xia et al., 2006; Xia et al., 2008a; Xia et al., 2008b).

Among the inherent properties of nanoparticles that may cause toxic effects to biological systems, charge seems to play a very important role, as cationic nanoparticles appear to be more toxic than negative or neutral nanoparticles, the latter being the most biocompatible (Lewinski et al., 2008). Size has also been suggested to be important for toxicity, with smaller particles being more toxic than bigger ones (Rabolli et al., 2010).

Another major concern that has been raised is the capacity of nanoparticles to induce immune responses (Nel et al., 2006). Indifferent to the entry route used by the nanoparticles, they will come in contact with the reticuloendothelial system which is composed by phagocytic cells present in the liver, spleen and lymph nodes, which will help in the clearance of nanoparticles from circulation. Interaction with these cells, which are also responsible for antigen presentation, could lead to the stimulation of immune responses. Although this is still not widely studied, there are some indications that contact with nanoparticles might indeed cause immune responses (Brown et al., 2001; Nel et al., 2006). Other serious concerns of the interaction of nanoparticles with humans are provoked by the translocation of nanoparticles into the brain (Calderon-Garciduenas et al., 2008; Oberdorster et al., 2004). Although this has obvious potential for human application, deleterious effects such as those seen in neurodegenerative disorders have also been described (Calderon-

Garciduenas et al., 2008), thereby raising concerns about the use of nanoparticles in humans.

Although some advances have been made to understand how nanoparticles interact with biological systems, there are still major questions to be addressed before they can be used safely in humans. Different studies have been made indicating that nanoparticles induce cellular toxicity, although many times the dosage used is very high. Moreover, the majority of the studies reported in literature refer to *in vitro* studies which might not directly correlate to *in vivo* scenarios. In addition there is a lack of studies investigating in detail the molecular and cellular mechanisms of nanoparticle-induced toxicity, in particular with biocompatible nanoparticles. The concerns for the safety of human and environmental exposure to nanoparticles are, therefore very pertinent and must be addressed in order to ensure safe usage of nanotechnology.

II. Cell Death

Cell death is a necessary mechanism prevalent in all multi-cellular organisms during development and adulthood used to dispose of unnecessary cells or old and damaged ones (Golstein and Kroemer, 2007; Hotchkiss et al., 2009). When the balance between cell growth and death is not maintained, diseases such as cancer develop (Hotchkiss et al., 2009; Jaattela, 2004).

In mammalian cells, cell death has historically been divided into two types of cell death: regulated (apoptosis) and unregulated (necrosis) (Figure 1.1) (Degterev and Yuan, 2008). Autophagy has also been described as another cell death mechanism, but its role is still under debate (Levine and Yuan, 2005), as autophagy is a process by which cells generate energy and

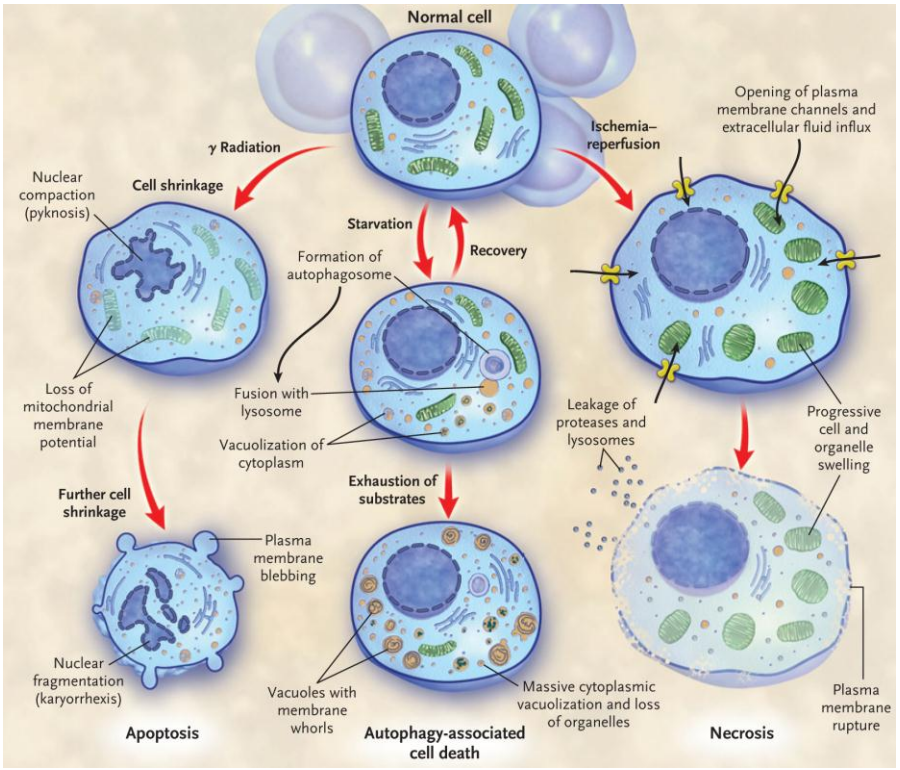

Figure 1.1. *Pathways of cell death in mammalian cells.* A variety of mechanisms of cell death can occur in mammalian cells, the three most important ones being: apoptosis, autophagy-associated cell death and necrosis. Depending on the type of stimulus and cell, one of the three types might predominate and there may be cross-talk between the different mechanisms (not shown). Figure taken from Hotchkiss et al., 2009.

metabolites by digesting their own organelles and macromolecules, but if this continues for a long time without the supply of nutrients, the cells die by a process called autophagy-associated cell death (Klionsky, 2007; Yang and Klionsky, 2010a).

The prevalent type of cell death depends on several aspects such as the type of cell or stimulus applied (Galluzzi et al., 2007). However, blocking one particular type of cell death mechanism might not prevent the destruction of the cell, but instead induce a change in the observed type of

cell death (Galluzzi et al., 2009c; Golstein and Kroemer, 2005; Hotchkiss et al., 2009). For example, it has been observed that in certain cell types, when apoptosis is blocked using caspase inhibitors the cell still dies, but with a different phenotype (Cauwels et al., 2003). In the same way, preventing autophagy makes the cells more susceptible to apoptosis (Boya et al., 2005). The three cell death types mentioned above will be described in the following sections focusing on the molecular and cellular events as well as on the morphological changes observed in the cells.

1. Mechanisms of cell death

1.1. Apoptosis

Apoptosis, a name that derives from an ancient Greek word that suggests "leaves falling from a tree", was first described in 1972 by Kerr and colleagues as a mechanism of controlled and programmed cell demise (Kerr et al., 1972).

Apoptosis is characterised by morphological changes that include rounding of the cell with retraction of pseudopodia, and a reduction of cellular volume (named pyknosis). DNA condensation (Figure 1.2), nuclear fragmentation (karyorrhexis) and plasma membrane blebbing occur (Figure 1.1). The formation of small round bodies surrounded by membranes, so-called apoptotic bodies, which are eventually engulfed by resident phagocytic cells such as epithelial cells or fibroblasts are also characteristic. When phagocytosis is inefficient, the apoptotic bodies eventually lose their integrity, spilling their contents into the surrounding environment, an event that is termed secondary necrosis (Vandenabeele et al., 2010). Despite these

Figure 1.2. *Morphological ultrastructural features of apoptosis by transmission electron microscopy.* Human non-small cell lung carcinoma (H1975) cell undergoing apoptosis, induced by treatment with an inhibitor of the epidermal growth factor receptor. Note the cell's shrinkage and complete nuclear condensation (pyknosis). Adapted from Galluzzi et al., 2007.

dramatic changes, the plasma membrane maintains its integrity until late stages of apoptosis (Galluzzi et al., 2007; Kroemer et al., 2005).

Several biochemical changes occur within the cell while it is going through apoptosis, but one of the key events specific to this mechanism of cell death is the cleavage of cellular proteins involved in the maintenance of cellular architecture and function. This proteolytic cleavage is orchestrated by caspases (cysteinyl aspartate proteinases), a family of cysteine proteases that cleave their substrates at specific aspartate residues (Alnemri et al., 1996; Kumar, 2007). These enzymes are usually produced as inactive precursors (zymogens or procaspases), which become active after specific proteolysis (Boatright and Salvesen, 2003). Other events including phosphatidylserine exposure on the outer leaflet of the plasma membrane (where its presence is required for recognition by the phagocytic cells), and induction of mitochondrial outer membrane permeability (MOMP) with release of intermembrane space (IMS) proteins to the cytoplasm also occur during the process of apoptosis (Krysko et al., 2008).

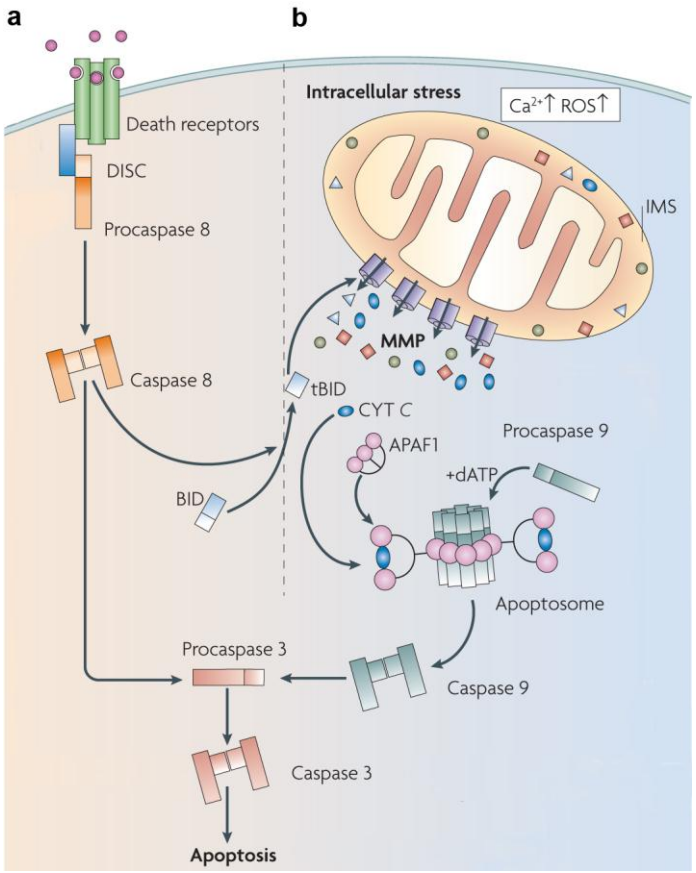

Figure 1.3. *Pathways of apoptosis.* Apoptosis can result from the activation of two distinct biochemical cascades known as the extrinsic (a) and the intrinsic (b) pathways. The extrinsic pathway is initiated at the cell membrane by the oligomerisation of death receptors, whereas the intrinsic pathway is triggered by intracellular signals such as calcium overload or over-generation of ROS. In both pathways, initiator caspases (CASP8 and CASP9, respectively) are activated within specific supramolecular platforms and so can catalyse the proteolytic maturation of executioner caspases, such as CASP3, which mediate (at least partially) the catabolic processes that characterise end-stage apoptosis. In the intrinsic pathway, following MOMP, apoptogenic proteins present in the intermembrane space (IMS), such as cytochrome c, are released into the cytosol. Cytochrome c, interacts with APAF1 and procaspase 9, forming the apoptosome, which results in the activation of downstream executioner caspases. One of the major links between the extrinsic

Two different apoptotic signalling pathways have been described, and their distinction depends on the origin of the stimulus and the sequence of caspase activation that occurs (Degterev and Yuan, 2008; Hotchkiss et al., 2009). In addition to the caspases, several other proteins help to modulate the apoptotic response. Many of these proteins belong to the BCL-2 (B-cell lymphoma protein 2) family of proteins, which will be described later in this chapter.

1.1.1. Pathways of apoptosis

There are essentially two signalling pathways of apoptosis that are identified by the location of the stimulus and the caspases that are activated in the process, but which intersect at different points. If apoptosis is induced by binding of ligands to plasma membrane death receptors, the *extrinsic* pathway of apoptosis is stimulated (Figure 1.3.a). On the other hand, if the stimulus arises from a perturbation of the intracellular homeostasis, the *intrinsic* pathway is initiated (Figure 1.3.b) (Ferri and Kroemer, 2001; Hotchkiss et al., 2009).

When death receptors are bound to their ligands, they oligomerise and in turn promote the assembly of a multiprotein platform – the denominated death-inducing signalling complex (DISC) – that transmits extracellular signals of danger thereby triggering apoptosis (Galluzzi et al., 2009b). Upon oligomerisation of the death receptors, an adaptor protein – FADD (Fas-associated via death domain) – promotes the binding of procaspases 8 and 10 leading to the formation of the DISC. Caspases 8

and intrinsic pathways of apoptosis is provided by the BCL-2 homology domain 3 (BH3)-only protein BID, which can promote MOMP following CASP8-mediated cleavage. Adapted from Galluzzi et al., 2009b.

(CASP8) and 10 (CASP10) then form dimers and are proteolytically activated (Boatright and Salvesen, 2003; Boldin et al., 1996; Muzio et al., 1996). These two caspases are denominated initiator caspases, as they begin the signalling pathway (Boatright and Salvesen, 2003).

In contrast to the extrinsic pathway, the intrinsic pathway begins after stress signs such as DNA damage, reactive oxygen species (ROS) generation or the unfolded protein response (UPR), are sent from within the cell (Hotchkiss et al., 2009). In this pathway, the mitochondria play a central role by integrating both pro- and anti-apoptotic signals (Galluzzi et al., 2009b). The mitochondrial contribution to apoptosis can be subdivided into three distinct phases: pre-mitochondrial initiation, integration, and execution phases (Galluzzi et al., 2009b). In the first phase, cells recognise danger signals and activate both death-inducing and pro-survival pathways in an attempt to cope with stress. Following this, during the integration phase, pro- and anti-apoptotic signals converge at the mitochondria and if the lethal signals are predominant, the outer mitochondrial membrane (OMM) becomes permeable. When MOMP becomes permanent, and affects a considerable fraction of the mitochondria, cells are committed to die. During the post-mitochondrial execution phase, several events occur at the level of the mitochondria that cause a profound bioenergetic and redox crisis, activating several catabolic processes that finally lead to an apoptotic cell death. Such events range from dissipation of mitochondrial transmembrane potential, respiratory chain uncoupling with consequent overproduction of ROS, and adenosine triphosphate (ATP) synthesis arrest (Galluzzi et al., 2009b; Hotchkiss et al., 2009). The ultimate event is the spillage of pro-apoptotic IMS proteins, such as cytochrome c and SMAC/DIABLO, into the cytosol (Du et al., 2000; Goldstein et al., 2000).

Release of the pro-apoptotic proteins from the IMS antagonises the effects of anti-apoptotic proteins and the path to caspase activation is

begun. Cytochrome c released into the cytosol binds to apoptosis protease associated factor-1 (APAF1), procaspase 9 and the co-factor dATP/ATP, together forming a supramolecular complex denominated the apoptosome (Bao and Shi, 2007; Li et al., 1997; Riedl and Salvesen, 2007). Similar to what happens at the DISC, caspase 9 (CASP9) is activated in the apoptosome and can in turn proteolytically activate downstream effector caspases 3 (CASP3) and 7 (CASP7), as well as other pro-apoptotic factors such as the BH3-only protein, BH3 interacting domain death agonist (BID) (Galluzzi et al., 2009b). In contrast to that seen for the effector caspases, the activation of CASP8 and CASP9 occurs via dimerisation, and it is thought that cleavage plays only a small role in this process (Boatright and Salvesen, 2003; Riedl and Salvesen, 2007).

Upon activation, the effector caspase CASP3 and to a lesser extent caspase 6 and CASP7, initiate the destruction of the cell by cleaving numerous structural proteins (for example lamins), repair enzymes (such as poly (ADP) ribose polymerase – 1 (PARP1)), and apoptotic regulators (such as BID), (Cohen, 1997; Degterev et al., 2003), ultimately leading to cell demise.

The involvement of other caspases and activating complexes in apoptosis has also been suggested. The PIDDosome, conveys the signalling arising from genotoxic insults such as nuclear DNA damage leading to the proteolytic activation of caspase 2 which then activates downstream effector caspases culminating in apoptosis (Mace and Riedl, 2010). Another platform, the inflammasome, has a very important role in inflammation as it promotes the activation of caspase 1, and possibly that of caspases 4 and 5, which are required for secretion of mature interleukine 1β and 18 (Tschopp, 2011).

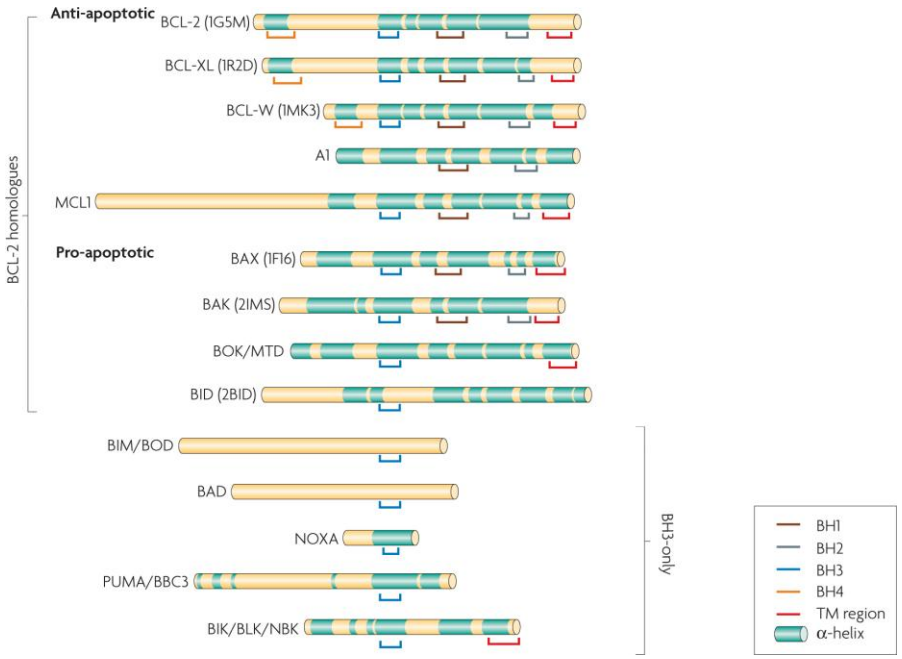

Figure 1.4. *Sequence alignment of core proteins belonging to the BCL-2 family of proteins.* Illustration of the overall structural arrangement of anti- and pro-apoptotic members of the BCL-2 family of proteins. The BH domains are indicated by brown (BH1), grey (BH2), blue (BH3) and orange (BH4) lines. The BH1, BH2 and BH3 domains fold to line a hydrophobic pocket that can bind BH3-only peptides. The BH3 domain mediates interaction between BH3-only proteins and other BCL-2 proteins thereby promoting apoptosis. The upper five proteins are considered anti-apoptotic, whereas the lower nine are pro-apoptotic. BID has a unique role as both a BCL-2 homologue and a BH3-only protein, and links the intrinsic and extrinsic apoptosis pathways. Adapted from Youle and Strasser, 2008.

1.1.2. The BCL-2 family of proteins

The BCL-2 family of proteins has been extensively studied in the last decade due to its importance in modulating the apoptotic response. This family contains both pro-apoptotic members and anti-apoptotic members,

and it is their combined action that modulates apoptosis (Youle and Strasser, 2008).

The BCL-2 gene was identified in 1985 at the t(14;18) chromosome translocation breakpoint in B-cell follicular lymphomas (Bakhshi et al., 1985; Tsujimoto et al., 1985), in which its expression becomes highly upregulated by the immunoglobulin heavy chain promoter and enhancer on chromosome 14. In contrast to the oncogenes known at the time of BCL-2 discovery, this gene was found to work by preventing cell death rather than inducing cell proliferation (Vaux et al., 1988), and this led to the identification and characterisation of other members of the BCL-2 family as essential modulators of a wide variety of apoptosis programmes including tissue turnover, host defence against pathogens, and development.

The BCL-2 family in mammals is composed of at least twelve core proteins, including BCL-2 itself and other proteins that either have a three-dimensional structural similarity or a predicted secondary structure that is similar to BCL-2 (Figure 1.4) (Petros et al., 2004; Soriano and Scorrano, 2010). These proteins display a range of bioactivities from inhibition to promotion of apoptosis, mitochondrial dynamics, and regulation of endoplasmic reticulum (ER) calcium stores (Chipuk et al., 2010; Youle and Strasser, 2008). The molecular mechanism of action of the BCL-2 family proteins depends mainly on the BCL-2 homology (BH) domains, as these domains, which despite not having enzymatic activity, play a key role in interaction between pro- and anti-apoptotic proteins (Soriano and Scorrano, 2010). Certain proteins of the BCL-2 family possess structural homologies to bacterial toxins which led to the hypothesis that they could form ion- or protein-conducting channels as part of their mechanism of action (Muchmore et al., 1996). In fact, several studies have demonstrated the ability of BCL-2-related gene long isoform (BCL-xL), BCL-2 and BCL-2-

associated X protein (BAX) to form channels upon self-oligomerisation (Saito et al., 2000; Schendel et al., 1997).

Anti-apoptotic BCL-2 proteins contain four different BH domains (BH1 to 4) (Figure 1.4) and although they are usually integrated in the OMM, they can also be present in the cytosol, or in the ER membrane anchored via a transmembrane domain present at the carboxyl terminus of the protein (Soriano and Scorrano, 2010; Youle and Strasser, 2008). Examples of this sub-group include BCL-2 and BCL-xL, and they act by directly inhibiting the pro-apoptotic BCL-2 proteins (Chipuk et al., 2010; Youle and Strasser, 2008).

The pro-apoptotic members can be further subdivided into two groups: the multidomain group, which are effectors of apoptosis, and the BH3-only members, which contain only a conserved BH3 domain and act by binding to and regulating the activity of the anti-apoptotic BCL-2 proteins thereby promoting apoptosis (Soriano and Scorrano, 2010; Youle and Strasser, 2008).

The multidomain proteins BAX and BCL-2 antagonist/killer (BAK), the activities of which are inhibited by the anti-apoptotic proteins BCL-2 and BCL-xL, are crucial for the induction of MOMP. They act by homo-oligomerising into proteolipid pores within the OMM from where apoptogenic molecules such as cytochrome c and SMAC/DIABLO are released into the cytosol with consequent caspase activation (Munoz-Pinedo et al., 2006). Due to structural similarities with BAX and BAK, another potential multidomain effector molecule, BCL-2 related ovarian killer (BOK), is also speculated to belong to this group, however there is no biochemical evidence that yet supports such function (Chipuk et al., 2010; Tait and Green, 2010).

The different BH3-only proteins act in distinct cellular stress scenarios by interacting either with the anti-apoptotic proteins

(sensitisers/derepressors: phorbol-12-myristate-13-acetate-induced protein 1 (PMAIP1/NOXA), BCL-2 interacting killer (BIK), BCL-2 associated agonist of cell death (BAD)) or with both the anti-apoptotic proteins and the multidomain pro-apoptotic proteins (direct activators: BCL-2 like 11 (BCL2L11/BIM), BID and BCL-2 binding component 3 (BBC3/PUMA)). These interactions determine MOMP and apoptosis, and also play a role in the cross-talk between the two different pathways of apoptosis (Chipuk et al., 2010; Li et al., 1998; Youle and Strasser, 2008). In mammals there are at least seven BH3 only proteins (Figure 1.4) and each member seems to be critical for tissue homeostasis and development (Soriano and Scorrano, 2010).

1.1.2.1. BCL-2 family protein activation

BH3-only proteins function as initial sensors of apoptotic stimuli originating from different cellular compartments. In healthy cells, these proteins are present in inactive forms and only become activated upon an apoptotic stimulus. Among the events that result in the activation of BH3-only proteins are transcriptional induction, phosphorylation and proteolysis (Soriano and Scorrano, 2010; Youle and Strasser, 2008). PUMA and NOXA can be transcriptionally activated by the tumour suppressor p53 in response to DNA damage (Nakano and Vousden, 2001; Oda et al., 2000), whereas BCL-2 expression is repressed by the C/EBP homologous protein (CHOP) in response to ER stress (McCullough et al., 2001). BID on the other hand can be regulated by either proteolysis or phosphorylation. As described above, BID is involved in the crosstalk between the two apoptotic pathways. When cleaved by CASP8, it gives rise to truncated BID (tBID), which in turn relays the apoptotic signal to the mitochondria (Li et al., 1998;

Luo et al., 1998). When BID is phosphorylated it becomes resistant to cleavage by caspases (Desagher et al., 2001). BID has also been shown to be cleaved by cathepsins, which are proteolytic enzymes released from the lysosomes upon induction of lysosomal membrane permeabilisation (LMP) (Droga-Mazovec et al., 2008).

The multidomain proteins BAX and BAK are known as the "effectors" of the BCL-2 family of proteins, since upon activation they form pores in the OMM through where apoptogenic molecules are released into the cytosol. The regulation of their activity occurs at the post-translational level rather than at the level of transcription, however the exact mechanism of their activation is presently under debate (Yuan et al., 2011). What is generally accepted is that upon activation BAX and BAK undergo a conformational change that in the case of BAX re-locates it from the cytosol to the OMM. These molecules then oligomerise and form pores (Soriano and Scorrano, 2010), however whether they are directly or indirectly activated by BH3-only proteins, and the identity of their activators, remain to be resolved.

There are two non-mutually exclusive theories to explain how the activation of BAX and BAK is regulated: the direct activation model and the indirect model (Galonek and Hardwick, 2006; Youle and Strasser, 2008). The direct activation model states that a subset of BH3-only proteins, including tBID and BIM, interact directly with BAX and BAK inducing conformational changes in them (Gavathiotis et al., 2008; Lovell et al., 2008). At the same time, anti-apoptotic BCL-2 proteins prevent MOMP by either sequestering BH3-only proteins or by inhibiting activated BAX and BAK. This repression is released by neutralisation of the anti-apoptotic BCL-2 proteins by other BH3-only proteins (Kuwana et al., 2005; Tait and Green, 2010). The indirect model postulates that BAX and BAK are constitutively active, but are bound to anti-apoptotic members of the BCL-2

family, which prevent their pro-apoptotic activity. Competitive interactions between BH3-only proteins and the anti-apoptotic members of the family release BAX and BAK promoting MOMP. This hypothesis is based on the fact that BAX- and BAK-dependent apoptosis proceeds in the absence of BID and BIM (Willis et al., 2007). However, other groups have also reported the role of other BH3-only proteins, such as PUMA and NOXA, in the direct activation of BAX and BAK (Du et al., 2011; Gallenne et al., 2009). Recently, experiments in knock-out animals have demonstrated that it is the combined action of BIM, BID and PUMA that are responsible for the activation of BAX and BAK (Ren et al., 2010).

Considerable research into the mechanisms of BAX and BAK activation continues, however a consensus on the biochemical mechanism responsible for their activation has still not been reached (Youle and Strasser, 2008).

1.1.2.2. Regulation of mitochondrial morphology by BCL-2 family members

Mitochondria are regarded as essential organelles for the transmission of the apoptotic cascade in cells, as well as serving to integrate signals from both the intrinsic and the extrinsic pathways of apoptosis. Indeed, loss of mitochondrial membrane potential and cytochrome c release from the mitochondria are often considered as "the point of no return" in apoptosis (Danial, 2007). Loss of mitochondrial membrane potential usually precedes MOMP, which in tum results in release of cytochrome c and other apoptogenic proteins, leading to massive caspase activation (Galluzzi et al., 2007; Galluzzi et al., 2009c). During apoptosis, mitochondria also undergo morphological changes, resulting in small, round and more numerous

organelles, as well as internal membrane changes which are in part modulated by proteins from the BCL-2 family (Soriano and Scorrano, 2010).

Mitochondria are highly versatile and complex organelles that participate in several cellular processes such as energy production, regulation of cell signalling, and apoptosis. Pioneering work from Palade and Sjostrand showed that the mitochondria are double-membrane organelles with the OMM delimiting the organelle, and containing a highly convoluted membrane termed the inner mitochondrial membrane (IMM) folded in a series of ridges called cristae (Palade, 1952; Sjostrand, 1953). The IMM surrounds a dense matrix that contains many soluble proteins important for metabolism, several copies of the mitochondrial genome, as well as the RNA molecules necessary for translation (Frey and Mannella, 2000).

Mitochondrial morphology can be very diverse, ranging from small spheres to interconnected tubules (Cereghetti and Scorrano, 2006; Frey and Mannella, 2000), with this shape being determined by mitochondria-shaping proteins that regulate the equilibrium between fission and fusion events during the life time of the cell (Soriano and Scorrano, 2010). Mitochondrial fusion events in mammalian cells are regulated by optic atrophy 1 (OPA1) of the IMM and by mitofusins (MFN) 1 and 2 of the OMM (Chen et al., 2003; Cipolat et al., 2004; Santel and Fuller, 2001). Mitochondrial fission is controlled by the cytosolic dynamin related protein 1 (DRP1) and fission 1 homolog (FIS1) (Smirnova et al., 2001; Yoon et al., 2003).

During the life cycle of the cell, the pro-apoptotic BCL-2 family members BAX and BAK seem to play an additional role in controlling mitochondrial morphology. These two proteins have been found to interact with mitofusins and their ablation reduces the rate of mitochondrial fusion. Moreover, apart from a role in the regulation of mitofusins, the presence of

BAX and BAK has also been shown to alter the assembly, mobility and distribution of MFN2 complexes in healthy cells (Karbowski et al., 2006).

In apoptotic cells, activated BAX is localised to small focal regions on the mitochondrial surface, with BAK also migrating to these sites during apoptosis induction (Nechushtan et al., 2001). These sites of BAX accumulation colocalise with DRP1 and MFN2 and often evolve into mitochondrial fission sites (Karbowski et al., 2002). This links BAX to the promotion of mitochondrial fragmentation that occurs almost simultaneously with the release of cytochrome c into the cytosol (Youle and Karbowski, 2005). In fact, studies have shown that inhibiting DRP1 activation before induction of apoptosis not only inhibits mitochondrial fission, but also delays caspase activation and cell death itself (Frank et al., 2001; Karbowski et al., 2002). Inhibition of FIS1, apart from preventing mitochondrial fission, also inhibits apoptosis (Lee et al., 2004), whereas its overexpression promotes cell death (James et al., 2003). By contrast, overexpression of MFN1 and MFN2 promotes mitochondrial fusion and is protective against cell death (Sugioka et al., 2004), while downregulation of OPA1 induces mitochondrial fragmentation with cytochrome c release and apoptosis (Olichon et al., 2003).

Cytochrome c, which is normally stored in the mitochondrial cristae, is released to the cytosol upon induction of apoptosis. A key event in the understanding of the mechanism by which this occurs was the discovery of cristae remodelling early in apoptosis (Scorrano et al., 2002). After receiving different signals, including those from the BH3-only proteins BID (Scorrano et al., 2002) and BIK (Germain et al., 2005), mitochondria remodel their internal structure: individual cristae fuse and cristae junctions widen at the region of contact with the OMM, and cytochrome c is mobilised from the intra-cristae compartment towards the IMS for subsequent release across the OMM. Loss of OPA1 expression has also been shown to widen the

mitochondrial cristae (Olichon et al., 2003) while inhibition of DRP1 prevents cristae widening induced by BIK (Germain et al., 2005).

1.1.3. Lysosomes and apoptosis

Lysosomes are dynamic cellular organelles that receive input from the different membrane traffic pathways that are active within the cell: secretory, endocytic and autophagic pathways (Luzio et al., 2007). They contain more than 50 acid hydrolases in their lumen, making them capable of digesting all the different types of macromolecules present in the cells and recycling the products for further metabolism (Kroemer and Jaattela, 2005). Of the different classes of enzymes present in the lysosome, the best-studied is the cathepsin family. Cathepsins are proteolytic enzymes that have optimal activity at acidic pH, although they can also act at neutral pH (Stoka et al., 2007). They are divided into three different subgroups according to their active-site amino-acid: cysteine, aspartate or serine.

In addition to their role in the secretory, endocytic and autophagic pathways, lysosomes can also play an important role in cell death. Stimuli such as ROS and sphingosine, as well as lysosomotropic toxins, can induce LMP resulting in the release into the cytosol of the catabolic enzymes present in the lumen of the organelle without loss of lysosomal morphology (Bidere et al., 2003). Indeed, this event can occur upstream of other cell death events, thereby triggering cell death, which depending on the amount of luminal contents released into the cytosol might evolve either into apoptosis or necrosis (Kroemer and Jaattela, 2005).

LMP drives the cell into apoptosis by inducing MOMP followed by the activation of the caspases involved in the intrinsic pathway of apoptosis (Boya et al., 2003). Cathepsins seem to be the molecules responsible for the

crosstalk between lysosomes and mitochondria (Chwieralski et al., 2006), however other cellular effects that might derive from LMP, such as cytoplasm acidification have still to be ruled out.

The crosstalk between lysosomes and mitochondria mediated by cathepsins might occur via BID cleavage followed by BAX and BAK activation and MOMP (Cirman et al., 2004). Moreover, BAX and BAK have been recently shown to promote LMP and cathepsin release, which might function as a positive feedback loop to amplify apoptosis (Oberle et al., 2010). ROS production by the mitochondria is stimulated upon LMP and has also been found to positively modulate the release of cathepsins from lysosomes (Chwieralski et al., 2006; Zhao et al., 2003).

1.1.4. Endoplasmic reticulum stress and apoptosis

The ER is the primary site of protein synthesis and folding of secretory, membrane and some organelle targeted proteins. For these events to occur correctly, the ER needs a special oxidizing environment, high calcium concentration and ATP. If there are perturbations to this environment, the protein folding capacity of the ER is reduced, resulting in the accumulation and aggregation of unfolded proteins, a condition that is called 'ER stress' (Woehlbier and Hetz, 2011).

To combat the deleterious effects of ER stress, cells have evolved various protective strategies collectively called the unfolded protein response (UPR) (Figure 1.5) (Szegezdi et al., 2006; Woehlbier and Hetz, 2011). The UPR adjusts the capacity of the ER to fold and remove abnormally folded proteins in order to recover homeostasis. Misfolded proteins are transported out of the ER into the cytosol where they are targeted to degradation by the proteasome by a process that is called

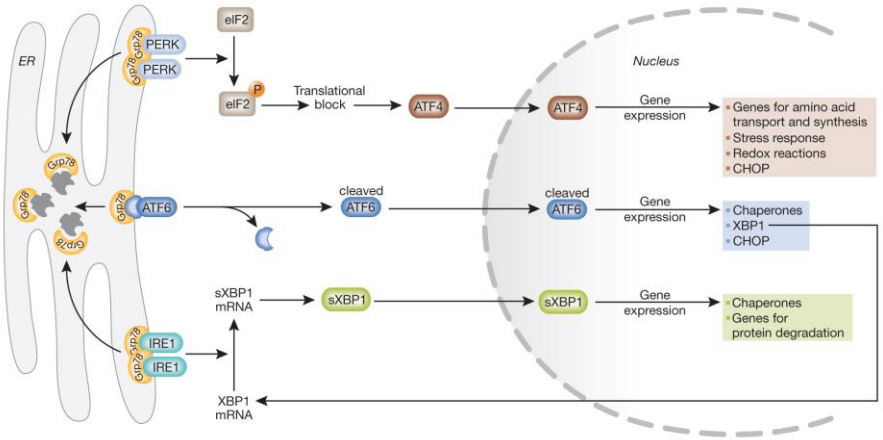

Figure 1.5. *Molecular mechanisms of the unfolded protein response.* Aggregated unfolded proteins in the ER are recognised by three different stress receptors: PERK, ATF6 and IRE1α. Their activation leads to a series of cellular events, such as transcription of protein folding machinery and of protein synthesis blocking, that are aimed at restoring normal ER function by blocking further build-up of proteins, enhancing the folding capacity of the ER and initiating the degradation of protein aggregares. Adapted from Szegezdi et al., 2006.

retrotranslocation or ER-associated protein degradation (ERAD) (Liu and Ye, 2011). However, if homeostasis is not recovered, the UPR drives the cell into apoptosis via the mitochondria (Woehlbier and Hetz, 2011).

UPR is a concerted and complex cellular response that is mediated by three ER transmembrane receptors that relay the information of the protein folding status from the ER into the nucleus of the cell: protein kinase RNA-activated-like ER kinase (PERK), activating transcription factor 6 (ATF6) and inositol-requiring enzyme 1α (IRE1α). In resting cells, all three ER stress receptors are maintained in an inactive state through their association with the ER chaperone, GRP78/BiP. On accumulation of unfolded proteins, GRP78 dissociates from the three receptors, leading to their activation and thereby triggering the UPR (Figure 1.5) (Szegezdi et al., 2006; Woehlbier and Hetz, 2011).

IRE1α and PERK are both transmembrane proteins that contain a cytosolic kinase domain. In addition, IRE1α also contains a cytosolic RNase domain which is involved in messenger RNA (mRNA) degradation upon UPR induction (Hollien et al., 2009; Hollien and Weissman, 2006). Activation of IRE1α leads to the unconventional splicing of X-box binding protein 1 (XBP1), which controls the expression of genes involved in protein folding and ERAD, among others (Calfon et al., 2002; Yoshida et al., 2001). PERK on the other hand, phosphorylates the eukaryotic translation initiation factor 2α (eIF2α) leading to an overall reduction in protein translation (Harding et al., 1999).

It has been hypothesised that the UPR develops in four different phases that occur consecutively. The initial aim of the UPR is to immediately reduce the unfolded protein load in the ER by decreasing protein influx to the ER through attenuation of translation. During this phase PERK and IRE1α are active (Woehlbier and Hetz, 2011). A second phase then ensues, in which transcription of UPR target genes such as transcription factors and ERAD components is stimulated, leading to a reduction of unfolded proteins in the ER. In this phase the transcription factors activating transcription factor 4 (ATF4), ATF6 and the alternative spliced version of XBP1 are involved (Yamamoto et al., 2007). A third phase follows in which transition of the signalling to pro-apoptosis occurs. Although the precise mechanisms that lead to this change of signalling are yet not well understood, the participation of CHOP, a transcription factor that acts downstream of ATF4, in the activation of pro-apoptotic events has been observed. In the final phase of UPR, IRE1α signalling is turned off leading to a decrease in the expression of the alternatively spliced form of XBP1 (Lin et al., 2007). During this phase, CHOP also modulates the expression of members of the BCL-2 family such as BCL-2 itself, PUMA and BIM (Galehdar et al., 2010; McCullough et al., 2001; Puthalakath et al., 2007). The consequence of these

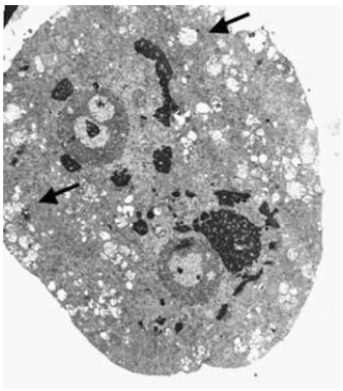

Figure 1.6. *Morphological ultrastructural features of necrosis by transmission electron microscopy.* Human epithelial cell undergoing necrosis after oxidative stress. Note the plasma membrane rupture, intracellular vesicle swelling and loss of mitochondrial ultrastructure (arrows). Adapted from Kroemer et al., 2005.

events is the activation of BAX and BAK with transmission of the signal to the mitochondria which evolves into apoptosis via the intrinsic pathway.

1.2. Necrosis

Necrosis (a word that comes from the Greek "nekros" meaning corpse) is normally considered as non-programmed cell death in response to overwhelming stress (Degterev et al., 2005). This type of cell death is harmful for the organism, as it often results in pathological cell loss and in tissue inflammation (Galluzzi et al., 2007; Hotchkiss et al., 2009).

Due to the convention that necrosis is an unregulated event, there are only a limited number of reported studies attempting to elucidate the mechanisms behind necrosis (Degterev et al., 2005). Consequently, necrosis is traditionally characterised in a negative fashion, as a type of cell death that leads to cell membrane rupture without the hallmarks of apoptosis and also without the characteristic autophagic vacuolisation present in autophagy-associated cell death (Galluzzi et al., 2007). Necrosis is

characterised by an increase in the cellular (oncosis) and organellar volumes with a consequent rupture of the cellular membrane and spillage of the cellular contents into the surrounding tissue (Figures 1.1 and 1.6). Also, in contrast with apoptosis, swollen and damaged organelles are disposed of in a disorganised fashion. The classical biochemical markers of apoptosis, such as caspase activation, are absent in necrosis.

Necrosis can be mediated by many different stimuli, such as metabolic failure that results in rapid depletion of ATP (Leist et al., 1997) and ROS (Hotchkiss et al., 2009), and over-activation of PARP1 (Zong et al., 2004). Interestingly, it has been repeatedly shown that if apoptosis or autophagy are inhibited, cell still death occurs, but with necrotic characteristics (Cauwels et al., 2003; Kroemer et al., 2009; Vercammen et al., 1998).

Recently some investigations have suggested that necrosis might be partially regulated, both in terms of its initiation and mechanism (Galluzzi and Kroemer, 2008; Moquin and Chan, 2010). In 2005, Degterev and colleagues characterised a mechanism with morphological characteristics of necrosis and activation of autophagy, but that was induced by the stimulation of death receptors in apoptosis-deficient conditions (Degterev et al., 2005). This mechanism has been called necroptosis and is dependent on the serine/threonine kinase activity of receptor interacting protein-1 (RIP1) (Degterev et al., 2005; Galluzzi and Kroemer, 2008). In 2008 an extensive systems biology study using RNA interference (RNAi) techniques, as well as *in silico* analyses, identified an extensive network of genes mediating necroptosis via death receptor activation (Hitomi et al., 2008). Despite this, the field of programmed necrosis is still at its infancy, and more studies are needed in order to fully understand how necroptosis is regulated (Moquin and Chan, 2010).

1.3. Autophagy

The name 'autophagy', which is derived from Greek and means 'self-eating' was proposed more than 40 years ago by Christian de Duve to describe the changes observed in the ultrastructure of rat liver after injection with glucagon (Deter and De Duve, 1967). Autophagy is a catabolic process conserved from lower to higher eukaryotes, and is essential for maintaining cellular homeostasis during demanding conditions such as nutrient depletion, hypoxia and during development (Mizushima and Levine, 2010). Autophagy levels are also increased in response to extracellular stressors such as oxidative stress or pathogen infection (Shintani and Klionsky, 2004). Additionally, a basal, constitutive level of autophagy is necessary for normal functioning of the cell by playing a key role in the degradation of superfluous or damaged/old organelles as well as removal of long-lived proteins and protein aggregates (Yang and Klionsky, 2010a).

Three different pathways of autophagy have been characterised based on the cargo delivery to the lysosome – macroautophagy, microautophagy and chaperone-mediated autophagy (Todde et al., 2009). Macroautophagy is initiated by the formation in the cytosol of the phagophore which expands into a double-membrane, engulfing the cargo to be degraded. The external membrane of the autophagosome fuses with the lysosomal membrane resulting in the degradation of the inner vesicle together with its cargo (Tooze and Yoshimori, 2010). The resulting nutrients are recycled back to the cytosol through membrane permeases (Figure 1.7) (Klionsky, 2007). Microautophagy differs from macroautophagy in the fact that cytosolic components are directly sequestered by the lysosome via an invagination of the lysosomal membrane. Chaperone-mediated autophagy has only been described in mammals and mediates the translocation of

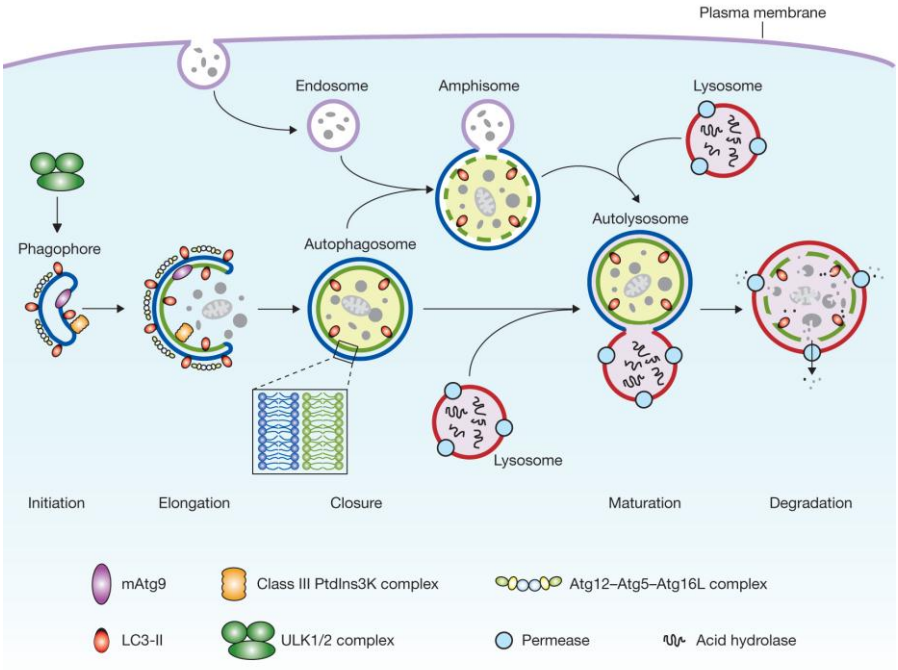

Figure 1.7. *Mechanisms of mammalian autophagy.* Autophagy is initiated by the formation of the phagophore, which is followed by elongation and expansion of the phagophore which is completed by closure with the formation of a double-membrane autophagosome which surrounds a portion of the cytosol. Autophagosome maturation occurs through the fusion with an endosome (product is known as amphisome) and/or a lysosome (the product known as autolysosome). Degradation of the autophagosome inner membrane and cargo is mediated by the acid hydrolases present in the autolysosome with recycling of the products to the cytosol through permeases. The core molecular machinery is also depicted. Adapted from Yang and Klionsky, 2010.

soluble proteins from the cytosol into the lysosome across a translocon-like complex in the lysosomal membrane (Kaushik et al., 2010).

1.3.1. Molecular mechanisms of autophagy

Although autophagy was first described in mammalian cells, much of the current understanding of its molecular mechanism is based on studies in yeast. Thirty-five autophagy-related genes (ATG) have been identified in yeast and many of them present homologues in higher eukaryotes (Yang and Klionsky, 2009). ATG proteins are organised into functional complexes that mediate the different steps of autophagy. The core proteins required for autophagosome formation are organised into four supramolecular complexes: ATG1/unc-51-like kinase (ULK) complex; class III phosphatidylinositol 3-kinase (PtdIns3K)/Vps34 complex I; two ubiquitin-like protein conjugation systems, ATG5-ATG12 and ATG8/light chain 3 (LC3); and, two transmembrane proteins, ATG9/mATG9 and vacuole membrane protein 1 (VMP1) (Xie and Klionsky, 2007).

An essential event that must take place for autophagosome formation is the production of phosphatidylinositol (3)-phosphate by PtdIns3K complexes, which in turn promotes the recruitment of ATG proteins to the membrane. Blockage of this event by 3-methyladenine hampers autophagy progression (Seglen and Gordon, 1982; Wu et al., 2010). There are two different classes of PtdIns3K complexes in mammals and it is the interaction between one of these complexes with beclin 1 (BECN1) that promotes its catalytic activity (Furuya et al., 2005). It is thought that the production of phosphatidylinositol (3)-phosphate is crucial for the special organisation of the core autophagic proteins at the phagophore during the process of membrane nucleation, which makes this a tightly controlled event. BCL-2 is one of the proteins that regulates this process by disrupting the PtdIns3K via interaction with BECN1, thus repressing autophagy. Upon autophagy induction, BCL-2 is phosphorylated

by c-Jun N-terminal kinase (JNK), thereby dissociating from BECN1, ultimately leading to autophagy induction (Maiuri et al., 2007a).

Two ubiquitin-like proteins – ATG12 and LC3 – together with their conjugation systems have been identified in yeast and mammals. These proteins are proposed to act during elongation and expansion of the phagophore membrane. ATG12 interacts with ATG5 in a reaction that requires ATG7 and ATG10 (E1 and E2-like enzymes, respectively). ATG8/LC3 is cleaved at its C-terminus by ATG4 to generate the cytosolic LC3-I. Phosphatidylethanolamine is then conjugated to LC3 (Ichimura et al., 2000; Kabeya et al., 2000; Kirisako et al., 2000). In contrast with the ATG12-ATG5 conjugate that only inserts in the outer membrane of the phagophore, the lipidated form of LC3 (LC3-II) does not display any membrane preference. However, later in the process, LC3-II is removed from the outer membrane of the autophagosome and is recycled into other conjugation reactions (Kirisako et al., 2000). This is followed by fusion of the autophagosome with a late endosome or a lysosome (Yang and Klionsky, 2010b).

1.3.2. Autophagy-associated cell death

During certain cell death conditions, the cell displays a lack of nuclear DNA condensation and presents a highly vacuolated appearance due to an increase in the number of autophagosomes. As a result of these observations, the hypothesis that autophagy is associated with a controlled cell death mechanism arose. However, there is still much debate within the scientific community on the true contribution of autophagy to the process of cell death (Kroemer and Levine, 2008).

The question of whether cell death occurs by an excess of autophagy or after autophagy has failed to rescue the cell from death is pertinent, however literature suggests that autophagy has mainly a pro-survival role by helping the cell to adapt to nutrient-depleted conditions (Maiuri et al., 2007b). In fact, in cells deficient in proteins involved in autophagy induction, an acceleration of cell death has been observed (Galluzzi et al., 2007).

Components of the autophagy molecular machinery have also been described to be involved in the induction of apoptosis, for example ATG5. This protein, which is involved in the early stages of autophagosome formation, has been shown to be proteolytically activated by calpain after which it migrates to the mitochondria where it induces MOMP, thereby working as a pro-apoptotic molecule (Shimizu et al., 2004).

The role of autophagy in cell death is therefore still not clear, and further investigation is needed in order to resolve this. However, it is interesting to note the cross-talk that exists between apoptosis and autophagy, specifically via ATG5 and proteins of the BCL-2 family.

2. Methodologies to study cell death

As described above, cell death has traditionally been characterised by taking into account morphological aspects of the cell (Galluzzi et al., 2007). Other methods are now employed to specifically look at biochemical changes, such as enzymatic activity or membrane potential.

The traditional approach for investigating the morphology of a dying cell is transmission electron microscopy (TEM), by which the various intracellular structures can be easily identified and any changes observed. Despite the power of this technique, there are also drawbacks associated

with it, including the small number of cells that can be analysed, the laborious sample preparation, and the need for specialised personnel to operate the microscope (Galluzzi et al., 2009a; Krysko et al., 2008).

Many of the biochemical tests currently employed, assess the various biochemical events that occur when a cell is dying. Changes at the level of the cellular membrane are studied using a combination of cell permeable dyes such as YoPro-1 or ToPro-3 and cell impermeable dies such as propidium iodide (PI) (Bouchier-Hayes et al., 2008). When a cell enters apoptosis, the permeability of its plasma membrane changes due to differences in the permeability of the ion channels present there (Plantin-Carrenard et al., 2003; Xiao et al., 2002). The cell permeable dyes can enter dying or dead cells whereas the cell impermeable dyes are only able to enter when the plasma membrane is disrupted as occurs during necrosis or secondary necrosis. In this way, combining the two dyes together, using either a flow cytometry or a light microscopy approach (Bouchier-Hayes et al., 2008; Galluzzi et al., 2009a), allows the distinction between apoptotic and necrotic cells. Labelling of phosphatidylserine, present at the outer leaflet of the plasma membrane, using Annexin V is also a common way of investigating the biochemical changes that occur at the cell membrane (Bouchier-Hayes et al., 2008).

In order to investigate the activation of caspases, a variety of different methods, including immunoblotting and light microscopy, can be used. To directly observe caspase activation using imaging approaches, consideration needs to be given as to whether live or fixed cells are most appropriate for the particular question in mind. When live cells are to be analysed, cell permeable fluorescent substrates (Galluzzi et al., 2009a) or FRET probes (Bouchier-Hayes et al., 2008) can be used. A similar rationale can be employed in fluorimetry- and luminometry-based approaches (Galluzzi et al., 2009a). These different approaches rely on the presence of

a specific peptide sequence that is recognised by the caspase, and which is then cleaved thereby releasing a fluorophore that can then be visualised and quantified. The problem with this general approach is that caspase substrates are not particularly specific, with almost all of them reacting with CASP3 with even greater affinity than that for the enzyme against which they were designed (McStay et al., 2008). For fixed cells, one can use antibodies that specifically recognise the active state of the enzyme (de La Motte Rouge et al., 2007). Again, the same problem as described above arises. To confirm that there is activation of the caspase under investigation, the most robust approach is immunoblotting, using antibodies that recognise either the active form of the protein or both the active and inactive (Krysko et al., 2008).

Immunoblotting can also be useful to examine other proteins that are cleaved upon apoptosis onset, or which relocate to a different compartment of the cell. Two such cases are BID, which is activated by cleavage into tBID (Li et al., 1998), and PARP1, which after cleavage becomes inactive and is therefore impaired in its ability to repair DNA strand breaks (Boulares et al., 1999).

LC3, cytochrome c and BAX are three proteins that see their sub-cellular localisation modified upon induction of cell death. Upon induction of autophagy LC3 is cleaved and recruited from the cytosol to the membranes of autophagosomes (Kabeya et al., 2000); upon induction of apoptosis cytochrome c is released from the IMS of the mitochondria into the cytosol, and BAX does the inverse by migrating from the cytosol to the mitochondria (Wolter et al., 1997). These movements can be observed by light microscopy using proteins labelled with a fluorescent tag (Goldstein et al., 2000; Nechushtan et al., 1999; Wolter et al., 1997), or by performing cell fractionation followed by immunoblotting (Goldstein et al., 2000).

In order to complement the study of cell death, many researchers investigate different aspects related to the normal functioning of the cell, such as lysosomal integrity, ATP content, maintenance of the mitochondrial membrane potential and ROS production. The results of these tests are not indicative of the type of cell death, but instead can point to the molecular mechanism behind it.

As described above, lysosomes play an important role in cell death as they can stimulate or potentiate cell death mechanisms. There are several ways to analyse integrity of the lysosomal membrane. Analysis by TEM can reveal damage to the lysosomal membrane, however there are drawbacks with this technique, as one can interpret sample preparation-induced artefacts as physiological cell damage. Release of lysosomal contents, including cathepins or internalised dextran molecules, can be more reliable, and has the advantage that it can be observed by fluorescence microscopy in either living or fixed cells (Bidere et al., 2003). Acidification of the cellular compartments can also be analysed using acridine orange or LysoTracker™, two fluorescent probes that change colour or become fluorescent in an acidic environment, respectively (Freundt et al., 2007; Sorensen and Novak, 2001).

Measurement of the ATP/ADP ratio has also been suggested to be useful in discriminating the different cell death types (Bradbury et al., 2000), however the relative amounts of ATP and ADP can be rapidly affected by extracellular or intracellular conditions, and therefore cannot be used alone to discriminate the type of cell death. The levels of ATP and ADP are usually measured using luminescence (Galluzzi et al., 2009a).

The loss of mitochondrial membrane potential usually occurs when the electron transport chain becomes uncoupled and can be measured using fluorescently labelled probes such as TMRE or TMRM (Tetramethyl rhodamine ethyl- or methyl-ester), which accumulate in mitochondria with

high membrane potential and are released when it is dissipated. This change in fluorescence can be followed by both flow cytometry and light microscopy (Bouchier-Hayes et al., 2008). Another consequence of the mitochondrial dysfunction is the formation of ROS (Indo et al., 2007). This can be measured by using non-fluorescent probes that become fluorescent upon oxidation by ROS, which can be detected by flow cytometry (Bass et al., 1983).

There are many other techniques that can be used to detect events in relation to cell death (Galluzzi et al., 2009a), however the ones described above are among those most commonly used. The number and variety of techniques existing at the moment reflects the complexity of the field, and highlights the necessity of using multiple techniques when characterising the type of cell death under study. Indeed, use of only a single technique may lead to an erroneous classification of the cell death pathway (Kroemer et al., 2009).

III. RNA interference

RNAi is a conserved biological response to double-stranded RNA (dsRNA) which mediates resistance to both endogenous parasitic and exogenous pathogenic nucleic acids, and regulates the expression of protein-coding genes (Hannon, 2002).

RNAi was first described in 1998 by the Nobel prize winners Craig Mello and Andrew Fire in *Caenorhabditis elegans*, where introduction of foreign dsRNA led to specific downregulation of gene expression (Fire et al., 1998). Soon after this, RNAi was discovered in different organisms, including mammals where it was found that long dsRNA elicited anti-viral responses dependent on interferon pathways (Kim and Rossi, 2007; Rana, 2007). It

was also found that target mRNA degradation was mediated by 21-23-nucleotide RNA fragments derived from long dsRNA (Zamore et al., 2000), thereby indicating that short dsRNA sequences were the triggers for RNAi and suggesting that these small 21-nucleotide long sequences did not elicit any interferon-based response (Rana, 2007).

The logical step that came afterwards was to try to apply this knowledge to develop a tool that could be used in molecular biology. And indeed, two independent groups reported that short synthetic dsRNA sequences could be transfected into mammalian cells where sequence-specific gene silencing was efficiently induced (Caplen et al., 2001; Elbashir et al., 2001). These small sequences are denominated small interfering RNA (siRNA) and are widely used in laboratories as a tool to study gene function. Endogenous, non-coding RNA, known as microRNA, has also been identified and plays important roles in different processes including development, proliferation and apoptosis (Ambros, 2001; Lee et al., 1993).

RNAi can occur either through degradation of the target mRNA or via translation repression followed by target mRNA degradation (Kim and Rossi, 2007). Exogenous siRNA target mRNA for cleavage and degradation in a process called post-transcriptional gene silencing (Zamore et al., 2000). Long, dsRNA molecules are processed by Dicer, an RNase II enzyme, into siRNAs containing a 2-nucleotide overhang at the 3' end and phosphate groups at the 5' end, that mediate the RNAi response (Bernstein et al., 2001; Ketting et al., 2001). This step is circumvented when synthetic siRNAs are exogenously introduced in the cells (Rana, 2007).

Effective silencing requires perfect or near-perfect base pairing between the mRNA sequence and the antisense strand of the siRNA and results in the cleavage of the mRNA by the RNA induced silencing complex (RISC) (Martinez et al., 2002). One of the components of the RISC complex, argonaute 2 (AGO2), is responsible for the mRNA cleavage (Liu et al.,

2004) which begins with the degradation of the sense strand of the double-stranded siRNA thereby generating a single-stranded antisense molecule which guides the RISC complex to the target mRNA (Matranga et al., 2005; Rand et al., 2005) (Figure 1.8). The cleavage of the target mRNA occurs between bases 10 and 11 relative to the 5' end of the siRNA antisense strand (Elbashir et al., 2001) with subsequent mRNA degradation being carried out by cellular exonucleases (Orban and Izaurralde, 2005). After activation by the antisense siRNA strand, the RISC complex remains active to mediate cleavage of other target mRNA molecules, which confers RISC very potent gene-silencing capacities (Kim and Rossi, 2007; Paroo et al., 2007).

RNAi is a very appealing tool both to medicine and to research due to its specificity and potency in gene silencing (Kim and Rossi, 2007). RNAi strategies could be very useful therapeutically against viral and neurodegenerative disorders as well as cancer, by promoting the silencing of defective proteins and/or proteins that are required for the normal life cycle of the virus or neoplastic cell (Kim and Rossi, 2007). The problem here is how to successfully deliver of these nucleic acids to the cells avoiding degradation and clearance from the blood. One of the strategies under study is the use of nanoparticles to protect and deliver the siRNAs to cells (Yuan et al., 2011). On a basic research level, RNAi has been successfully employed in genome-wide screens to understand how certain processes such as apoptosis, cell devision or secretion are regulated (Aza-Blanc et al., 2003; Neumann et al., 2010; Simpson et al., 2007).

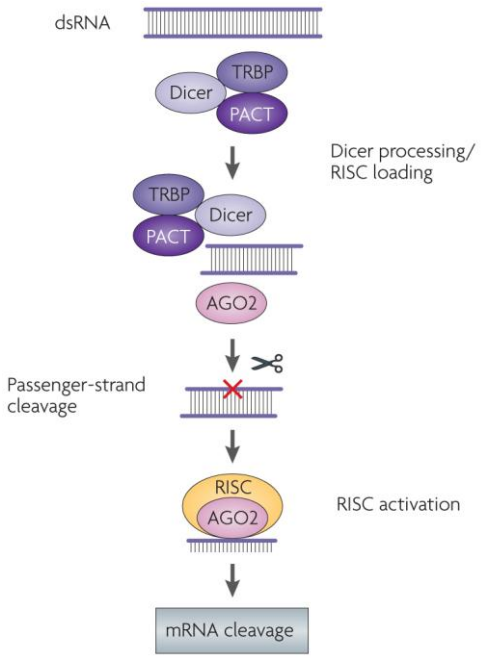

Figure 1.8. *Mechanism of RNAi in mammalian cells.* dsRNAs are recognised and processed by a complex formed by Dicer, TAR RNA-binding protein (TRBP) and protein activator of protein kinase PKR (PACT), thereby facilitating loading of the siRNA duplex into AGO2 and RISC. RISC then cleaves the sense (passenger) strand, thereby activating RISC. The specific mRNA is recognised and cleaved by AGO2 and further degraded by cellular exonucleases. Adapted from Kim and Rossi, 2007.

IV. Objectives

As described above, there is still much to be done in the field of nanotechnology, and in particular in the area of nanotoxicology, before nanoparticles can be safely used in humans. For that reason, the overall objective of this work was to understand how cationic nanoparticles interact with cells, in particular with the main cell type present in the central nervous system, astrocytes.

Specifically, the aim of this work was to provide a greater understanding of the cell death mechanism that is elicited when cells come into contact with NH_2-modified nanoparticles (Chapter 3). The second major goal was to dissect the signalling pathways and identify the intervening molecules that lead to cell death (Chapters 3 and 4). In parallel, it was also sought to understand if two stress adaptive responses – autophagy and ER stress – played any role in the process (Chapter 5). The final goal was to establish a methodology for using RNAi to study the interactions between nanoparticles and cultured mammalian cells (Chapter 4).

CHAPTER 2

MATERIALS AND METHODS

2.1. Nanoparticles

50 nm amine-modified fluorescent polystyrene (NH_2-PS) nanoparticles (Sigma Aldrich) and 50 nm unmodified and carboxylated (COOH-PS) unlabelled polystyrene nanoparticles (Polysciences) were used without further modification. Nanoparticles of the same batch were used throughout this work.

2.2. Cell culture

Human brain astrocytoma 1321N1 cells were cultured at 37 °C in Dulbecco's modified Eagle medium (DMEM) containing 4.5 g/l D-glucose and 1 mM sodium pyruvate supplemented with 10 % foetal bovine serum (FBS) (Gibco) in a humidified atmosphere of 5 % CO_2/95 % air. Cells were routinely subcultured 1:5 by incubating them in 0.25 % trypsin (Gibco) on reaching confluency. Cells were used from passages 1 to 10, after which they were discarded.

2.3. Analysis of cell viability using YoPro-1/PI co-staining

Cells (3×10^4 cells/cm^2) were incubated with various concentrations (0, 12.5, 25, 50 and 100 μg/ml) of nanoparticles for 24 hours, or with a 50 μg/ml nanoparticle dispersion for varying lengths of time (0, 1, 3, 6, 9 and 24 hours) at 37 °C. Incubation with 1 μM staurosporine (Calbiochem) was used as a positive control for apoptosis. Following incubation, all cells, including those in the supernatant, were harvested. Cells were incubated for 5 minutes with 100 nM YoPro-1 (Molecular Probes) and with 20 μg/ml PI (Sigma Aldrich) for 1 minute on ice. Analysis was performed by Flow

Cytometry using a Cyan ADP cytometer (DAKO) using 488 nm excitation and measuring fluorescence emission at 530 nm and 575 nm. Post-acquisition analysis was carried out using Summit software (DAKO). Flow Cytometry was carried out in the Flow Cytometry Core Facility of the Conway Institute for Biomolecular and Biomedical Sciences, University College Dublin.

2.4. Measurement of caspases 3, 7, 8 and 9 activities and cellular ATP content

Measurement of CASP3, CASP7, CASP8 and CASP9 activities was carried out using the Caspase-Glo 3/7, Caspase-Glo 8 and Caspase-Glo 9 assays (Promega) and cellular ATP content was determined using the CellTiter-Glo assay (Promega), according to the manufacturer's instructions. Briefly, cells were incubated in a 96-well plate with various concentrations of nanoparticles for 24 hours, or with a 50 μg/ml nanoparticle dispersion for varying lengths of time (0, 1, 3, 6, 9 and 24 hours) at 37 °C. After incubation, an equal volume of the assay reagent was added to the cells and incubation was continued for a further 1 hour at room temperature. Luminescence was measured using a Wallac VICTOR^{2TM}, 1420 Multilabel Counter (Perkin Elmer). Results were normalised either against the untreated or the negative siRNA controls.

2.5. Incubation with caspase inhibitors

1321N1 cells were prepared as described in the previous section. The following day, cells were pre-treated for 1 hour with different irreversible caspase inhibitors (Calbiochem): z-VAD-fmk, a pan-caspase

inhibitor (final concentration of 20 μM); z-DEVD-fmk, a specific inhibitor for CASP3; z-IETD-fmk, a specific CASP8 inhibitor and z-LEDH-fmk, a specific CASP9 inhibitor all with at a final concentration of 30 μM. The inhibitors were then removed and cells were incubated for 24 hours with 50 μg/ml of NH_2-PS nanoparticles Cells were then analysed for CASP3 and CASP7 activity induction using the assay described in the previous section.

2.6. Preparation of whole cell extracts and Western blotting

Following incubation with nanoparticles, 3×10^5 cells were lysed with RIPA buffer (50 mM Tris-Cl pH 7.5; 150 mM NaCl; 1 % NP-40; 0.1 % sodium dodecyl sulphate (SDS); 0.5 % sodium deoxycholate, (Thermo Scientific)) supplemented with Complete™ protease inhibitor cocktail tablets (Roche). Proteins from each sample were quantified using the bicinchoninic acid (BCA) protein assay kit (Thermo Scientific) and were then subjected to SDS-PAGE gel electrophoresis. The proteins were transferred to polyvinylidene fluoride membrane (Perkin Elmer) and detected using the antibodies listed in Table I following incubation with Attophos fluorescent reagent (Roche) or Pierce ECL Western blotting substrate (Thermo Scientific).

To quantify the amount of cleaved product in LC3 and PARP1 Western blots, Image J 1.42q (National Institutes of Health) software was used. Briefly, for each lane, the background, the uncleaved and the cleaved bands were quantified using the same rectangular selection for all. Results were expressed as the percentage of the cleaved protein over the total amount of protein (cleaved + uncleaved protein).

Table I: Identification of the antibodies used for Western blotting

Specificity	Comments / Concentration	Company
APAF1	Mouse; clone 24/Apaf-1 (1:1000), 10 % gel	BD Transduction Laboratories
ATG5	Rabbit (1:1000), 10 % gel	Cell Signaling Technologies
BAX	Mouse; clone 3/Bax (1:1000), 12 % gel	BD Transduction Laboratories
BAK	Mouse; clone G317-2 (1:250), 12% gel	BD Pharmingen
BECN1	Mouse, clone 20/Beclin (1:1000), 10 % gel	BD Transduction Laboratories
BID	Rabbit (1:1000), 12 % gel	Cell Signaling Technologies
BIM	Rabbit (1:1000), 12 % gel	BD Pharmingen
BOK	Rabbit (1:1000), 12 % gel	Cell Signaling Technologies
CASP3	Rabbit (1:1000), 12 % gel	Cell Signaling Technologies
CASP7	Rabbit (1:600), 12 % gel	Cell Signaling Technologies
CASP8	Mouse; clone 3-1-9 (1:1000), 12 % gel	BD Pharmingen
CASP9	Rabbit (1:1000), 12 % gel	Cell Signaling Technologies
CASP10	Rabbit (1: 1000), 10 % gel	Abcam
GAPDH	Rabbit; clone 14C10 (1:1000)	Cell Signaling Technologies
GAPDH	Mouse; clone 6C5 (1:5000)	Abcam
LC3B	Rabbit (1:1000), 15 % gel	Cell Signaling Technologies
PARP1	Rabbit (1:1000), 10 % gel	Cell Signaling Technologies
PUMA	Rabbit (1:1000), 12 % gel	Cell Signaling Technologies

Anti-Rabbit	Goat; polyclonal; alkaline phosphatase (1:5000)	Sigma Aldrich
Anti-Mouse	Goat; polyclonal; alkaline phosphatase (1:5000)	Sigma Aldrich
Anti-Rabbit	Goat; polyclonal; horseradish peroxidase (1:2000)	Abcam
Anti-Mouse	Rabbit; polyclonal; horseradish peroxidase (1:2000)	Abcam

2.7. Transmission electron microscopy

Cells treated as described above were fixed with 2.5 % glutaraldehyde (BDH) and post-fixed in 1 % osmium tetroxide (OxKem Limited). The samples were dehydrated in an ethanol series and embedded in Epon. Ultrathin sections of 80 nm were stained with 2 % uranyl acetate, 0.4 % lead citrate (Agar Scientific) before being examined with an FEI TECNAI 120 TEM.

2.8. Measurement of ROS production

1321N1 cells were treated with various concentrations of NH_2-PS nanoparticles for 24 hours, as described above. As a positive control, incubation for 1 hour with 300 μM of *tert*-butyl hydroperoxide (TBHP) (Sigma Aldrich) was carried out. ROS production was measured using chloromethyl-H_2DCFDA (Molecular Probes) according to the manufacturer's instructions. Briefly, all cells, including those in the

supernatant, were harvested and stained with 2.5 μM chloromethyl-H_2DCFDA in phosphate buffered saline (PBS) (Sigma Aldrich), for 20 minutes at 37 °C. Analysis was performed by flow cytometry using a Cyan ADP cytometer (DAKO) using 488 nm excitation and measuring fluorescence emission at 530 nm. Post-acquisition analysis was carried out using Summit software (DAKO).

2.9. Coating of glass surfaces with collagen

Glass coverslips or 35 mm glass-bottomed dishes (MatTek Corporation) were coated with rat tail collagen type I (Sigma Aldrich) as recommended by the supplier. Briefly, the collagen stock solution was diluted 1:50 in sterile distilled water and left overnight at 4 °C. The following day the collagen solution was aspirated and the coverslips or dishes were left to dry at room temperature. Coated glass surfaces were kept at 4 °C until further use.

2.10. Analysis of lysosomal leakage

1321N1 cells were plated on 35 mm glass-bottomed dishes (MatTek Corporation) previously coated with rat tail collagen type I. Cells were incubated with 1 mg/ml of 10 kDa dextran conjugated to Texas Red (Molecular Probes) at 37 °C for 3 hours. Cells were washed with PBS to remove non-internalised dextran, and were left in complete DMEM for 1 hour, prior to incubation with 50 μg/ml of NH_2-PS nanoparticles for 6 hours at 37 °C. After particle exposure, the medium was removed and cells were carefully washed with PBS, followed by incubation in complete DMEM

at 37 °C. Imaging of cells was carried out at 37 °C in 5 % CO_2 and 60 % humidity using a spinning-disk confocal microscopy system (Andor). Fluorescent dextran was excited using a 561 nm laser line and images were acquired using a 60x 1.35 NA Olympus UPlanSAPO oil immersion objective. Image analysis was carried out with MATLAB R2007a (The Mathworks) and Image J 1.34e (National Institutes of Health) software. To quantify the differences between treated and untreated cells, a top-hat filter was used to identify punctate structures and measure their fluorescence intensity. Subtracting the filtered image from the original image, a measurement of the diffuse fluorescence intensity was obtained and compared with that of the discrete structures. A total of 10 cells from each treatment were analysed and quantified.

2.11. Alkalinisation of lysosomal pH

1321N1 cells were prepared as described in section 2.4. The following day cells were pre-incubated for 30 minutes with 20 μM chloroquine or 10 mM ammonium chloride (NH_4Cl) diluted in complete DMEM. Following this, cells were incubated with 50 μg/ml of NH_2-PS nanoparticles for 6 hours, after which CASP3 and CASP7 activities were measured as described in section 2.4.

2.12. Analysis of cathepsin L release from lysosomes

1321N1 cells (1×10^5 cells) were plated on glass coverslips previously coated with rat tail collagen type I. Cells were incubated with either 50 μg/ml of NH_2-PS nanoparticles for increasing lengths of time (0, 3, 6

and 9 hours) or 30 μg/ml chloroquine (Sigma Aldrich) for 3 hours, and were then fixed with absolute methanol (Fisher Scientific) at -20 °C for 4 minutes. Cells were stained with mouse anti-cathepsin L (BD Transduction Laboratories, clone 22/Cathepsin L) diluted 1:200 in PBS, for 1 hour at room temperature. Secondary staining was performed with goat anti-mouse antibodies conjugated to Alexa-568 (Molecular Probes) diluted 1:200 in PBS for 30 minutes at room temperature. Nuclei were stained with Hoechst 33342 (Sigma Aldrich) diluted 1:10 000 for 5 minutes at room temperature. Slides were mounted using Mowiol (Sigma Aldrich). Confocal images were acquired using a spinning-disk confocal microscopy system (Andor) with a 60x 1.35 NA Olympus UPlanSAPO oil immersion objective.

2.13. Analysis of cytochrome c release from mitochondria

1321N1 cells (1×10^5 cells) were plated on glass coverslips previously coated with rat tail collagen type I, as described in section 2.8 and left to adhere overnight. The following day cells were treated with 50 μg/ml of NH_2-PS for increasing lengths of time (0, 3, 6 and 9 hours) and fixed with 3 % paraformaldehyde (PFA) (Sigma Aldrich) for 15 minutes at room temperature, followed by incubation with 30 mM glycine (Fisher Scientific) for 5 minutes to quench the PFA. Cells were permeabilised using 0.1 % Triton-X100 for 5 minutes at room temperature. Following three 3 minute washes with PBS, cells were incubated for 1 hour at room temperature with mouse anti-cytochrome c (BD Pharmingen, clone 6H2.B4) diluted 1:100 in PBS and rabbit anti-Manganese superoxide dismutase (MnSOD) (Stressgene) diluted 1:200. Secondary staining was performed using goat anti-mouse antibodies conjugated to Alexa-488 and goat anti-rabbit antibodies conjugated to Alexa-568 (Molecular Probes) diluted 1:400 and

incubation proceeded for 30 minutes at room temperature. Nuclei were stained with Hoechst 33342 diluted 1:10 000 for 5 minutes at room temperature. Following five washes, each for 5 minutes, coverslips were mounted using Mowiol. Confocal images were acquired using an Olympus FluoView FV1000 confocal microscope with a 60x 1.35 NA Olympus UPlanSAPO oil immersion objective.

2.14. siRNA transfection

Cells (20×10^3 cells/cm^2) were transfected with Silencer Select siRNA (Table II) (Ambion) using Oligofectamine (Invitrogen). Briefly, 30 pmol of siRNA and Oligofectamine were diluted separately in OptiMEM® (Invitrogen) and incubated for 7 minutes at room temperature. When cells were transfected with more than one siRNA, 30 pmol of each were used without changing the amount of Oligofectamine. After that, diluted siRNA and Oligofectamine were mixed together and incubated for a further 20 minutes at room temperature to allow the formation of the transfection complexes. Transfection complexes were added to the cells, previously washed with serum-free DMEM, in a drop-wise manner and cells were then incubated at 37 °C for 4 hours. DMEM containing 30 % FBS was added to the cells and incubation proceeded for a further 44 hours.

2.15. Total RNA extraction

Total RNA from 1321N1 cells treated as described above was purified using Invisorb spin cell RNA mini kit (Invitek) as recommended by

Table II. Details of the siRNA molecules used

Target	siRNA Name	Ambion ID	Sense Sequence (5'→ 3')
ATG5	ATG5.1	s18158	GGAUGCAAUUGAAGCUCAUtt
	ATG5.2	s18160	GCUAUAUCAGGAUGAGAUAtt
APAF1	APAF1.1	s1413	CAUGAUUAGUGAUGGAUUUtt
	APAF1.2	s1414	GAGACAAGAGUGUUACAGAtt
BAK	BAK.1	s1880	GGUUUUCCGCAGCUACGUUtt
	BAK.2	s1881	GGAUUCAGCUAUUCUGGAAtt
BAX	BAX.1	s1888	GUGCCGGAACUGAUCAGAAtt
	BAX.2	s1889	ACAUGUUUUCUGACGGCAAtt
BECN1	BECN1.1	s16537	CAGUUACAGAUGGAGCUAAtt
	BECN1.2	s16539	CAGAUACUCUUUUAGACCAtt
BID	BID.1	s1985	GCACAUCUGUAAAUCUACAtt
	BID.2	S1086	CUUGCUCCGUGAUGUCUUUtt
BIM	BIM.1	s195011	CAUGAGUUGUGACAAAUCAtt
	BIM.2	s195012	UGACCGAGAAGGUAGACAAtt
BOK	BOK.1	s194313	GCAAGGUGGUGUCCCUGUAtt
	BOK.2	s194314	CCGAGAUCAUGGACGCCUUtt
CASP3	CASP3.1	s397	GGAAUAUCCCUGGACAACAtt
	CASP3.2	s398	GUCUAACUGGAAAACCCAAtt
CASP7	CASP7.1	s2423	CCACGGUUCCAGGCUAUUAtt
	CASP7.2	s2424	UACCGUCCCUCUUCAGUAAtt

CASP8	CASP8.1	s2425	GAUAAUCAACGACUAUGAAtt
	CASP8.2	s2427	GAUACUGUCUGAUCAUCAAtt
CASP9	CASP9.1	s2428	CGGUGAAAGGGAUUUAUAAtt
	CASP9.2	s2430	CUUCGUUUCUGCGAACUAAtt
CASP10	CASP10.1	s2431	GGACAGACAAGGAACCCAUtt
	CASP10.2	s2433	GGUUCACAGUGCAUAUACAtt
	CASP10.3	s2432	CAGAUGCUCUGAACCCUGAtt
Negative control	NEG	Negative Control #1	Not available
PUMA	PUMA.1	s25840	GCCUGUAAGAUACUGUAUAtt
	PUMA.2	s25842	GGAGGGUCCUGUACAAUCUtt

the supplier. Briefly, cells were lysed directly in the plate and the lysate was then transferred to a DNA-binding spin filter. 70 % molecular biology grade ethanol (Sigma Aldrich) was added to the flow-through and this was applied to a RNA-binding spin filter. After several washing steps, RNA was eluted in 40 µl of elution buffer. RNA concentration was determined using NanoDrop3000 (Thermo Scientific), and then stored at -20 °C until further use.

2.16. cDNA synthesis and quantitative Real-Time PCR

Complementary DNA (cDNA) synthesis was performed using the High Capacity cDNA Reverse Transcription kit (Applied Biosystems) according to the supplier's instructions. Briefly, 500 ng of RNA were reverse-

Table III. Primer sequences

Target	Primer	Sequence
APAF1	Forward	cagtggtaaagattcagttagtggaa
	Reverse	aaaacaactggcctctgtgg
ATG5	Forward	caacttgtttcacgctatatcagg
	Reverse	cactttgtcagttaccaacgtca
BAK	Forward	aaactgggctcccactca
	Reverse	cagtggaggacgggatca
BAX	Forward	atgttttctgacggcaacttc
	Reverse	atcagttccggcaccttg
BCL-2	Forward	tacctgaaccggcacctg
	Reverse	gccgtacagttccacaaagg
BECN1	Forward	ggatggtgtctctcgcagat
	Reverse	ttggcactttctgtggacat
BID	Forward	ggagggctacgatgagctg
	Reverse	tccggatgatgtcttcttgac
BIM	Forward	catcgcggtattcggttc
	Reverse	gctttgccatttggtcttttt
BOK	Forward	cagtctgagcctgtggtgac
	Reverse	catacagggacaccaccttgc
CASP3	Forward	gtggaattgatgcgtgatgt
	Reverse	acaggtccatttgttccaaaa

CASP7	Forward	ggaccgagtgcctacatatca
	Reverse	cgtttcgaacgcccatac
CASP8	Forward	tccaaatgcaaactggatga
	Reverse	tcccaggatgaccctcttct
CASP9	Forward	ccatatgatcgaggacatcca
	Reverse	gactccctcgagtctccagat
CASP10	Forward	gcagcacctcaactgtacca
	Reverse	tgacagttcgtagagcaggttt
CHOP	Forward	cagagctggaacctgaggag
	Reverse	ctgcagttggatcagtctgg
EDEM1	Forward	agtcatcaactccagctccaa
	Reverse	aaccatctggtcaatctgtcg
ERdj4	Forward	tggtggttccagtagacaaagg
	Reverse	cttcgttgagtgacagtcctgc
HERPUD1	Forward	tcctcctcctgaccttgtaaa
	Reverse	tgctcgccatctagtacatcc
NOXA	Forward	ggagatgcctgggaagaag
	Reverse	cctgagttgagtagcacactcg
PUMA	Forward	gacctcaacgcacagtacga
	Reverse	gagattgtacaggaccctcca

transcribed using random primers. The reaction was carried out in a GS2 thermocycler (G-Storm) and the cycling program used was the following: 25 °C, 10 minutes → 37 °C, 120 minutes → 85 °C, 5 minutes. When the

cycling program was complete samples were kept at 10 °C. Real-time PCR was performed using Power SYBR green PCR MasterMix (Applied Biosystems). Briefly, 1/20 of the cDNA reaction was used as template for the reaction and 200 nM of each primer (Table III) was used. Quantitative real-time PCR was performed in a 7500 FAST real-time PCR system (Applied Biosystems) using the following cycling program: 50 °C, 2 minutes → 95 °C, 10 minutes → (95 °C, 15 seconds → 60 °C, 1 minute) × 40. A melting curve stage was also included in every run in order to assess the synthesis of only the specific PCR product. All samples were run in quadruplicate. Results were obtained using the $-\Delta$Ct method.

2.17. Statistical Analysis

Unless mentioned otherwise, results were expressed as the mean and standard error of the mean between three independent experiments. Each experiment consisted of three technical replicates. Analysis of variance (one-way ANOVA) was performed to compare between the experimental conditions. Univariate analysis was used throughout, with the exception of the YoPro-1/PI co-staining experiments, where multivariate analysis was used. *Post hoc* analysis was carried out using Tukey test. All statistical analyses were performed with PASW Statistics v.18 software (SPSS Inc.).

CHAPTER 3

MECHANISMS OF CELL DEATH INDUCED BY NH_2-PS NANOPARTICLES

The results presented in this chapter were published in:

Bexiga, M.G.; Varela, J.A.; Wang, F.; Fenaroli, F.; Salvati, A.; Lynch, I.; Simpson, J.C.; Dawson, K.A. (2010) Cationic nanoparticles induce caspase 3- and 7-mediated cytotoxicity in a human astrocytoma cell line. *Nanotoxicology*. DOI: 10.3109/17435390.2010.539713

Nanoparticles are present in our daily lives as a result of applications in nanotechnology and cosmetic industries, and with potentially more deleterious effects they are also present in atmospheric pollution (Nel et al., 2006). As a consequence of their small size, large surface area, chemical composition, and other physicochemical properties, nanoparticles are able to interact with biological systems in ways not yet known (Nel et al., 2009), and therefore a greater understanding of this is vital if they are to be fully exploited. Various studies have shown that nanoparticles can distribute to many compartments in the body, including the liver, lungs and the central nervous system (Calderon-Garciduenas et al., 2008; Li and Huang, 2008). Although these observations may lead to revolutionary applications in drug delivery, at the same time they raise concerns about the safety of their use in humans (Nel et al., 2006).

Many of these nanoparticles, such as liposomes and metallic nanoparticulates, display a positive charge on their surface and are known to induce cytotoxicity (Aillon et al., 2009; Lv et al., 2006), but the molecular mechanism of how this occurs has never been described in detail. Interaction of nanoparticles at the level of the mitochondria with consequent production of ROS (AshaRani et al., 2009; Xia et al., 2008a; Xia et al., 2008b) and damage at the level of the cell membrane have been reported in the literature, but information about the signalling pathways that lead to these effects is still lacking.

In this study we begin characterising the molecular mechanism of cationic nanoparticle-induced cell death in a model human brain cell line, 1321N1 astrocytoma cells. The use of this biological system is relevant because it has been reported that nanoparticles present in air pollution not only affect the respiratory tract, but may also cross to the brain causing inflammation, deposition of amyloid-β, and other pathological events (Calderon-Garciduenas et al., 2008), which are in turn characteristic of

neurological diseases such as Alzheimer's and Parkinson's Disease (Jellinger, 2009).

3.1. Amine-modified nanoparticles induce toxicity in 1321N1 cells

To study the cytotoxic effects of cationic nanoparticles we used, as a model, polystyrene nanoparticles with a NH_2- modification at the surface, which conferred them a positive charge (Table AI.I), and a human astrocytoma cell line, 1321N1, combined with YoPro-1/PI co-staining and analysis by flow cytometry (Figure 3.1.a). During apoptosis, the permeability of the plasma membrane has been reported to be affected, with one consequence being changes in ionic movements across this membrane (Plantin-Carrenard et al., 2003; Xiao et al., 2002). This phenomenon can be utilised to probe for apoptotic and necrotic processes. Specifically, certain dyes such as YoPro-1 can enter apoptotic cells, whereas other dyes, such as PI, can only enter cells if the plasma membrane has been severely damaged (Bouchier-Hayes et al., 2008), as would be the case in late apoptosis/necrosis. Thus, the respective uptake of these dyes can be used as both a measure of the degree and the stage of apoptosis/necrosis in cells. Incubation with increasing concentrations of 50 nm NH_2-PS nanoparticles for 24 hours led to a decrease in the overall number of viable cells, with a corresponding increase in the numbers of early and late apoptotic and necrotic cells (Figure 3.1.b). In subsequent studies, a concentration of 50 μg/ml of nanoparticles was used, because although there was an increase in the numbers of early and late apoptotic and necrotic cells at this nanoparticle concentration, the viable cell population was still relatively well represented. In contrast, incubation for 24 hours with increasing concentrations of either COOH-PS or unmodified polystyrene nanoparticles

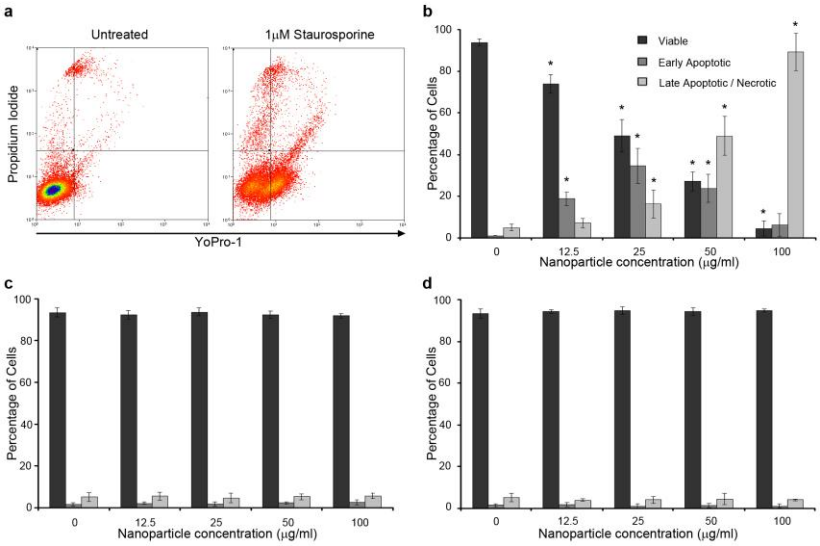

Figure 3.1. *50 nm NH_2-PS nanoparticles induce cell death in 1321N1 cells in a concentration-dependent manner.* YoPro-1/Propidium Iodide (PI) staining was used to assess the viability of cells. In **a.**, an example of how the different cell populations were defined is shown, for either untreated or cells treated for 6 hours with 1 μM of staurosporine, a known inducer of apoptosis. 1321N1 cells incubated for 24 hours with varying concentrations of **b.** NH_2-PS, **c.** COOH-PS, or **d.** unmodified 50 nm polystyrene nanoparticles. Viable cells are YoPro-1$^-$PI$^-$, early apoptotic cells are YoPro-1$^+$PI$^-$, late apoptotic/secondary necrotic YoPro-1$^+$PI$^+$ and necrotic are YoPro-1$^-$PI$^+$. Results show means and standard deviations from three independent experiments, each with three replicates. * indicates p-values <0.001. In each case comparisons are made to untreated cells of the same population class.

(Figures 3.1.c and d), did not induce any significant change in the levels of the different cell populations as compared to untreated cells.

3.2. Cell death kinetics

Kinetic analysis using YoPro-1/PI co-staining of 1321N1 cells incubated with 50 μg/ml of NH_2-PS nanoparticles revealed that the

number of viable cells decreased over the period of time studied (Figure 3.2.a). This is in contrast with the results obtained for untreated cells, in which all cell populations remained constant over a period of 24 hours (Figure 3.2.b). Kinetic analysis also revealed that the early apoptotic cell population only increased after 6 hours of incubation, whereas the late apoptotic/necrotic cell population had already increased after just one hour of incubation with NH_2-PS nanoparticles (Figure 3.2.a).

3.3. Cell death is associated with activation of caspases 9, 3 and 7 and PARP1 cleavage

In order to confirm the type of cell death that was being induced by the NH_2-PS nanoparticles, apoptosis-specific events were studied. It is well known that, in contrast to necrosis, apoptosis is a highly controlled mechanism of cell death involving the proteolytic activation of specific enzymes called caspases (Hotchkiss et al., 2009; Riedl and Shi, 2004). Depending on the cellular organelle triggering the apoptotic events, the caspase that initiates the signalling pathway will be different. For events starting with a stimulus at the level of the plasma membrane, the activation of CASP8 and CASP10 leads to apoptosis via the so-called extrinsic pathway; whereas if the initial stimulus is at the level of the mitochondria, CASP9 will be activated via the intrinsic pathway (Ferri and Kroemer, 2001; Riedl and Shi, 2004).

The cationic nanoparticle-specific activation of two effector caspases, CASP3 and CASP7, which are downstream of the initiator events of the apoptotic cascade and are common to both the extrinsic and the intrinsic apoptotic pathways was investigated. A chemiluminescence assay in which activated caspases react with a specific substrate, with the product of

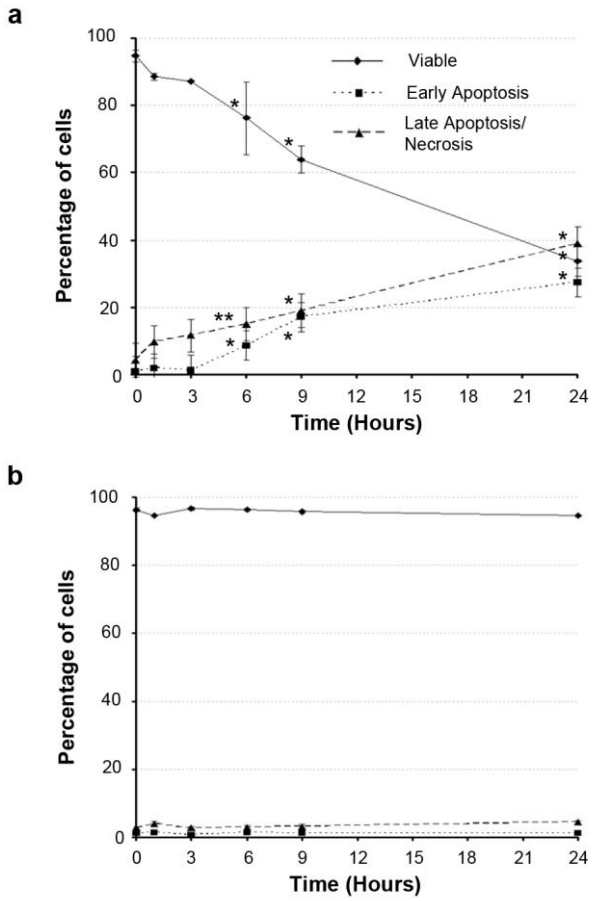

Figure 3.2. *Kinetics of cell death induced by NH_2-PS nanoparticles.* **a.** YoPro-1/PI staining of 1321N1 incubated with 50 μg/ml of 50 nm NH_2-PS nanoparticles shows an increase in the population of dead cells (early apoptotic and late apoptotic/necrotic) and a decrease in the viable cell population over a 24-hour period. **b.** The same assay carried out with untreated cells shows no change in the relative proportions of each cell population. Results show means and standard deviations from three independent experiments, each with three replicates. * indicates p-values <0.01, ** indicates p-values <0.05. In each case comparisons are made to untreated cells of the same population class.

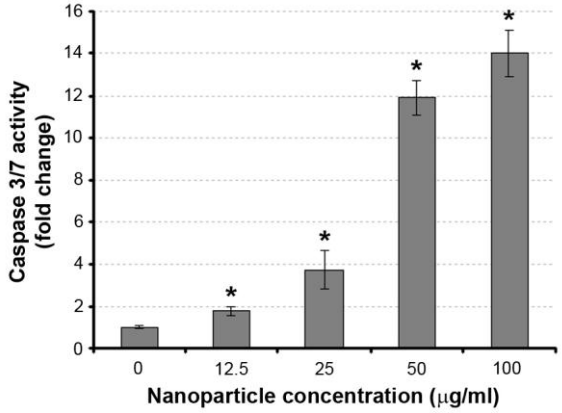

Figure 3.3. *NH_2-PS nanoparticles induce CASP3 and CASP7 activity in a concentration-dependent manner.* Analysis of the apoptosis-specific activity of CASP3 and CASP7 in 1321N1 cells treated with increasing concentrations of NH_2-PS nanoparticles reveals an increase in caspase activity as the nanoparticle concentration increases. This indicates that apoptosis is one of the mechanisms involved in cell death induced by 50 nm NH_2-PS nanoparticles. Results were normalised to the untreated sample and show means and standard deviations from three independent experiments, each with three replicates. * indicates p-values <0.001 compared to untreated cells.

the reaction serving as substrate for luciferin was chosen. This results in the release of light, which is proportional to the level of caspase activation.

1321N1 cells were first incubated with increasing concentrations of NH_2-PS nanoparticles (12.5, 25, 50 and 100 μg/ml) for 24 hours after which the chemiluminescence assay was performed. At all the concentrations tested, the activities of CASP3 and CASP7 increased significantly when compared to the untreated control (Figure 3.3). In order to understand the kinetics of CASP3 and CASP7 activation, 1321N1 cells were incubated with 50 μg/ml of NH_2-PS nanoparticles for increasing lengths of time up to a maximum of 24 hours, and were then subjected to the chemiluminescence assay (Figure 3.4.a). This nanoparticle concentration was also used for all subsequent experiments. An increase in CASP3 and CASP7 activation was

first detected after 9 hours of incubation with particles. This increase continued with time, and after 24 hours of exposure to the NH_2-PS nanoparticles, caspase activity in the treated cells was nine-fold higher than that of the untreated cells.

Caspase activation during apoptosis involves several energy-dependent steps, including activation of the caspases themselves through a cleavage mechanism and translocation of proteins to the nucleus (Chiarugi, 2005). In the early stages of apoptosis, cytoplasmic ATP levels increase and then gradually decrease (Zamaraeva et al., 2005). This is in contrast to necrosis, during which energy levels can be dissipated by 90 % within 30 minutes (Leist et al., 1997). In our studies we observed that 1 hour after addition of NH_2-PS nanoparticles to cells there was a transient increase of 3 % in the total ATP content followed by a slow decline, reaching 43 % after 24 hours incubation with nanoparticles (Figure 3.4.a). Other studies using macrophage cells have also reported a similar modest increase (10 %) in ATP content shortly after particle addition followed by a slow decline (Xia et al., 2008b).

In order to assess the specific pathway of apoptosis that was being activated in the system two different techniques were used: a luminescence technique similar to the one described above but using CASP8 and CASP9 substrates (Figure 3.4.b), and a biochemical approach to detect specific cleavage of CASP8 and CASP9, the initiator caspases for the extrinsic and intrinsic pathways of apoptosis respectively. In addition, cleavage of CASP3, an effector caspase common to both pathways was also monitored by Western blotting (Figure 3.5.a). Studies on the cleavage of the CASP8 and the CASP9 substrates were inconclusive, as both displayed a low luminescence signal and also a similar profile of activation (Figure 3.4.b). In addition, the profile of CASP8 and CASP9 activation was analogous to that of CASP3. This is in line with reports stating that many caspase substrates

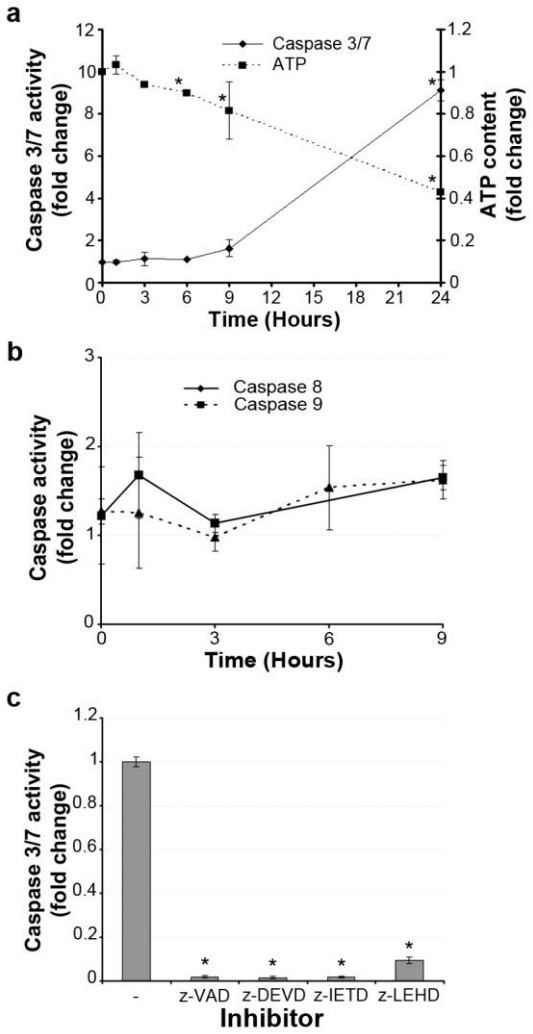

Figure 3.4. *NH_2-PS nanoparticles induce CASP3 and CASP7 activity in 1321N1 cells.* a. Analysis of the apoptosis-specific activity of CASP3 and CASP7 reveals an increase over time, indicating that apoptosis is one of the mechanisms involved in cell death induced by 50 nm NH_2-PS nanoparticles. Analysis of cellular ATP content shows that there is also energy depletion in the cells. Results were normalised to the untreated sample and represent means and standard deviations from three independent experiments, each with three replicates. * indicates p-values <0.01 compared to untreated cells. b. Analysis of CASP8 and CASP9 activities in 1321N1 cells treated with NH_2-PS nanoparticles over a period of 9 hours did not indicate

available commercially are not specific to the caspase against which they are designed, and often preferentially interact with CASP3 with a higher affinity than for their corresponding caspase (McStay et al., 2008). Experiments using caspase inhibitors were also performed, but again no clear effect were observed. This is most likely due to the poor specificity of the reagents, as typically they are small peptides with a recognition sequence similar to that of the caspase substrates used in the chemiluminescence assay. As expected, when z-VAD, a pan-caspase inhibitor was used, CASP3 and CASP7 activities were similar to those of the untreated cells (Figure 3.4.c). The same was true when CASP3 was blocked by its specific inhibitor (z-DEVD). However, when the inhibitors for CASP8 (z-IETD) and for CASP9 (z-LEHD) were used, no significant effect at the level of CASP3 and CASP7 was observed (Figure 3.4.c), therefore making it difficult to identify which was the caspase responsible for the initiation of the apoptotic pathway elicited by the NH_2-PS nanoparticles.

Due to the technical difficulties surrounding the assessment of initiator caspase activity, the preferred option for analysis of the activation of these enzymes was the use of Western blotting to monitor their proteolytic cleavage and subsequent activation. Cleavage of CASP3 and CASP9 could be detected after 9 hours of exposure to NH_2-PS

any clear induction of caspase activity. Results were normalised to the untreated sample and show means and standard deviations from three replicates. **c.** Incubation of 1321N1 cells with medium only (-) or pan-caspase (z-VAD), CASP3 (z-DEVD), CASP8 (z-IETD) and CASP9 (z-LEHD) inhibitors followed by 24 hours of incubation with NH_2-PS nanoparticles resulted in a decrease in CASP3 and CASP7 activities. Results were normalised to the sample not treated with inhibitor, but treated with NH_2-PS nanoparticles and represent means and standard deviations from three independent experiments, each with three replicates. * indicates p-values <0.01 compared to cells not treated with inhibitors, but treated with NH_2-PS nanoparticles.

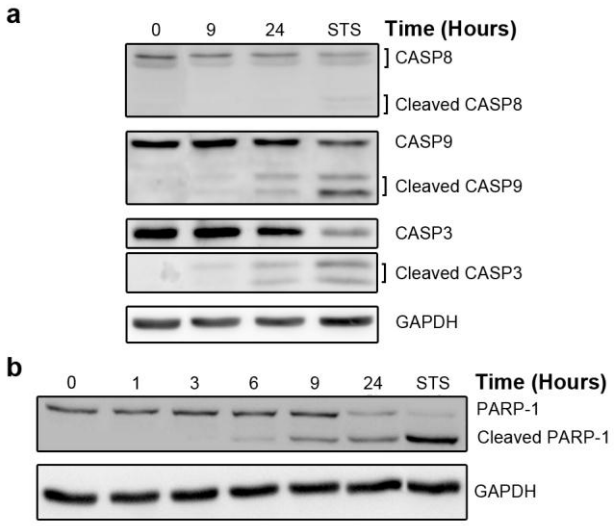

Figure 3.5. *NH_2-PS nanoparticles induce CASP3, CASP9 and PARP1 cleavage in 1321N1 cells.* **a.** Western blot detection of apoptosis-specific cleavage of CASP8, CASP9 and CASP3 after incubation with 50 μg/ml of nanoparticles for 9 or 24 hours shows cleavage of CASP9 and CASP3, but not of CASP8. **b.** Western blot for the apoptosis-specific cleavage of PARP1 (116 kDa) shows an increase of the cleaved protein (89 kDa) over time in the presence of 50 μg/ml of nanoparticles. Incubation with staurosporine (STS) for 6 hours was used as positive control for the experiment and GAPDH was used as the loading control. Three independent experiments were performed and a representative example is shown.

nanoparticles, with the cleaved protein being distinctly visible after 24 hours of exposure (Figure 3.5.a). In contrast, cleavage of CASP8 was not detected at any of the incubation times tested (Figure 3.5.a).

Next the apoptosis-specific cleavage of PARP1 by CASP3 and CASP7 was investigated. PARP1 is a highly abundant nuclear enzyme that in response to DNA-strand breaks catalyses the transfer of ADP-ribose polymers onto different proteins, including itself. During apoptosis full length PARP1 (116 kDa) is cleaved by CASP3 and CASP7 into two fragments of

89 kDa and 24 kDa, resulting in the inactivation of its catalytic activity (Boulares et al., 1999; Jagtap and Szabo, 2005). This cleavage has become a useful hallmark of apoptosis. The study of PARP1 cleavage is not possible using chemiluminescence methods, so therefore we probed the cellular status of PARP1 by Western blotting. Similar to the kinetic profile of CASP3 and CASP7 activation, these experiments revealed that cleavage of PARP1 was also initially detectable 6 hours after nanoparticle addition to the cells, and the amount of cleaved protein increased with time, with a corresponding decrease in the amount of full length protein (Figure 3.5.b).

3.4. NH_2-PS nanoparticles induce damage to the mitochondria

In order to understand which organelle was being affected by the nanoparticles and therefore responsible for initiating the apoptotic cascade, 1321N1 cells either untreated or treated with 50 μg/ml of NH_2-PS nanoparticles for 6 hours, were analysed by TEM. As shown in Figure 3.6.a compared to untreated cells, the mitochondria of the treated cells appeared highly electron translucent, an observation that is consistent with the disappearance of the mitochondrial cristae and damage to the mitochondria (Germain et al., 2005). Given that damage to the inner mitochondrial membrane results in the generation of ROS (Indo et al., 2007), we used the oxidation of chloromethyl-H_2DCFDA as a means to analyse ROS production in cells treated with NH_2-PS nanoparticles for 6 hours. Chloromethyl-H_2DCFDA is a non-fluorescent cell permeable molecule, which is retained in the cell after hydrolysis by cellular esterases. Oxidation of this compound by ROS results in the emission of fluorescent light that can be detected by flow cytometry (Bass et al., 1983). As shown in Figure 3.6.b, the production of ROS was observed to increase as the cells

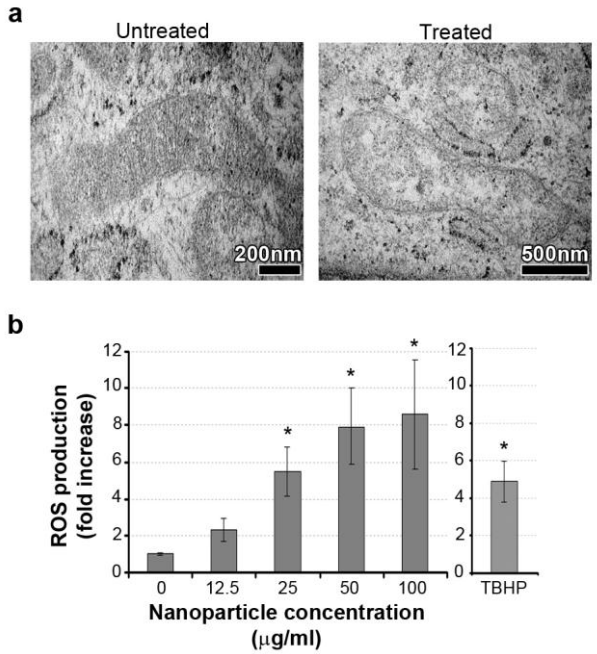

Figure 3.6. *Apoptosis induced by 50 nm NH_2-PS nanoparticles is mediated through damage to the mitochondria.* **a.** TEM images mitochondria in untreated 1321N1 cells and cells treated for 6 hours with 50 μg/ml nanoparticles. **b.** ROS production by 1321N1 cells treated with increasing amounts (12.5, 25, 50 and 100 μg/ml) of NH_2-PS nanoparticles for 6 hours or with 300 μM of *tert*-butyl hydroperoxide (TBHP) for 1 hour was measured using chloromethyl-H_2DCFDA. Results were normalised to the untreated sample and show means and standard deviations from three independent experiments, each with three replicates. * indicates p-values <0.001 compared to untreated cells.

were exposed to increasing concentrations of nanoparticles, with an eight-fold increase in ROS production at the highest particle concentration tested.

3.5. NH_2-PS nanoparticles induce lysosomal membrane permeabilisation with release of their contents

To analyse the contribution of the endocytic pathway, and in particular the lysosomes, to the mechanism of cell death induced by NH_2-PS nanoparticles, cells were incubated with fluorescently labelled 10 kDa dextran, a hydrophilic polysaccharide commonly used to analyse fluid phase endocytosis and label lysosomes (Watson et al., 2005). Under control conditions the lysosomes become loaded with this internalised cargo, and they can be viewed as discrete punctate structures by fluorescence microscopy. However, if the lysosomal membrane is permeabilised, the contents of the lysosomal lumen, including the dextran, are released into the cytoplasm of the cell resulting in a diffuse pattern of fluorescence (Bidere et al., 2003). In 1321N1 cells treated with 50 μg/ml of NH_2-PS nanoparticles, it was indeed observed that the dextran localisation pattern became diffuse compared to control cells in which the fluorescence remained concentrated in punctate structures (Figure 3.7.a). Quantitative single cell image analysis confirmed the relative increase in the presence of diffuse fluorescent structures (55 %) in nanoparticle-treated cells, compared to untreated control cells (24 %) (Figure 3.7.a).

Similar to the results obtained from the fluorescence-based analyses of gross lysosome morphology, TEM images of lysosomes also revealed apparent damage to their membranes (Figure 3.7.b). In addition, the electron-dense regions within the lysosome lumen were reduced in size, indicating a loss of proteolytic enzymes from this organelle (Figure 3.7.b). Furthermore, 50 nm nanoparticles could be clearly observed inside the lysosomes showing these defects (Figure 3.7.b, arrowheads). Lysosomal damage was confirmed using an immunofluorescence approach to investigate the subcellular localisation of one of the proteolytic enzymes

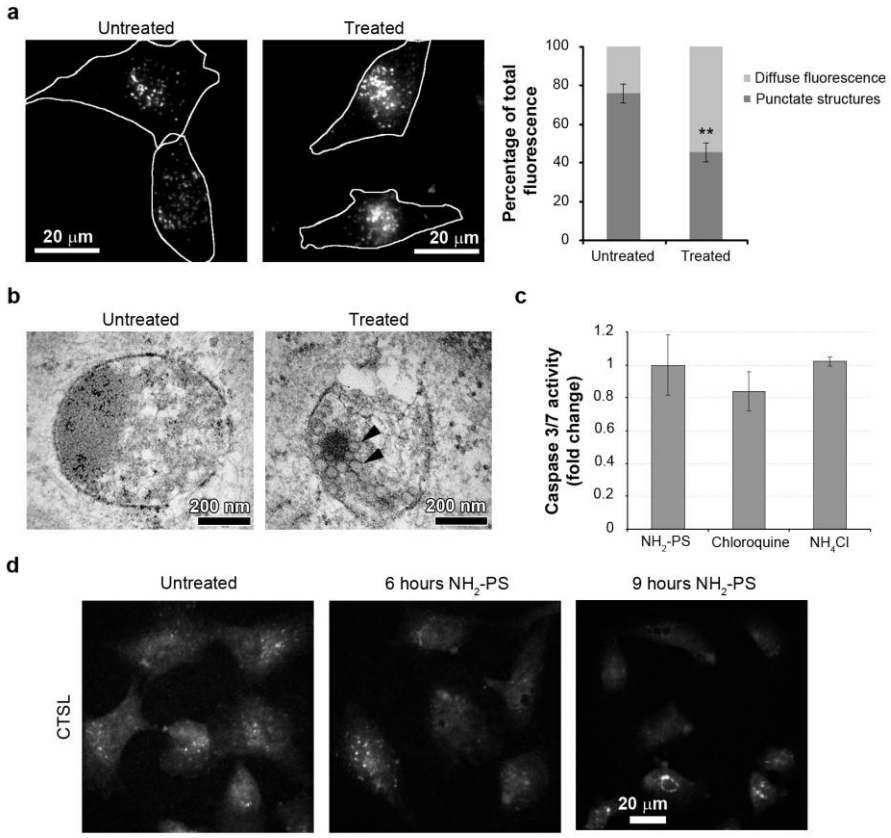

Figure 3.7. *Apoptosis induced by 50 nm NH_2-PS nanoparticles is mediated through damage to lysosomes.* **a.** Projections of spinning-disk confocal microscopy images of 1321N1 cells loaded with 10 kDa dextran-Texas Red, untreated or treated with 50 μg/ml of NH_2-PS nanoparticles for 6 hours. The outline of the cells, as determined from corresponding bright field images, is depicted as a white line. On the right, a graph showing analysis of the relative proportion of discrete and diffuse fluorescent structures in the cells treated as indicated above. A total of 10 cells were analysed for each condition. ** indicates p-value <0.05 compared to untreated cells. **b.** TEM image of lysosomes in untreated 1321N1 cells and cells treated for 6 hours with 50 μg/ml nanoparticles. **c.** Cells were pre-treated with 20 μM chloroquine or 10 mM NH_4Cl and then treated for 6 hours with NH_2-PS nanoparticles, after which CASP3 and CASP7 activities were measured. Results are represented as the means and standard deviations of one experiment with three

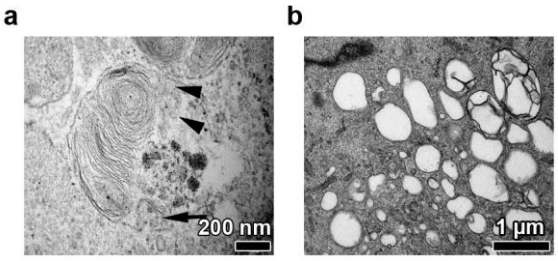

Figure 3.8. *NH_2-PS nanoparticles induce vacuolation of internal cellular membranes.* **a.** A multi lamellar body (MLB) containing nanoparticles. Arrowheads indicate NH_2-PS nanoparticles inside the lysosome and MLB. Arrow indicates a vesicle fusing with the outer membrane of the MLB. **b.** In treated cells, an increase in the vacuolation of the cells was observed, with some of these vacuoles presenting cellular debris inside.

(cathepsin L - CTSL) present in the lysosome. As can be observed in Figure 3.7.d as the incubation time with the nanoparticles increased from 0 to 9 hours, the distribution of the stained CTSL changed from punctate to diffuse and indeed some of the cells treated for 6 hours with nanoparticles no longer displayed defined CTSL-positive membrane structures. This effect was particularly visible in the cells that had been treated with the NH_2-PS nanoparticles for 9 hours (Figure 3.7.d). An increase in the apparent size of the lysosomes was also observed, in addition to an increase in the intensity of the immunofluorescence signal. In order to analyse if lysosomal damage was connected with the effects of lysosomal acidification, incubation with two chemicals that have been shown to alkalinise the lysosome (NH_4Cl (Christensen et al., 2002) and chloroquine) was performed. As shown in Figure 3.7.c, pre-incubation with either chemical followed by 6 hours of incubation with NH_2-PS nanoparticles was unable to prevent induction of

replicates. **d.** Projections of spinning-disk confocal microscopy images of 1321N1 cells untreated or treated with 50 µg/ml of NH_2-PS nanoparticles for 6 or 9 hours, stained for CTSL. A minimum of 10 cells was observed for each condition.

CASP3 and CASP7 activities.

In the treated cells, TEM analysis also revealed the presence of multi-lamellar bodies (MLBs) containing nanoparticles (Figure 3.8.a). Membrane-like structures containing nanoparticles, apparently fusing with the membrane of MLBs (Figure 3.8.a arrow), were also occasionally visible, indicating a potential route of entry of the NH_2-PS nanoparticles into the cytoplasm. In general, the cells treated with NH_2-PS nanoparticles were extremely vacuolated and many of these vacuoles seemed to contain cellular debris (Figure 3.8.b).

3.6. Discussion and Conclusions

A greater understanding of the cellular response on encountering nanoparticles is essential if we are to extend their use in the biological arena. One critical aspect in this regard relates to their potential cytotoxicity, and specifically understanding the molecular details of this event. In this study we have applied a combination of biochemical and imaging techniques to begin the process of dissecting the molecular detail of nanoparticle-induced toxicity, and specifically correlate these events with visual changes in the cellular organelles.

The cationic nanoparticles used here were observed to induce cell death in a concentration- and time-dependent manner in a model human brain cell line, 1321N1 astrocytoma cells. These cells were particularly selected for this study because they are derived from the most abundant cell type in the brain and have been linked to cerebral inflammatory and degenerative processes upon contamination with ambient ultrafine nanoparticles (Calderon-Garciduenas et al., 2008). In addition, they are amenable to cell culture, and can be examined by both biochemical and cell

biology methodologies. The nanoparticle concentration used throughout the majority of this study was 50 μg/ml, and was chosen because the different cell populations we observed (viable, early apoptotic and late apoptotic/necrotic) were equally represented at this particle concentration. In stark contrast to the NH_2-PS nanoparticles, neither the unmodified nor the COOH-PS nanoparticles induced cell death in 1321N1 cells, indicating that the effects observed are not due to polystyrene, or to the presence of the nanoparticles *per se*, but are rather a consequence of the charge that the $–NH_2$ surface modification confers.

Recently, efforts to identify the mechanism of cell death induced by nanoparticles have begun to be reported (Frohlich et al., 2009; Xia et al., 2008b). One such study has indicated that necrosis may be involved in the mechanism of toxicity induced by NH_2-PS nanoparticles (Xia et al., 2008b). Consistent with this our flow cytometry analyses indicate that even very soon after initial exposure to the nanoparticles, a fraction of the cells display necrosis-like characteristics. This suggests that for at least part of the cell population the initial stimulus induced by the particles is so strong that the cells cannot cope with it, thus dying in an uncontrolled necrotic manner. Release of necrotic contents from these particular cells may have an apoptotic influence on the surviving cells, although this specific possibility remains to be confirmed. Nevertheless, our data indicate that following exposure to cationic nanoparticles, apoptosis appears to play a significant role in the death of the cells.

In order to identify the pathway of cell death being induced in the cells treated with NH_2-PS nanoparticles, the specific activation of two initiator caspases (CASP8 and CASP9) and of two effector caspases (CASP3 and CASP7) as well as their cleavage, in addition to that of one of their substrates (PARP1) was investigated. Activation of CASP9, CASP3 and CASP7 and PARP1 cleavage occurred after the viable cell population

started to decrease. Complementary chemiluminescence and biochemical methods were necessary to evaluate the effects on these classes of molecules, and it was striking that both approaches were consistent in showing clear activation of the apoptotic molecular machinery between 6 and 9 hours after particle exposure. In these experiments we were unable to detect cleavage of CASP8, together suggesting that intrinsic apoptotic mechanisms play a significant role in the cell death observed in 1321N1 cells after exposure to NH_2-PS nanoparticles. It is also noteworthy to mention that the use of commercially available 'specific' caspase substrates/inhibitors was unable to provide any clear conclusion with respect to which caspases may be involved in the observed apoptosis events (Figure 3.4.b and c). The most likely explanation for this, in accordance with reports from the literature (McStay et al., 2008), is that many of these reagents lack caspase specificity.

The flow cytometry, chemiluminescence and biochemical assays together suggest that apoptotic damage to cells is occurring after addition of cationic nanoparticles. At the subcellular level, apoptosis can be visualised at the mitochondria (Germain et al., 2005; Scorrano et al., 2002), and analysis of TEM images revealed that mitochondrial damage could be observed, in addition to nanoparticles being detected in the lysosomes. Interestingly, apoptosis only seemed to be triggered in response to NH_2-PS nanoparticles, which have a positive ζ-potential (Table AI.I). The values of ζ-potential typically vary with the ionic strength and local pH environment. In the specific case of the nanoparticles used in this study, we observed that *in vitro* the ζ-potential values increased with the decrease in pH (Figure AI.2). By lowering the pH of the solution, unsaturated amines present at the surface of the nanoparticles become protonated, hence displaying a positive charge, which is in tum reflected in the increase in their ζ-potential. In physiologically relevant conditions, as the nanoparticles travel through

endosomal-lysosomal pathways, the pH they encounter varies from relatively neutral values (between 6 and 6.7 for endosomes) to acidic (4.7 for lysosomes) (Casey et al., 2010), and as a consequence their charge increases. Thus, the low pH of the lysosomal environment, where we detected the accumulation of cationic nanoparticles, could enhance their cytotoxic effects. In this regard we also observed lysosomal membranes that appeared to be ruptured, therefore suggesting that lysosomal contents could be being released into the cytoplasm. Fluorescence studies in living and in fixed cells also indicated that lysosomal structures were compromised after exposure to nanoparticles. One interpretation of these observations is that the cytoplasmic release of proteolytic enzymes such as cathepsins may provide the stimulus for activating or enhancing apoptotic pathways from the mitochondria (Chwieralski et al., 2006). Indeed, cells treated for 6 or 9 hours with NH_2-PS nanoparticles displayed a more diffuse CTSL localisation pattern, with some cells lacking any CTSL-positive punctate structures (Figure 3.7.d). Inhibition of the damage to the lysosomes was attempted using chemical treatments (chloroquine and NH_4Cl) to make the lysosomal pH more basic, however no significant difference in CASP3 and CASP7 activities could be observed when compared to the cells not treated with these reagents (Figure 3.7.c). As these chemicals can also induce other cellular behaviours such as autophagy induction, one solution could be to try a more biologically relevant drug such as bafilomycin A, a specific inhibitor of the vacuolar-type H^+-ATPase (Yoshimori et al., 1991).

Similar to that previously reported (Xia et al., 2006), we found that NH_2-PS nanoparticles induced ROS production in 1321N1 cells in a concentration dependent-manner. ROS are well known to induce lysosomal leakage and, in turn, lysosomal proteins can promote the generation of ROS by mitochondria, thereby creating a feedback loop leading to a further increase in lysosomal permeabilisation (Zhao et al., 2003). Consistent with

this, we indeed observed a loss of normal mitochondrial architecture after treatment with nanoparticles, also suggesting a critical role for this organelle in the mechanism of cell death.

In summary, our results indicate that 50 nm NH_2-PS nanoparticles can enter 1321N1 cells and can be routed to lysosomes. There, and in accordance with the proton sponge hypothesis (Nel et al., 2009), the positive charge on the particles leads to the destabilisation of the lysosomal membrane, thereby instigating the release of both nanoparticles and proteolytic enzymes such as cathepsins into the cytoplasm. This in turn results in damage to the mitochondria, activation of CASP9, CASP3 and CASP7, with consequent cleavage of PARP1. The ultimate consequence of these events is that the cell is driven into apoptosis.

CHAPTER 4

USING RNA INTERFERENCE TO DISSECT THE APOPTOSIS PATHWAY INDUCED BY NH_2-PS NANOPARTICLES

A manuscript with the results presented in this chapter is in preparation:
Bexiga, M.G.; Dawson, K.A.; Simpson, J.C. Using RNA interference to identify key proteins involved in apoptosis induced by cationic nanoparticles

With the advent of nanotechnology, new concerns about the safety of use of nanoparticles have risen (Oberdörster et al., 2007). Cationic nanoparticulates, including liposomes and polyplexes, have been shown in the past to be toxic to cells (Aramaki et al., 2001; Iwaoka et al., 2006) and we and others have shown that engineered cationic nanoparticles can interact with mammalian cells and induce apoptosis (Bexiga et al., 2010). However, in depth studies of the molecular and cellular mechanisms underlying these events have been lacking. Previously we have shown, using positively charged NH_2-PS nanoparticles as a model (Table AI.I) (Bexiga et al., 2010), that this process occurs via activation of CASP3, CASP7 and CASP9 (Bexiga et al., 2010). If nanoparticles are to be used for applications where humans will be exposed, the exact molecular and cellular mechanisms of toxicity must be fully understood. This is not only important in terms of nanotoxicology, but also because understanding the pathways of toxicity can lead to the development of new therapies via controlled manipulation of the nanoparticle's properties (Oberdörster et al., 2007).

The complete sequencing of the human genome, its detailed level of annotation (Rual et al., 2004), and the discovery of RNAi and its ability to specifically and rapidly silence individual genes and accordingly downregulate their corresponding proteins in mammalian cells (Fire et al., 1998; Kim and Rossi, 2007; Rana, 2007), have been key events in the study of cellular function. Large-scale RNAi studies have been successfully employed to dissect a variety of cellular pathways, including cell division (Neumann et al., 2010), protein secretion (Simpson et al., 2007), and indeed apoptosis (Aza-Blanc et al., 2003). RNAi is a highly conserved innate mechanism of gene-specific gene silencing, which works via the targeted destruction of individual mRNA molecules by homologous double-stranded siRNA (Fire et al., 1998; Kim and Rossi, 2007). siRNAs can be generated by both chemical synthesis *in vitro* or *in vivo* by transcription through vector-

based expression systems and have proven to be very useful tools in study of gene loss-of-function in mammalian cells (Kim and Rossi, 2007).

Here we use a highly focussed RNAi screen to identify key proteins involved in the cytotoxicity induced by NH_2-PS nanoparticles. We provide evidence that siRNA can be used to study the mechanisms of interaction of nanoparticles with cells. We also confirm that the apoptosome is central to the observed mechanism of toxicity and show that pro-apoptotic proteins BAX, BAK, BID, BIM and PUMA are critical modulators of the process.

4.1. Validation of the RNAi approach – Providing proof-of-concept

4.1.1. Analysis of the knockdown efficiency at the mRNA and protein levels

In order to gain further insight into the molecular pathways involved in the cell death response to nanoparticle interaction, genes involved in both the intrinsic and the extrinsic pathway of apoptosis, namely CASP3, CASP7, CASP8, CASP9, CASP10 and APAF1, were selected. The choice for these targets was primarily made in accordance with the results obtained in Chapter 3, in which it was found that the intrinsic, but not extrinsic, pathway of apoptosis was involved in the cytotoxicity process induced by NH_2-PS nanoparticles. A minimum of two different siRNA sequences were used to target each gene (Table II), and after 48 or 72 hours of transfection the amount of mRNA remaining in the cells was measured by real-time quantitative PCR. As can be seen in Figure 4.1.a, treatment with the various siRNAs led to an effective knockdown of gene expression after both 48 and 72 hours, with the majority of siRNAs reducing levels of their cognate mRNAs to below 30 % of those seen in cells transfected with non-silencing control sequences. In general, knockdown

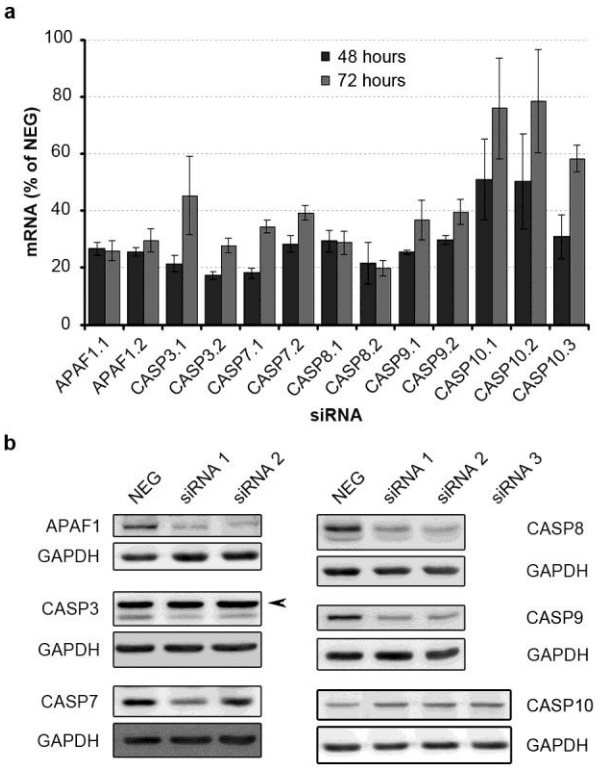

Figure 4.1. *Validation of the efficiency of siRNA-mediated knockdowns.* **a.** mRNA levels were measured by real-time quantitative PCR as described in Chapter 2. Bars indicate relative mRNA levels after 48 or 72 hours in cells treated with different siRNAs, compared to cells treated with non-silencing siRNA (NEG). Results shown represent the mean and standard deviations of four technical replicates and are representative of three independent experiments. **b.** Western blotting showing the efficiency of the siRNA-mediated knockdowns at the protein level 48 hours post-transfection. Results are representative of 3 independent experiments. Arrowhead indicates a cross-reactive protein. GAPDH is used as a loading control.

efficiencies seemed to be better after 48 hours, so this incubation time was chosen for all subsequent experiments. The amount of protein left in the cells 48 hours after transfection was also measured by Western blotting (Figure 4.1.b). As can be observed, siRNA treatment successfully decreased

the amount of protein in the cells and this correlated well with the results obtained for the mRNA measurements. For example in the case of CASP7, the CASP7.1 siRNA produced a stronger knockdown effect compared to CASP7.2 at both the mRNA and protein levels. The only exception for this was CASP10, where the knockdown obtained was poor at both the mRNA and protein levels with all three siRNAs tested. Of these, the CASP10.3 siRNA produced the strongest knockdown effects, and was therefore used in subsequent experiments involving multiple siRNAs.

4.1.2. siRNA transfection confirms involvement of the intrinsic pathway of apoptosis in the cytotoxicity mechanism

Having established the effectiveness of gene expression knockdown by the siRNAs available, their phenotypic effects were investigated. In order to do this, the methods described in the previous chapter were used, specifically measurement of CASP3 and CASP7 activity together with the cleavage of one of their targets, PARP1.

One important aspect to take into account when studying mechanisms of cytotoxicity is whether the reagents being used are cytotoxic by themselves. As described in Appendix II, with the transfection conditions chosen, siRNA transfection *per se* was not toxic to cells. Another aspect to consider is whether the treatment with the siRNAs would somehow change the toxicity observed after incubation with NH_2-PS nanoparticles for 24 hours. This was not the case in the system in use, as there was no significant difference between the non-transfected cells and the cells transfected with the negative control siRNAs (NEG) with respect to the levels of CASP3 and CASP7 activation (Figure 4.2). Therefore, in all subsequent experiments, normalisations were carried out relative to cells treated with NEG siRNA,

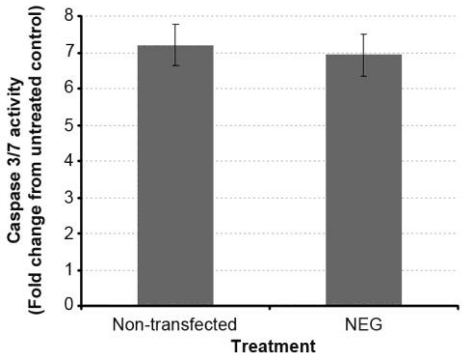

Figure 4.2. *siRNA transfection does not induce changes in CASP3 and CASP7 activities of 1321N1 cells treated with NH_2-PS nanoparticles.* 1321N1 cells were transfected with NEG siRNA or treated with OptiMEM for 48 hours and then exposed to 50 μg/ml of NH_2-PS nanoparticles for a further 24 hours followed by CASP3 and CASP7 activities measurement. Results were normalised to the untreated and non-transfected control. Results represent the mean and standard error of the mean of 3 independent experiments, each with 3 replicates.

as this is a more robust negative control than the untreated cells since it also takes into account the effects of the siRNA transfection process.

Consistent with the results presented in the previous chapter (Bexiga et al., 2010), when 1321N1 cells were transfected with siRNAs against CASP3, CASP7, CASP9 and APAF1, the CASP3 and CASP7 activities were significantly reduced compared to NEG siRNA-treated cells (Figure 4.3). This activity also correlated with the amount of knockdown observed in Figures 4.1.a and b. By contrast, when cells were transfected with siRNAs targeting CASP8 and CASP10, with the exception of one of the siRNAs targeting CASP10 (CASP10.2), there was no significant difference in CASP3 and CASP7 activities compared to the control (Figure 4.3). Interestingly, analysis of the mRNA levels after 48 hours of transfection revealed that this siRNA was not the most effective targeting CASP10, but was instead CASP10.3 (Figure 4.1.a). It was also observed that in cells not

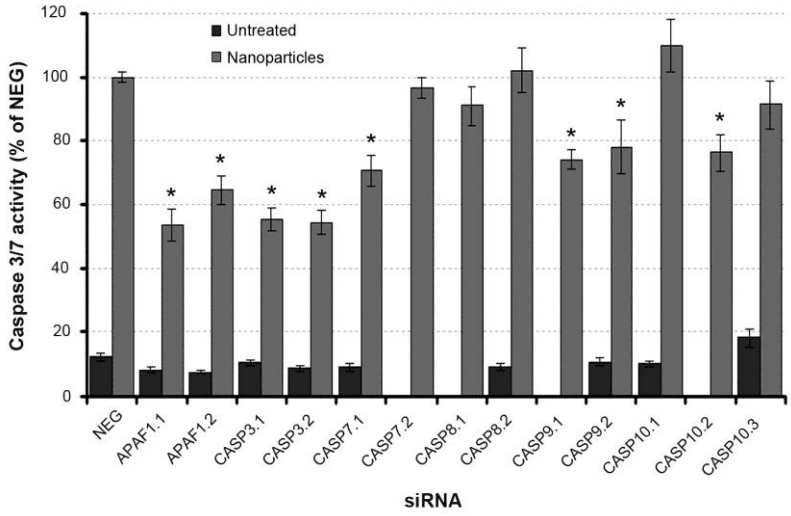

Figure 4.3. *Transfection of siRNAs against members of the two apoptotic pathways.* CASP3 and CASP7 activities in 1321N1 cells treated for 48 hours with different siRNAs targeting genes involved in the intrinsic or extrinsic pathways of apoptosis, followed by 24 hours of incubation with 50 μg/ml NH_2-PS nanoparticles or medium alone (untreated). Shown is the percentage of CASP3 and CASP7 activities compared to cells transfected with NEG siRNA and treated with NH_2-PS nanoparticles. Results represent the mean and standard error of the mean from three independent experiments each with three replicates. * indicates p-value < 0.001

treated with nanoparticles, but transfected with the siRNAs targeting the different genes alone, no significant change in the caspase activity when compared to the untreated NEG control was observed (Figure 4.3).

Since many of the caspases work together in supramolecular complexes we next assessed their relevance to nanoparticle-induced apoptosis events by combining the downregulation of multiple genes operating in the same pathway. For these experiments, the siRNAs that gave the best knockdown results at the mRNA and protein level were used (Figure 4.1.a), specifically CASP3.2, CASP7.1, CASP8.2, CASP9.1, CASP10.3

and APAF1.1. As expected, since it was the activities of CASP3 and CASP7 that were being detected, when these two genes were downregulated together, the CASP3 and CASP7 activities that were detected were significantly reduced when compared to NEG-treated cells (Figure 4.4.a).

Not only do these results serve as a control to confirm that the approach is valid, they also highlight the fact that phenotypes can be much more striking when multiple components of a network or interaction complex can be targeted. We therefore next assessed the effect of combining the siRNAs against CASP8 and CASP10 or CASP9 and APAF1 (initiators of the extrinsic and intrinsic pathways of apoptosis, respectively). In strong agreement with the results presented in the previous chapter (Bexiga et al., 2010), prevention of apoptosome formation by downregulation of CASP9 and APAF1, significantly reduced the CASP3 and CASP7 activities to 30 % of those seen in NEG control cells. By contrast, the combination of siRNAs against CASP8 and CASP10 did not result in any detectable decrease in CASP3 and CASP7 activities (Figure 4.4.a). Similar results were observed when we investigated the cleavage of PARP1. Knockdown of CASP9 and APAF1 completely abrogated the cleavage of PARP1 during the period of time studied, whereas no difference was detected between the NEG siRNA transfected cells and those treated with the combination of CASP8 and CASP10 siRNAs (Figure 4.4.b). These results confirmed the validity of the experimental approach, indicating that it could be used to study in greater depth the cellular and molecular processes occurring in cells upon exposure to nanoparticles, and in particular in 1321N1 cells exposed to the NH_2-PS nanoparticles. To that end therefore, the involvement of other regulatory proteins in the process of cytotoxicity observed was investigated, specifically pro-apoptotic members of the BCL-2 family of proteins.

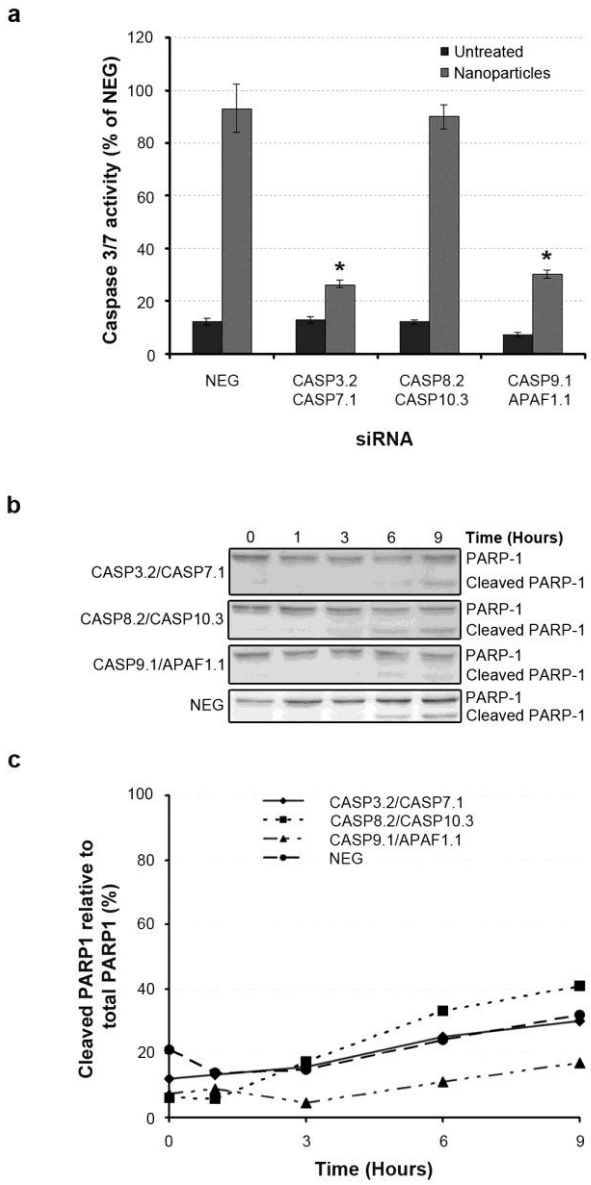

Figure 4.4. *Impairment of apoptosome formation leads to a decrease in apoptosis markers.* **a.** CASP3 and CASP7 activities in cells transfected for 48 hours with siRNAs targeting two different molecules in the same apoptotic pathway, followed by 24 hours of incubation with 50 μg/ml of NH_2-PS nanoparticles or treated with complete DMEM (untreated). Results are shown as the percentage of the caspase activity compared to cells treated with NEG siRNA. Results represent the mean

4.2. Involvement of members of the BCL-2 family of proteins in the cytotoxicity mechanism elicited by NH_2-PS nanoparticles

The BCL-2 family of proteins is essential for many different apoptotic events, such as those involved in development, tissue turnover and host defence against pathogens (Youle and Strasser, 2008). In mammals, there are at least 12 BCL-2 members organised into three classes. One class inhibits apoptosis, whereas a second class promotes apoptosis, despite both classes being BCL-2 homologues. A third divergent class termed 'BH3-only' proteins, has a conserved BH3 domain that can bind to and regulate the anti-apoptotic BCL-2 proteins to promote apoptosis (Youle and Strasser, 2008).

In this study all of the pro-apoptotic BCL-2 homologues (BAX, BAK, BOK and BID) as well as two of the BH3-only proteins (BCL2L11/BIM and BBC3/PUMA) were targeted. BAX and BAK are crucial to the induction of the permeabilisation of the outer membrane of the mitochondria, thereby releasing into the cytoplasm apoptogenic molecules, including cytochrome c (Chipuk and Green, 2008; Degterev et al., 2001). BID, in contrast, after being proteolytically activated, for example by CASP8 or cathepsins, interacts with BAX inducing cytochrome c release from the mitochondria with consequent activation of downstream CASP3 and CASP7 (Luo et al., 1998). The mechanism by which BAX and BAK become activated is still only poorly understood, although there are two current models under consideration. In one model, the anti-apoptotic members of the BCL-2

and standard error of the mean from three independent experiments each with three replicates. * indicates p-value < 0.001. b. 1321N1 cells were treated as for a. and 30 μg of protein were then subjected to Western blotting to detect PARP1 cleavage. **c.** Quantification of the percentage of cleaved PARP1 over the total PARP1 protein was determined by densitometry.

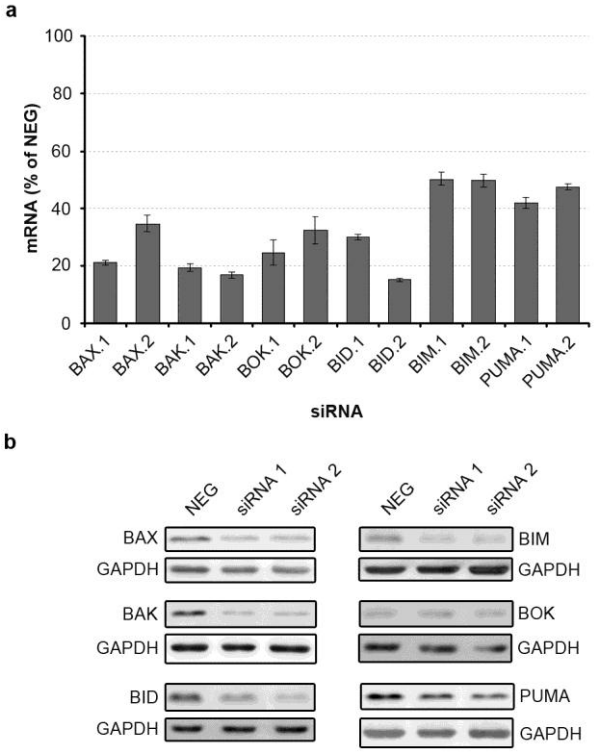

Figure 4.5. *Validation of siRNA knockdown efficiency of BCL-2 family members.* **a.** mRNA levels were measured by real-time quantitative PCR as described in Chapter 2. Bars indicate relative mRNA levels after 48 hours in cells treated with different siRNAs, compared to cells treated with non-silencing siRNA (NEG). Results shown represent the mean and standard deviations of four technical replicates and are representative of three independent experiments. **b.** Western blotting shows the efficiency of the siRNA knockdown at the protein level 48 hours post-transfection. Results are representative of 3 independent experiments. GAPDH is used as a loading control.

family are inhibited by direct binding of other pro-apoptotic proteins (Chipuk and Green, 2008; Galonek and Hardwick, 2006), whereas in a second model, the direct activation of BAX and BAK by certain BH3-only proteins such as BIM, truncated BID and PUMA occurs (Ren et al., 2010).

4.2.1. Validation of the siRNA knockdown

Similar to the previous experiments, we first determined the efficacy of the various siRNAs used. As shown in section 4.1.1., this was carried out by looking at the percentage of mRNA left in the cells following siRNA transfection, in addition to determining the remaining protein levels.

Transfection of 1321N1 cells with siRNAs against the pro-apoptotic BCL-2 homologues BAX, BAK, BOK and BID resulted in efficient mRNA downregulation, and in the cases of BAX, BAK and BID at least one of the siRNAs used (BAX.1, BAK.1, BAK.2 and BID.2) resulted in a downregulation of more than 80 % of the respective mRNA (Figure 4.5.a). For the two BH3-only proteins used in this study, BIM and PUMA, the efficiencies of knockdown were lower than for the previous genes analysed, resulting in a downregulation of only 50-60 % at the mRNA level (Figure 4.5.a). These results also correlated well with the protein levels found in the cells after treatment with the various siRNAs (Figure 4.5.b).

4.2.2. Depletion of members of the BCL-2 family of proteins leads to a decrease in caspases 3 and 7 activation

To evaluate how the cells reacted to the depletion of the selected proteins of the BCL-2 family upon treatment with NH_2-PS nanoparticles, CASP3 and CASP7 activities were again used as a read-out. As shown in Figure 4.6, only the siRNAs BOK.2, BID.1 and BIM.2 failed to lead to a significant decrease in the activity of the caspases. It was interesting to note that in the case of BID, this effect correlated very well with the results obtained both at the mRNA and the protein levels (Figure 4.5.a and b, respectively), where BID.1 siRNA treatment led to reduced downregulation compared to BID.2 siRNA treatment. It was also observed that downregulation of the various BCL-2 family members had no significant

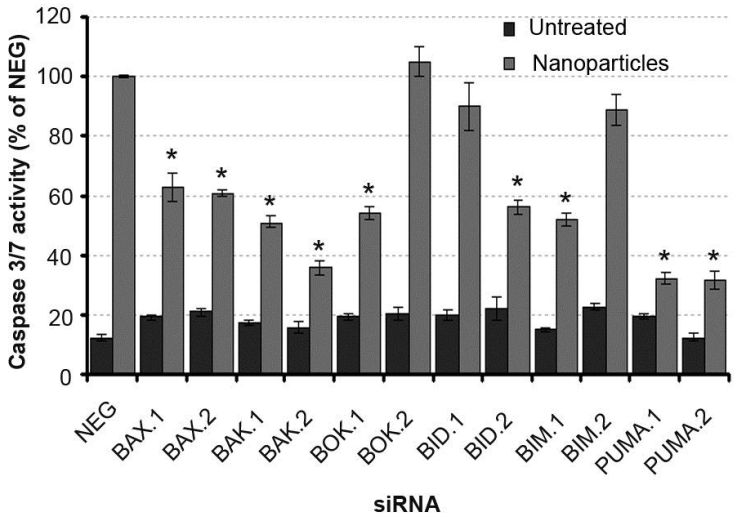

Figure 4.6. *Single knockdown of pro-apoptotic members of the BCL-2 family of proteins results in downregulation of CASP3 and CASP7 activities.* CASP3 and CASP7 activities in 1321N1 cells treated for 48 hours with different siRNAs followed by 24 hours of incubation with NH_2-PS nanoparticles or medium alone is shown as percentage of the activity of cells treated with NEG siRNA. Results represent the mean and standard error of the mean from three independent experiments each with three replicates. * indicates p-value < 0.001.

effect of CASP3 and CASP7 activities in the absence of nanoparticles (Figure 4.6), providing another indication that the transfection itself was not influencing the results obtained.

4.2.3. BAX and BAK are key regulators of the apoptotic process observed

Due to the known role of BAX and BAK in the permeabilisation of the mitochondrial outer membrane, and the consequent release of apoptogenic molecules (Chipuk and Green, 2008; Soriano and Scorrano, 2010), it was investigated whether combined knockdown of these two

genes (BAX and BAK), and of their proposed activators (BID and BID, BIM and PUMA) would lead to a decrease in the CASP3 and CASP7 activities.

Combined downregulation of BAX and BAK led to a significant decrease in the activities of CASP3 and CASP7 (Figure 4.7.a), reducing their activation by greater than 75 % compared to NEG transfected cells in the presence of nanoparticles. The double knockdown of BAX and BID, and the triple knockdown of BID, BIM and PUMA, also led to a significant decrease in the activation of the two caspases, with the strongest effect of all seen in the triple knockdown. In this experiment, similar levels of CASP3 and CASP7 activation to those seen in the transfected cells not treated with NH_2-PS nanoparticles were observed (Figure 4.7.a). A similar scenario was observed when we analysed the cleavage of PARP1. When either BAX and BAK, or BID, BIM and PUMA were downregulated together, there was a decrease in the amount of cleaved PARP1 to less than half of that observed in cells treated with NEG siRNA (Figure 4.7.b and c). Combined knockdown of BAX and BID also led to a decrease in the amount of cleaved PARP1 detected, but to a lesser extent than the other combined knockdowns carried out (Figure 4.7 b and c).

PUMA is one of the most potent pro-apoptotic members of the 'BH3-only' class of proteins (Yu and Zhang, 2008), and unlike most of the other pro-apoptotic proteins its activation is regulated at the transcriptional level rather than post-translationally. Expression of PUMA is transactivated by several transcription factors, such as p53 or CHOP, in response to various apoptosis-inducing stimuli including genotoxic (Nakano and Vousden, 2001) and ER stress (Li et al., 2006). PUMA has been suggested to either directly (Gallenne et al., 2009) or indirectly (Jabbour et al., 2009) activate BAX thereby promoting MOMP and apoptosome dependent apoptosis. For this reason, the role of PUMA becomes more relevant when

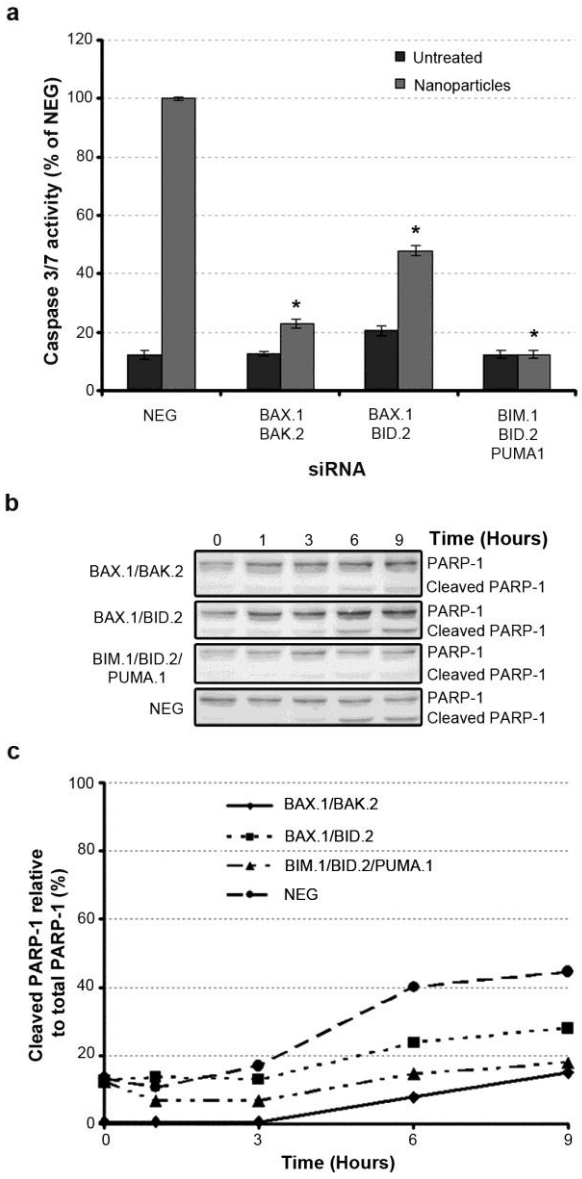

Figure 4.7. *Knockdown of BAX and BAK and their proposed activators leads to a reduction in apoptosis markers.* a. CASP3 and CASP7 activities in cells transfected for 48 hours with siRNAs targeting mRNAs coding for proteins involved in BAX- and BAK-mediated permeabilisation of the outer mitochondrial membrane, followed by 24 hours of incubation with 50 μg/ml of NH_2-PS nanoparticles or treated with DMEM (untreated) is shown as the percentage of the activity in cells

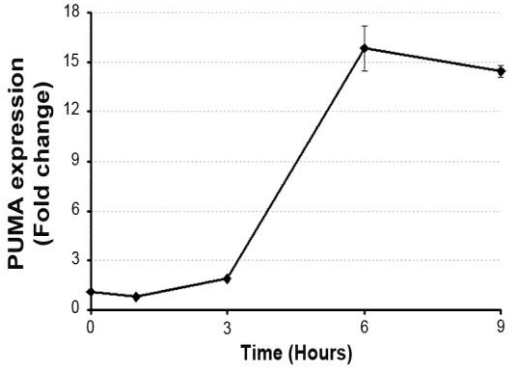

Figure 4.8. *Treatment of 1321N1 cells with NH_2-PS nanoparticles induces PUMA expression.* Expression of PUMA after exposure for different amounts of time to NH_2-PS nanoparticles measured by real-time quantitative PCR. Normalisation was performed against the untreated control at each time point. Results are representative of three independent experiments and show the mean and standard deviations of 4 technical replicates.

investigating its expression in 1321N1 cells following increasing duration of exposure to NH_2-PS nanoparticles. As shown in Figure 4.8, gene expression analysis revealed a doubling of PUMA expression after 3 hours of exposure to the nanoparticles, and after 6 hours it had increased 15-fold, maintaining this level of expression up to 9 hours of incubation with nanoparticles.

4.3. Effects on the mitochondria

Early during apoptosis, mitochondria undergo co-ordinated fragmentation and cristae remodelling to facilitate cytochrome c release

treated with NEG siRNA. Results represent the mean and standard error of the mean from three independent experiments each with three replicates. * indicates p-value < 0.001. **b.** 1321N1 cells were treated as for a. and 30 μg of protein were then subjected to Western blotting to detect PARP1 cleavage. **c.** Quantification of the percentage of cleaved PARP1 compared to the total PARP1 protein was assessed by densitometry.

from the mitochondria into the cytosol (Frank et al., 2001; Scorrano et al., 2002). This process results in the presence of numerous spherical mitochondria and is, at least in part, mediated by proteins of the BCL-2 family of proteins, namely BAX and BAK which interact with proteins involved in the maintenance of mitochondrial morphology, such as MFN and DRP1 (Frank et al., 2001; Soriano and Scorrano, 2010).

In Chapter 3, ultrastructural studies revealed that mitochondrial morphology was affected, and a loss of cristae occurred following exposure of cells to NH_2-PS nanoparticles. Due to the relevance of BAX and BAK in the apoptotic process induced by the NH_2-PS nanoparticles in 1321N1 cells, it was important to analyse whether these molecules may also play a role in altering mitochondrial structure and consequently release of cytochrome c from the IMS to the cytoplasm of the cell. In order to test this, siRNA-transfected cells treated or untreated with NH_2-PS nanoparticles for different amounts of time were stained for cytochrome c and for MnSOD, as a marker for mitochondria (Weisiger and Fridovich, 1973a, b), followed by visualisation using confocal microscopy. Surprisingly, in NEG-treated cells, despite the mitochondria being highly fragmented, the cytochrome c was retained in the mitochondria (Figure 4.9). In the BAX and BAK double-knockdown cells, no difference could be observed when comparing with the NEG-treated cells (Figure 4.9). In staurosporine-treated cells, mitochondrial fragmentation was observed as early as 1 hour and 30 minutes, but also without apparent cytochrome c release into the cytosol. Images at longer time points were not acquired, as the general cellular morphology had changed dramatically by this time, preventing clear visualisation of the cytoplasm and the organelles within. This may be one explanation why cytosolic cytochrome c was not observed in the cells.

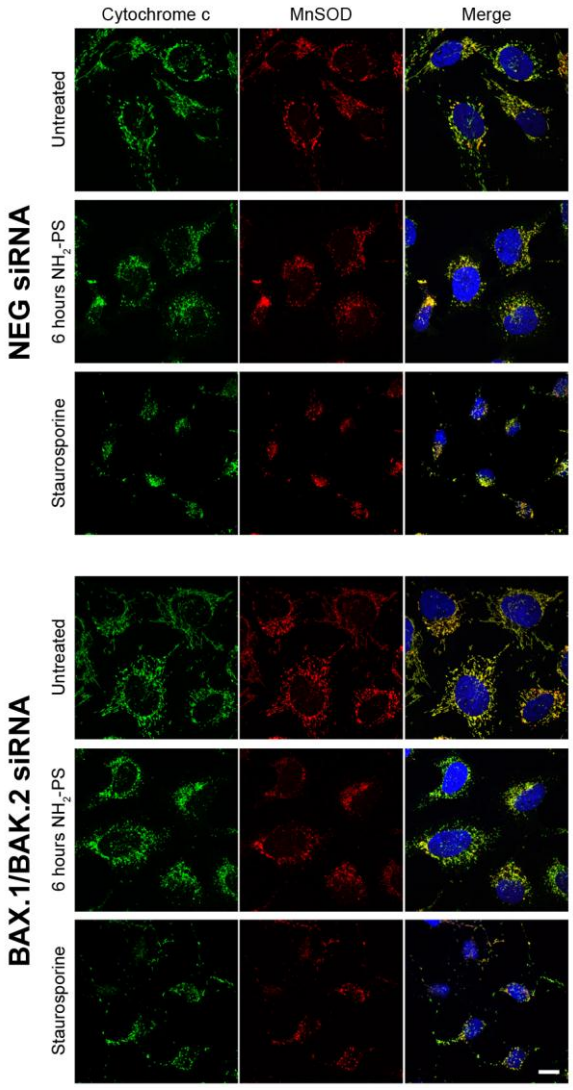

Figure 4.9. *NH_2-PS nanoparticles induce mitochondrial fragmentation independent of BAX and BAK.* 1321N1 cells were transfected for 48 hours with NEG or BAX.1/BAK.2 siRNAs and then treated with either 50 μg/ml of NH_2-PS nanoparticles for 6 hours or with 1 μM staurosporine for 90 minutes. Cells were then stained for cytochrome c (green) and MnSOD (red) and confocal images were acquired as described in Chapter 2. In both cases, mitochondria are fragmented and cytochrome c release to the cytosol could not be observed. Scale bar corresponds to 10 μm.

4.4. Discussion and Conclusions

Nanotechnology, as we understand it today, is still a relatively new field that gained impulse with the discovery of fullerenes in 1985 (Kroto et al., 1985), and a few years later with the discovery (Iijima, 1991) and synthesis of carbon nanotubes (Ebbesen and Ajayan, 1992). As a result of the field still being in its infancy, there is still much to be understood, particularly if nanoparticles are to be used in humans. This is why it is of paramount importance to comprehend how nanoparticles interact with living systems, and in particular with cells, both at the molecular and cellular level.

RNAi has been shown to be a very powerful tool to study different cellular events such as secretion (Simpson et al., 2007) and apoptosis (Aza-Blanc et al., 2003), however this approach has never been applied within the remit of understanding the cellular and molecular pathways of the interactions between nanoparticles and cells. By contrast, the potential use of nanoparticles as delivery agents for siRNAs to cells has been explored (Yuan et al., 2011). Combined with the data acquired in Chapter 3 (Bexiga et al., 2010), RNAi was therefore selected as an appropriate technology by which these interactions could be studied.

The use of RNAi technology in the cellular system under study, specifically where NH_2-PS nanoparticles caused damage to mitochondria with consequent activation of CASP3, CASP7 and CASP9 (Bexiga et al., 2010), was initially optimised. The first obvious targets were the initiators of both the extrinsic (CASP8 and CASP10) and intrinsic (CASP9 and APAF1) pathways of apoptosis and also, as a control, a common link between the two pathways, the effector caspases CASP3 and CASP7 (Boatright and Salvesen, 2003).

Two siRNAs were used against each target, in order to increase the chances of having at least one of the sequences effectively downregulating the expression of its target. The first step was to establish whether the siRNAs chosen were effective at downregulating the expression of the genes they were targeting. In order to asses this, two complementary techniques were used: (i) the amount of mRNA remaining in the cells was measured by real-time quantitative PCR and (ii) the amount of protein remaining after transfection was analysed by Western blotting. Whenever possible, the two approaches were used in parallel; in particular when long lived proteins were studied, as strong reductions at the mRNA level do not necessarily correspond to a similar effect at the protein level.

In the experiments presented in this chapter, both techniques were shown to have comparable efficiencies in detecting the effects of the siRNA on gene expression (Figure 4.1.a and b). Furthermore, in the cases of APAF1, CASP3, CASP7, CASP8 and CASP9, the efficiencies of knockdown were higher than 70 % and in some cases (CASP3.2 and CASP7.1) were higher than 80 % (Figure 4.1.a).

Another critical step in the optimisation of the transfection conditions was to determine the length of transfection time, with this depending on many different factors such as mRNA turnover and cell division (Dykxhoorn et al., 2003). Incubations of 48 or 72 hours with the siRNAs targeting the genes involved in the intrinsic and extrinsic pathway of apoptosis were tested, and it was found that 72 hours of incubation did not produce any advantage over 48 hours of incubation, and indeed the amount of mRNA remaining was not further reduced at these longer incubation times, but rather had begun to increase (Figure 4.1.a). Therefore, throughout the rest of the work, 48 hours was used as the optimal incubation time to have robust transfection efficiency and gene downregulation. In order to assess the phenotypic effects of the

downregulation of the proteins involved both in the extrinsic and intrinsic pathways, the activation of CASP3 and CASP7, which are common to both pathways, was first investigated. Cleavage of PARP1, a target of these two caspases, was also analysed. These are two classical markers of apoptosis and were used efficiently in Chapter 3 to identify the occurrence of apoptosis (Bexiga et al., 2010).

To analyse whether siRNA transfection prevented the induction of apoptosis in 1321N1 cells exposed for 24 hours to NH_2-PS nanoparticles, single or double transfections were performed. The reduction observed in the CASP3 and CASP7 activities when only one siRNA was transfected was lower than when two siRNAs were transfected together (Figure 4.3), and in the best cases, it was reduced to approximately 50 % of that seen in the NEG-treated cells. It was also observed that none of the siRNAs targeting CASP8 was effective in reducing the activities of CASP3 and CASP7, thereby indicating that the extrinsic pathway was not being invoked in these cells. When targeting either the intrinsic or extrinsic pathways of apoptosis by siRNA-mediated double-knockdowns of CASP9 and APAF1 or CASP8 and CASP10, respectively, followed by NH_2-PS nanoparticle treatment there was a striking cumulative effect resulting in only 30 % of CASP3 and CASP7 activities remaining when the intrinsic pathway of apoptosis was hindered (Figure 4.4.a). As expected, a similar effect (35 % of CASP3 and CASP7 activity) was also observed when CASP3 and CASP7 were downregulated together. By contrast, no significant difference in CASP3 and CASP7 activities was observed when CASP8 and CASP10, which target the extrinsic pathway of apoptosis, were downregulated together (Figure 4.4.a). A similar effect was observed at the level of PARP1 cleavage, whereby depletion of APAF1 and CASP9 led to an almost complete absence of PARP1 cleavage, but depletion of CASP8 and CASP10 together did not (Figures 4.4.b and c). These results strongly imply that the apoptosome

formed by CASP9, APAF1 and cytochrome c (Riedl and Salvesen, 2007) is central to the pathway of apoptosis induced by NH_2-PS nanoparticles. Together with the results shown in the previous chapter (Bexiga et al., 2010), these data now provide proof of principle for the application of RNAi in the study of nanoparticles, and in particular one consequence of when NH_2-PS nanoparticles interact with cells.

In order to extend our understanding of the molecular pathways of apoptosis that were being elicited by the NH_2-PS nanoparticles, the involvement of members of the BCL-2 family of proteins was next assessed. This family of proteins, grouped according to the different homology domains of the BCL-2 protein, contains both anti- and pro-apoptotic members that modulate the apoptotic response (Youle and Strasser, 2008). Only pro-apoptotic proteins were chosen as targets: four BCL-2 homologues (BAX, BAK, BOK and BID) and two proteins belonging to the 'BH3-only' protein class (BIM and PUMA).

A similar RNAi approach to that established previously was used to investigate the effect of siRNA transfection on 1321N1 cells treated with NH_2-PS nanoparticles. Again, the knockdown efficiencies were good for all the BCL-2 homologues (BAX, BAK, BOK and BID), with at least one of the siRNAs directed against each target causing a reduction in the levels of cognate mRNA of 80 % or greater (Figure 4.5.a). These results again correlated well with the protein levels detected in the cells 48 hours after transfection. For the two 'BH3-only' proteins studied (BIM and PUMA), the efficiency of knockdown was comparatively not as high, with only a 50-60 % decrease in expression observed (Figure 4.5.a).

One interesting observation was that the level of mRNA depletion in the cells for each of the targets did not necessarily correlate with the phenotypic effects observed. The siRNAs targeting BIM and PUMA that had resulted in only modest decreases in the mRNA levels, resulted in strong

phenotypes in terms of inhibition of CASP3 and CASP7 activities (Figure 4.6). By contrast, the BCL-2 homologues that were downregulated to a higher degree, did not present such a striking effect. This might be indicative that for some proteins, even small changes in their expression levels might lead to strong phenotypic effects.

BAX and BAK, two of the pro-apoptotic BCL-2 homologues that were studied, once activated, are responsible for the formation of pores in the mitochondrial outer membrane. This in turn can cause the release into the cytoplasm of apoptogenic molecules, such as cytochrome c and SMAC/DIABLO (Boatright and Salvesen, 2003; Youle and Strasser, 2008). Inactive BAX is normally found in the cytosol, but upon its activation is recruited to the mitochondrial outer membrane where it oligomerises with BAK, with consequent formation of pores (Leber et al., 2007). The mechanism of activation of BAX and BAK is still under debate. Two models have been proposed: one postulates direct activation of BAX and BAK by 'BH3-only' proteins, such as tBID or BIM, and another model proposes that BAX and BAK activation occurs by default through inactivation of all the anti-apoptotic members of the BCL-2 family as a result of being neutralised by the 'BH3-only' members (Galonek and Hardwick, 2006; Youle and Strasser, 2008). Recently another study has indicated that the concerted action of BIM, BID and PUMA is necessary for activation of the BAX- and BAK-dependent cell death programme (Ren et al., 2010).

Taking all this information into account, double or triple knockdowns of BAX and BAK and their proposed activators were performed to determine whether apoptosis could be prevented. When BAX and BAK were downregulated simultaneously, a significant reduction in CASP3 and CASP7 activities, together with the cleavage of PARP1 to half of that observed in the NEG-treated cells, was observed. This is a strong indication that BAX and BAK are involved in the modulation of the

signalling pathway involved in the apoptotic process induced by NH_2-PS nanoparticles. To further understand the regulation of BAX and BAK in this system, double knockdowns of BAX and BID, and triple knockdowns of BIM, BID and PUMA, were performed. Both CASP3 and CASP7 activities and PARP1 cleavage were reduced compared to NEG-treated cells (Figure 4.7.a and 4.7.b and c, respectively), but the most striking effect was obtained when BIM, BID and PUMA were silenced together. In fact, the CASP3 and CASP7 activation was reduced to levels similar to the untreated (no nanoparticles) NEG cells, and PARP1 cleavage was similar to that seen in the BAX and BAK double knockdown (Figure 4.7). This strongly points towards the involvement of these three proteins in the regulation of the activation of BAX and BAK, thereby preventing the formation of pores in the mitochondrial outer membrane and consequential release of pro-apoptotic proteins.

The release of cytochrome c from the mitochondria into the cytosol was analysed by immunofluorescence and confocal microscopy. These experiments indicated, at least during the period of time studied, that no release of cytochrome c occurred either in the NEG-treated or the BAX/BAK knockdown cells (Figure 4.9). By contrast, we observed extensive mitochondrial fragmentation, and surprisingly this could not be prevented by depleting BAX and BAK (Figure 4.9). Mitochondrial fragmentation occurs early during apoptosis, preceding cytochrome c release, and is at least in part modulated by BAX and BAK via interaction with fission and fusion machinery (Karbowski et al., 2006). The fact that mitochondrial fragmentation was not prevented in the double knockdown cells, might be indicative that in the system under study, their main function is not at the level of the regulation of mitochondrial morphology, but at a different level such as that of cytochrome c release from the mitochondria. Although cytochrome c release was not detected in either the NEG-treated cells or

the BAX and BAK double knockdown, our observation that CASP3 and CASP7 activities were inhibited following CASP9 and APAF1 downregulation, nevertheless suggests that cytochrome c is still released to the cytosol thereby allowing the apoptosome to form. The inability to observe this release, despite our use of antibodies to assess the localisation of endogenous cytochrome c, may simply reflect that only small amounts of this molecule are needed to invoke apoptosome formation. In addition, cells were only monitored for up to 6 hours, a time that may be insufficient to cause appreciable accumulation of cytochrome c in the cytoplasm. Two experiments could be suggested at this point to decipher the enigma of BAX and BAK regulation of the apoptotic response. Firstly, a longer kinetics of cytochrome c sub-cellular distribution should be attempted to confirm that it indeed occurs, and secondly, the relevance of mitochondrial fragmentation in the system should be assessed. One of the ways to do this, and following the rational of this work, would be to knockdown members of the fission and fusion machinery, such as MFN and DRP1, and analyse the effect on apoptosis.

Analysis of PUMA expression in 1321N1 cells treated with NH_2-PS nanoparticles (Figure 4.8) makes these results even more interesting as recently, Gallenne and colleagues have reported that PUMA can act as a potential activator of BAX and BAK through direct interaction with BAX (Gallenne et al., 2009). This interaction is prevented by the presence of anti-apoptotic members of the BCL-2 family of proteins. Therefore, these results strengthen the hypothesis that the apoptotic response observed occurs through the formation of the apoptosome, and is modulated by BAX and BAK activation regulated by BIM, BID and PUMA.

In conclusion, we have described a system where RNAi has been used to study the interactions of NH_2-PS nanoparticles with 1321N1 cells, and it is expected that this approach can be extended to a more detailed

study of the interactions of nanoparticles with cells. Moreover, this work has confirmed and extended the results described in the previous chapter, by showing that the formation of the apoptosome by CASP9 and APAF1 is central to the mechanism of apoptosis observed. This activation seems to be modulated by BAX and BAK, which are in turn regulated by BIM, BID and PUMA.

CHAPTER 5

UNDERSTANDING THE CYTOTOXICITY INDUCED BY NH_2-PS NANOPARTICLES AT THE CELLULAR LEVEL

The mechanisms of cytotoxicity induced by NH_2-PS nanoparticles in 1321N1 cells have been described in Chapters 3 and 4, and provide the first hints of which molecular mechanisms are being elicited in cells. Here in this chapter, a number of these processes are investigated in greater detail.

In Chapter 3, the involvement of autophagy in the process of nanoparticle-induced cell death was suggested following analysis of TEM images. These studies revealed that many cells exhibited a high degree of vacuolation, and many of them contained cellular debris. Autophagy is an adaptive response to sub-lethal stress, such as nutrient deprivation, and is a mechanism by which cells recycle damaged, redundant or non-essential organelles or macromolecules supplying the metabolites necessary for the cell, thereby contributing to cell survival (Hotchkiss et al., 2009). Autophagy also has a role in other processes such as the removal of misfolded proteins and elimination of intracellular microorganisms (Shintani and Klionsky, 2004). The role of autophagy in cell death is controversial, without a consensus on whether autophagy is the executioner of cell death or if it is a consequence of the cell no longer being able to compensate for the loss of vital components, a process referred to as autophagy-associated cell death (Kroemer and Levine, 2008). In fact, deletion of key autophagy proteins has been shown to potentiate cell death, pointing to a survival role of autophagy rather than a pro-death role (Boya et al., 2005; Kuma et al., 2004).

It has also been described previously that the lysosomes of NH_2-PS nanoparticle-treated cells become damaged and release their contents to the cytoplasm (Bexiga et al., 2010). Lysosomes, which account for up to 5 % of the total cellular volume, are dynamic organelles that receive and degrade macromolecules coming from the secretory, endocytic, autophagic and phagocytic membrane-trafficking pathways (Luzio et al., 2007). Because of their relevance to cellular homeostasis, one possibility is that the rupture

of lysosomes inhibits normal secretory activity, thereby inducing accumulation of newly synthesised proteins in the ER with promotion of ER stress.

When the conditions for the proper protein folding in the ER are impaired, there is an accumulation and aggregation of unfolded proteins in the lumen of the organelle, a process that is termed ER stress. To resolve this situation, the cell has evolved different cellular responses collectively called UPR (Szegezdi et al., 2006). UPR is a protective cellular mechanism through which the cell tries to reduce the accumulation of unfolded proteins and restore normal ER function. If however the stress is not resolved, the signalling switches from pro-survival to pro-apoptotic (Fribley et al., 2009).

Here, the induction and relevance of both autophagy and ER stress to the mechanism of cell death induced by the NH_2-PS nanoparticles were studied. To this end, an ensemble of molecular biology and biochemistry techniques were used.

5.1. Role of autophagy in cell death induced by NH_2-PS nanoparticles

5.1.1. NH_2-PS nanoparticles induce LC3 cleavage and autophagosome formation

The involvement of autophagy in the cell death mechanism induced by NH_2-PS nanoparticles in 1321N1 cells was first suggested by TEM, where it could be seen that the cells were highly vacuolated with some of the vacuoles presenting cellular debris inside (Figures 3.8 and 5.1) – a morphological hallmark of autophagy (Klionsky et al., 2008). In some of the vacuoles, it was also possible to visualise nanoparticles inside (Figure 5.1.b arrow).

To confirm that these vacuoles were indeed caused by autophagy, the cleavage of LC3 was analysed. LC3 is a cytosolic protein that upon

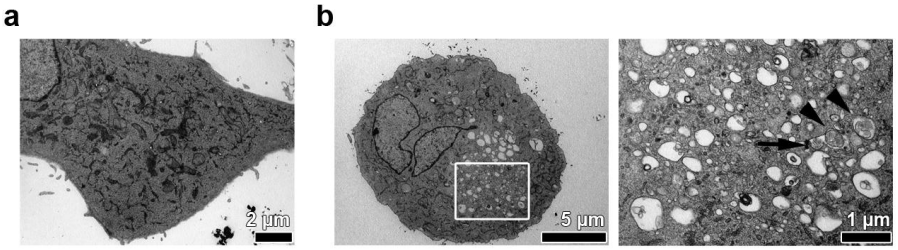

Figure 5.1. *NH_2-PS nanoparticles induce high levels of vacuolation in 1321N1 cells.* TEM images of 1321N1 cells either **a.** untreated or **b.** treated for 6 hours with 50 µg/ml of 50 nm NH_2-PS nanoparticles. **b.** A great increase in the levels of cytoplasmic vacuolation is observed. The image on the right is a magnification of the area surrounded by a white rectangle on the image on the left. In some of the vacuoles cellular debris can be observed (arrowheads), as well as nanoparticles (arrow).

induction of autophagy is cleaved into LC3-II and inserts in the phagophore membrane in a process denominated lipidation (Kabeya et al., 2000). Protein extracts obtained from 1321N1 cells incubated with NH_2-PS nanoparticles for increasing amounts of time were analysed for the presence of LC3-II by Western blotting (Figure 5.2). The relative proportion of LC3-II in the cells increased with the time of exposure of the cells to nanoparticles. This increase was of 60 %, from 20 % in untreated cells to 83 % in cells treated for 9 hours with NH_2-PS nanoparticles (Figure 5.2.b), indicating that autophagy was being induced in the system.

5.1.2. Using RNAi to understand the relevance of autophagy to the cytotoxicity mechanism

Having established the induction of autophagy in the system, it was pertinent to determine whether the blocking of autophagy could prevent cell death, and so an RNAi approach was again used. The core machinery

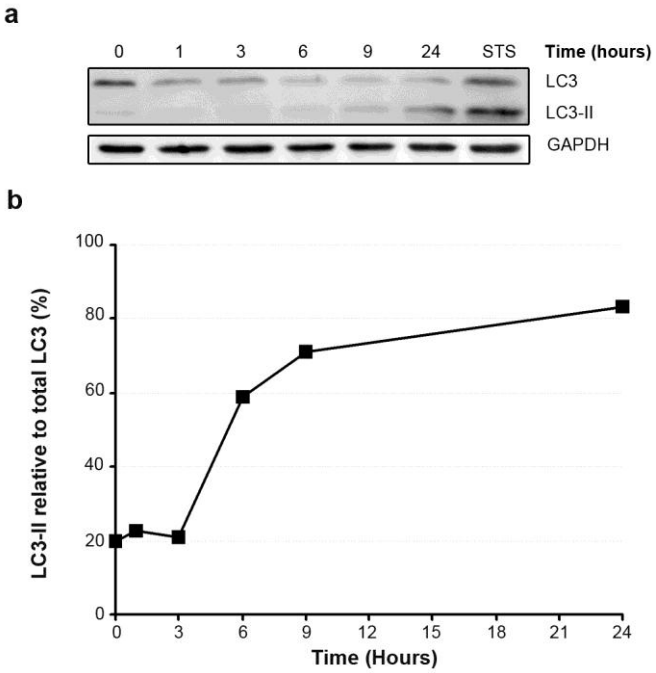

Figure 5.2. *NH_2-PS nanoparticles induce LC3 cleavage.* a. Western blotting showing the presence of full length LC3 and cleaved LC3-II in cell extracts of 1321N1 cells treated for increasing lengths of time with NH_2-PS nanoparticles. b. Quantification of the percentage of LC3-II compared to the total LC3 protein was performed by densitometry Results are represented as percentages. Results are representative of two separate experiments each with two replicates.

involved in the autophagosome formation is comprised of four protein complexes: the ATG9 and its cycling system, the PtdIns3K and the Ulk complexes and the ubiquitin-like systems. Here we targeted two of these systems: the PtdIns3K and the ubiquitin-like system by knocking-down BECN1 and ATG5, respectively.

The levels of siRNA knockdown achieved were very good both at the mRNA and at the protein levels. For ATG5, the levels of mRNA in the cell after 48 hours of siRNA treatment were 14 and 11 % for the siRNA 1 and 2, respectively, while for BECN1 they were 5 and 6 % (Figure 5.3.a).

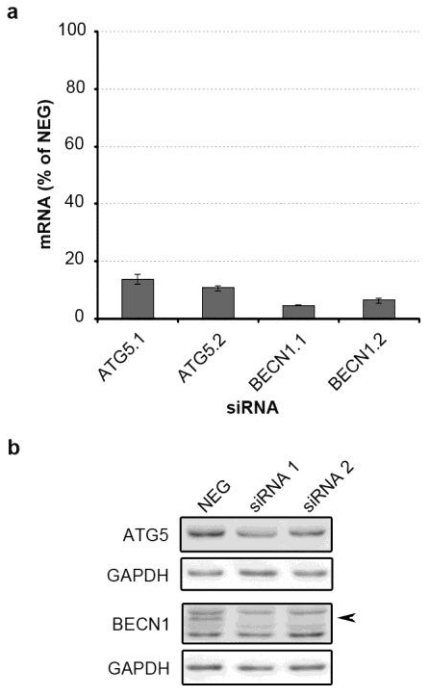

Figure 5.3. *Validation of the siRNA-mediated knockdown efficiency.* **a.** mRNA levels were measured by real-time quantitative PCR as described in Chapter 2. Bars indicate relative mRNA levels after 48 hours in cells treated with different siRNAs, compared to cells treated with non-silencing siRNA (NEG). Results shown represent the mean and standard deviations of four technical replicates and are representative of three independent experiments. **b.** Western blot showing the efficiency of the siRNA-mediated knockdowns at the protein level 48 hours post-transfection. Results are representative of 2 independent experiments. Arrowhead indicates the specific BECN1 band. GAPDH is used as a loading control.

These levels correlated well with those observed for the protein, with a near absence of protein in the BECN1-treated samples (Figure 5.3.b).

Having established the efficacy of the knockdowns, the effect of preventing the formation of the autophagosome, and hence autophagy, in apoptosis was determined. A similar strategy to that employed in Chapter 4 was used, namely the measurement of CASP3 and CASP7 activities. As

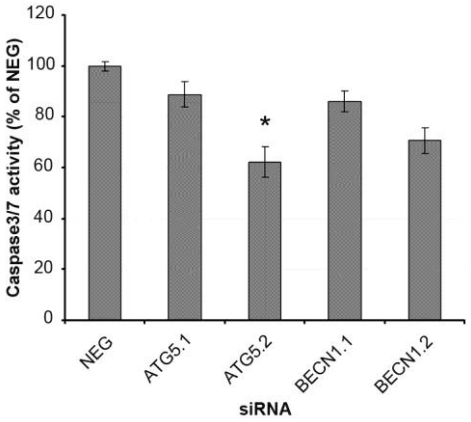

Figure 5.4. *Knockdown of proteins involved in autophagosome formation does not greatly affect CASP3 and CASP7 activities.* CASP3 and CASP7 activities in 1321N1 cells treated for 48 hours with different siRNAs followed by 24 hours of incubation with NH_2-PS nanoparticles is shown as percentage of the activity of cells treated with NEG siRNA. Results represent the mean and standard error of the mean from three independent experiments each with three replicates. * indicates p-value < 0.05.

shown in Figure 5.4, ablation of expression of BECN1 did not have any significant influence on the CASP3 and CASP7 activities, and only one of the siRNAs tested against ATG5 (ATG5.2), resulted in any significant decrease in the CASP3 and CASP7 activities, however even in this case the inhibition of CASP3 and CASP7 activities was not as pronounced as in the previous RNAi studies (Chapter 4).

5.2. ER stress induction

5.2.1. Induction of expression of ER stress-related genes

The ER is the site of synthesis and folding for membrane or secreted proteins (Vembar and Brodsky, 2008). In the ER lumen, a complex

network of chaperones, foldases and cofactors ensure the proper folding of proteins. However, if ER homeostasis is impaired, protein folding becomes unbalanced and misfolded proteins accumulate in the ER lumen, a condition referred to as ER stress develops, which in turn leads to the induction of several intracellular signalling pathways collectively known as the UPR (Woehlbier and Hetz, 2011). The UPR is an adaptive response of the cell to try to deal with the stress. If the stress is not resolved, the cell can be driven into apoptosis.

One of the ways in which the UPR acts on the cells is by modulation of transcription of different genes involved in protein synthesis and folding, and also transcription factors. One such factor is CHOP that is activated in response to the ATF6 and PERK signalling pathways of the UPR (Sato et al., 2000).

Analysis of CHOP expression revealed an upregulation of this gene up to 12-fold at 9 hours of treatment compared to the untreated cells (Figure 5.5.a). Enhanced expression of CHOP occurred relatively early during the incubation with NH_2-PS nanoparticles, being first visible at 3 hours of incubation, and then increasing at 6 hours, before stabilising its expression levels by 9 hours of incubation.

Other genes also see their expression upregulated in response to ER stress. Well studied examples include ER degradation enhancing α-mannosidase-like protein 1 (EDEM1) and homocysteine-inducible ER stress-inducible ubiquitin-like domain member 1 protein (HERPUD1), which are involved in ERAD, which is the cytosolic degradation of misfolded proteins expelled from the ER, and DnaJ homolog superfamily B, member 9 (DNAJB9/ERdj4) which is expressed upon activation of the IRE1α pathway. HERPUD1 and ERdj4 were found to have similar kinetics of expression, which started to increase at 3 hours after the beginning of incubation with NH_2-PS nanoparticles, increasing after 6 hours to approximately 3 and 3.5

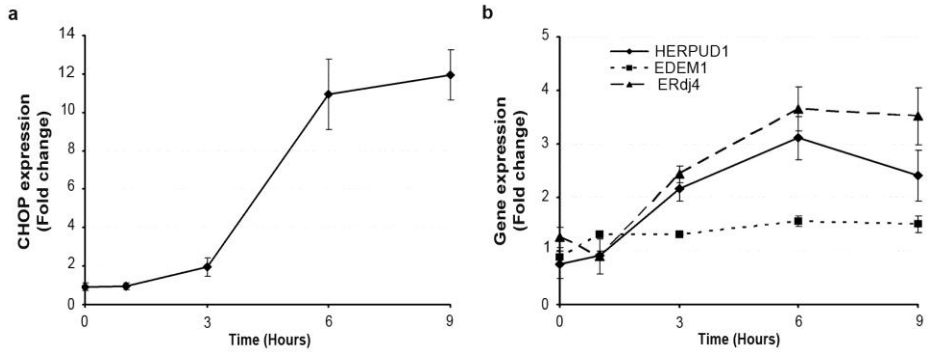

Figure 5.5. *NH_2-PS nanoparticles induce expression of ER stress-related genes.* 1321N1 cells were incubated with 50 μg/ml of NH_2-PS nanoparticles for increasing amounts of time (0, 1, 3, 6 and 9 hours) and the expression **a.** of an ER stress related gene (CHOP) or **b.** of genes involved in ERAD (HERPUD1, EDEM1) and IRE1α pathway (ERdj4) was measured by real-time quantitative PCR as described in Chapter 2. Results shown represent the mean and standard deviations between 4 technical replicates.

fold, respectively, before stabilising their expression level, compared to the untreated controls (Figure 5.5.b). EDEM1 also displayed an increase in its expression (Figure 5.5.b), however more studies need to be performed to be able to have statistically significant data.

5.2.2. Modulation of the expression of BCL-2 family proteins

Upon induction of ER stress, if the adaptive UPR is not able to resolve the stress, the signal switches to pro-death and the cell will die by apoptosis. This process can occur by various means, but usually involves modulation of the activity of proteins belonging to the BCL-2 family of proteins (Szegezdi et al., 2006). This modulation can occur either post-translationally through the JNK pathway, or at the transcription level by changes in gene expression. In this work only transcriptional changes were studied. As described above, CHOP is a transcription factor that is

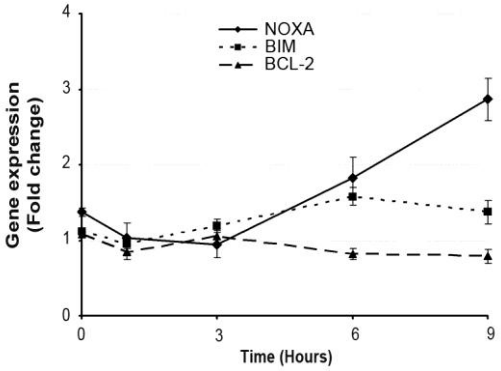

Figure 5.6. *Modulation of the expression of BCL-2 family members after incubation with NH_2-PS nanoparticles.* 1321N1 cells were incubated with 50 μg/ml of NH_2-PS nanoparticles for increasing lengths of time (0, 1, 3, 6 and 9 hours) and the expression of the pro-apoptotic genes NOXA and BIM, and of the anti-apoptotic gene BCL-2, was measured by real-time quantitative PCR as described in Chapter 2. Results shown represent the mean and standard deviations between 4 technical replicates.

expressed upon ER stress induction and has been connected to induction of apoptosis by upregulating various genes involved in apoptosis, including BIM, PUMA and NOXA (Galehdar et al., 2010; Puthalakath et al., 2007; Rodriguez et al., 2011). By contrast, CHOP also modulates apoptosis by decreasing the expression of the anti-apoptotic molecule BCL-2 (McCullough et al., 2001).

The expression of BCL-2, BIM and NOXA genes was analysed by real-time quantitative PCR and it was observed that their expression did not vary greatly after incubation with NH_2-PS nanoparticles (Figure 5.6). NOXA, a gene that can also be expressed in response to p53 (Oda et al., 2000) had its expression increase to 2.9 times higher than that of the untreated cells. BIM, which has also been shown to be overexpressed during ER stress in response to CHOP, was found to have its expression increased to only 1.5-fold. BCL-2, an anti-apoptotic protein that sees its expression

downregulated during ER stress in a CHOP-dependent manner, had its expression decreased to only 0.8-fold when compared to the untreated cells. These experiments need to be repeated to ensure that these so far preliminary results are statistically significant.

5.3. Discussion and Conclusions

In the previous chapters the molecular mechanisms of toxicity induced by NH_2-PS nanoparticles have begun to be unravelled, providing the first clues to the cellular machinery involved. Here, investigations of cell death-associated mechanisms have been broadened to take account of involvement of processes including autophagy and ER stress.

Autophagy is primarily a survival process by which the cell recycles old and malfunctioning organelles, thus serving as a pro-survival mechanism. However, as described above, autophagy has also been linked to cell death, although its role in this process is controversial. Some reports indicate that autophagy is a mechanism of cell death and that, if blocked, death would be prevented, while others argue that autophagy is merely a process that occurs during cell death (Kroemer and Levine, 2008).

Autophagy induction has been described following incubation with various types of nanoparticles (Liu et al., 2011; Stern et al., 2008), however information on cationic nanoparticles is scarce, with the only reports found in the literature being on 3 μm polystyrene nanoparticles (Kobayashi et al., 2010) or dendrimers (Li et al., 2009). In Chapter 3 it was suggested that autophagy might play a role in the mechanism of cell death observed upon exposure of 1321N1 to NH_2-PS nanoparticles, so this was studied in further detail in the present chapter.

Confirmation that autophagy was indeed being induced was studied using two different, but complementary, techniques to detect the accumulation of autophagosomes: TEM and Western blotting to detect LC3 cleavage into LC3-II. TEM studies revealed an increase in the number of vacuoles in the cells. In many of the cells observed, cellular debris and nanoparticles were visible inside (Figure 5.1). The occurrence of autophagy was further confirmed by detection of an increase in the relative abundance of LC3-II, compared to the total LC3, in cells treated for 24 hours with NH_2-PS nanoparticles (Figure 5.2). This analysis could be further complemented by microscopy analysis of LC3 lipidation using a LC3-GFP construct that is normally soluble in the cytosol but associates with autophagosome membranes after it has been cleaved, thereby changing its distribution from diffuse to punctate (Kabeya et al., 2000)

As autophagy has been inferred in both cell death and cell survival mechanisms, it was interesting to determine whether the induction of autophagy in the system under study was serving as a survival mechanism by which the cells were trying to dispose of the nanoparticles, or if autophagy was involved in the cell death process. RNAi was used to target two genes (ATG5 and BECN1) important for the formation of the autophagosome (Xie and Klionsky, 2007; Yang and Klionsky, 2010b). Both genes were efficiently downregulated both at mRNA and protein level, with an almost complete absence of targeted protein after 48 hours of incubation with the respective siRNAs (Figure 5.3). In general, despite the effectiveness of these silencing experiments, CASP3 and CASP7 activation was not significantly altered in these cells when treated with nanoparticles for 24 hours (Figure 5.4). Although one of the siRNAs (ATG5.2) targeting ATG5 did result in a statistically significant reduction in CASP3 and CASP7 activation, the protective effect was much milder than that seen with siRNAs targeting the core apoptosis machinery, suggesting that autophagy

is not making a major contribution to the cell death response. Nevertheless, further analysis using a wider panel of siRNAs targeting the autophagy machinery would be needed to confirm this.

ATG5 forms a complex with ATG12 and ATG16, which together drives the formation of the autophagosome (Xie and Klionsky, 2007; Yang and Klionsky, 2010b). The knockdown of ATG5 has been used previously to study autophagy induction and apoptosis (Colell et al., 2007; Grishchuk et al., 2011). Interestingly, ATG5 has also been shown to be involved in apoptosis induction following cleavage by calpain. This occurs via migration of one of the fragments to the mitochondria and association with BCL-xL and consequent release of cytochrome c and caspase activation (Yousefi et al., 2006). ATG5 depletion in BAX and BAK double knockout cells also efficiently protects cells from death (Shimizu et al., 2004), thus pointing towards an important role of ATG5 in cell death promotion other than that connected to autophagy induction. The results presented in this chapter together with those presented in Chapter 4 regarding the knockdown of BAX and BAK, may point towards a role for ATG5 in promoting apoptosis in this system. This, however, would need to be confirmed by attempting to rescue cells from nanoparticle-induced death by performing triple knockdowns of BAX, BAK and ATG5 or by inhibiting calpain activity in the BAX and BAK double knockdown cells. In this regard it would also be interesting to investigate whether there is any connection between ATG5 and the mitochondrial fragmentation that was observed in the 1321N1 cells treated with NH_2-PS nanoparticles.

Several experiments are still required to provide further clarification of some of the results presented in this chapter. One such experiment would be to validate if the ATG5 and BECN1 knockdown cells did indeed have impaired autophagy, by analysing this phenomenon in starved cells. According to Klionsky and colleagues when investigating autophagy it is

also advisable to study the autophagic flux by analysing if autophagy substrates reach the lysosomes and, when appropriate, if they are degraded (Klionsky et al., 2008).

The second cellular adaptive mechanism studied – ER stress – was also found to be activated in 1321N1 cells incubated with NH_2-PS nanoparticles. A canonical ER stress marker, CHOP, which is a transcription factor that has an increased expression during ER stress and that is implicated in the switching of the signalling into a pro-apoptotic direction, was shown to be highly upregulated in response to incubation with NH_2-PS nanoparticles (Figure 5.5.a). Other genes that are known to have their expression increased upon ER stress include EDEM1, ERdj4 and HERPUD1. These molecules, apart from ERdj4, are all involved in ERAD (Dong et al., 2008; Olivari et al., 2006), the process by which misfolded proteins in the ER are retrotranslocated and then degraded in the cytoplasm. All of these candidates were found to be upregulated on nanoparticle uptake (Figure 5.5.b), thus further suggesting that ER stress can be induced after incubation with NH_2-PS nanoparticles.

Since ER stress can push the cell towards apoptosis if the stimulus is not overcome, a link between these two events was also investigated. Members of the BCL-2 family of proteins are central to the induction of apoptosis during ER stress, and once activated BAX and BAK lead to the release of cytochrome c from the mitochondria with consequent formation of the apoptosome (Woehlbier and Hetz, 2011). The mechanisms by which the UPR signal is transformed into apoptosis is still not understood, however several of the BCL-2 family of proteins members are known to show increased expression upon ER stress in a CHOP-dependent way (Galehdar et al., 2010; Puthalakath et al., 2007; Rodriguez et al., 2011), so their expression was investigated. Preliminary results indicate that NOXA and BIM are mildly overexpressed in 1321N1 cells after incubation with NH_2-PS

nanoparticles (Figure 5.6), although these observations need further confirmation. Another gene, the expression of which is upregulated by CHOP, is PUMA (Galehdar et al., 2010). As shown in the previous chapter, PUMA is highly upregulated upon exposure to NH_2-PS nanoparticles (Figure 4.8). Indeed, its expression follows a very similar kinetics to that of CHOP: an increase in the expression is first observed at 3 hours of incubation and then it increases at 6 hours with a stabilisation of the expression levels up to 9 hours. This suggests that the PUMA upregulation observed in the system might be promoted by CHOP, however, the transcription factor responsible for the induction of PUMA expression needs to be investigated in further detail as PUMA is also expressed in response to p53 (Nakano and Vousden, 2001). Nevertheless, these are interesting observations, as PUMA is a highly potent pro-apoptotic member of the BCL-2 family of proteins, and has been shown to be involved in the modulation of the apoptotic process induced by the cationic nanoparticles (Figure 4.7). The other gene that was investigated was BCL-2, which is reported to be downregulated by CHOP (McCullough et al., 2001). In this study, preliminary results indicate only a small effect on BCL-2 expression (Figure 5.6), so more experiments will be needed in order to confirm and assess the significance of these results. However, BCL-2 is also known to be negatively regulated post-translationally through phosphorylation by JNK, depending on IRE1α signalling, so it is important to investigate whether this pathway is active in this system.

The results presented in this chapter are still preliminary and need to be further developed, however they provide indications that two cellular adaptive mechanisms – autophagy and ER stress – may also be involved in the cell death mechanism induced by NH_2-PS nanoparticles in 1321N1 cells. More detailed studies on the signalling pathways and the relevance of ER stress and autophagy to the mechanism of cell death are currently being

performed, and the results should help clarify the cellular processes elicited by cationic nanoparticles. Finally, it is worth noting that the mechanism by which nanoparticles arriving in the lysosomal system are able to invoke an ER stress response is also an intriguing issue that needs clarification, and therefore studies of secretory pathway function will also be needed to resolve this point.

CHAPTER 6

CONCLUDING REMARKS AND FUTURE PERSPECTIVES

Nanoparticles surround us everywhere: they are present in food, clothes, cosmetics, the environment, and in nanotechnology applications. Despite this, nanotechnology is a field in its infancy and detailed knowledge of how nanoparticles interact with living matter is still limited. Concerns over the safety of use of nanomaterials in humans and in the environment are therefore pertinent.

In this work, some of these concerns have begun to be addressed, by specifically assessing nanoparticle toxicity at the cellular level. It has been reported previously that ultrafine particles present in pollution are able to cross to the brain, and once there induce various pathological conditions such as inflammation and deposition of amyloid-β (Calderon-Garciduenas et al., 2008). However, little is known about the cellular and molecular mechanisms of toxicity that are elicited by nanoparticles in cells. Many of the nanoparticles humans come in contact with display a positive charge at their surface, and so it is of utmost importance to study how these nanoparticles interact with cells.

To this end, 50 nm NH_2-PS nanoparticles, displaying a positive ζ-potential (Table AI.I), have been used as a model for cationic nanoparticles and, as a cellular model, an astrocytoma cell line (1321N1) was chosen. The choice of this cellular model was relevant, as the brain is an organ that is affected by contact with nanoparticles and also because of the pivotal role astrocytes play in maintaining the homeostasis of the central nervous system (Giaume et al., 2007).

Incubation of 1321N1 cells with NH_2-PS nanoparticles was shown to be toxic to cells, while incubation with a wide range of concentrations of nanoparticles carrying a negative ζ-potential (COOH-PS and unmodified nanoparticles) was found not to elicit toxic effects. Using an assay in which the integrity and relative permeability of the plasma membrane is tested, and that is able to differentiate between live, early apoptotic, and late

apoptotic/necrotic cells, it was determined that cells were primarily dying through an apoptotic process. This was further validated by additional biochemical experiments that confirmed the presence of other apoptotic hallmarks, such as caspase activation and PARP1 cleavage.

Apoptosis is a highly controlled mechanism of cell death in which caspases play a central role. CASP3 and CASP7 are the primary executioners of this process and are common to the two known apoptotic signalling pathways. These pathways are termed the extrinsic pathway, which begins at the cell surface, and the intrinsic pathway that is initiated from within the cell. There are also particular caspases that are responsible for the start of the signal relay in each of these pathways, specifically CASP8 and CASP10 in the extrinsic pathway, and CASP9 in the intrinsic pathway. In this study a variety of approaches were used to investigate which of these routes were pertinent to nanoparticle-induced cell death. Caspase activation was assessed using a luminescent substrate; chemical inhibitors were employed to compare cleavage of caspases into their active forms; and a targeted RNAi strategy was used to delineate the key molecular players. Together these studies established that on exposure to NH_2-PS nanoparticles, the intrinsic pathway is the mechanism by which apoptosis proceeds.

In addition to identifying the specific initiation pathway of cell death invoked by the nanoparticles this study also assessed the downstream consequences. Two molecular events that occur during apoptosis were detected, namely activation of CASP3 and CASP7, and cleavage of CASP9 and PARP1. Various biochemical and molecular biology techniques, including Western blotting and RNAi, were used. Although not all techniques were found to be efficient in delineating the pathway of apoptosis, by combining the results obtained from the RNAi studies and the biochemical analyses of caspase activation and PARP1 cleavage, it can be concluded that the

mechanism of apoptosis induced by NH_2-PS nanoparticles in 1321N1 cells occurs via activation of the intrinsic pathway, with an active role of the apoptosome, formed by CASP9, APAF1 and cytochrome c. Consistent with these results, it was also noted that the ultrastructure of the mitochondria was severely compromised and production of ROS was detected.

This work also began to investigate the mechanism by which mitochondrial damage was occurring. During apoptosis, mitochondrial damage is known to occur through loss of mitochondrial ultrastructure and permeabilisation of the mitochondrial membrane, which in turn leads to cytochrome c release and apoptosome formation (Riedl and Salvesen, 2007; Scorrano et al., 2002). In order to evaluate these processes in the context of nanoparticle-induced toxicity, RNAi was used to assess the possible processes initiating mitochondrial damage. Cellular depletion of BAX and BAK, which modulate the apoptotic response and act directly on the mitochondria to induce MOMP and fragmentation, was found to strongly abrogate the apoptotic cascade, as measured by CASP3 and CASP7 activation and PARP1 cleavage. Similarly it was also noted that the combination of BIM, BID and PUMA, which have been described as activators of BAX (Ren et al., 2010), also strongly affected the apoptotic response of the cells upon exposure to NH_2-PS nanoparticles. These observations suggest that after entering the cells, NH_2-PS nanoparticles promote BAX and BAK activation in a process that is dependent on the 'BH3-only' proteins BIM, BID and PUMA. Upon activation, BAX translocates to the mitochondria where it interacts with BAK, thereby inducing MOMP with cytochrome c release to the cytoplasm and formation of the apoptosome. The consequences of these events are CASP9 activation, followed by CASP3 and CASP7 activation, thereby resulting in controlled cleavage of cellular proteins and cellular demise.

Although this work has clearly identified the nature of the cell death response invoked by nanoparticles, the more fundamental question of how nanoparticle-cell interaction leads to this trigger remains to be resolved. Imaging experiments carried out in this study and others (Bexiga et al., 2010; Xia et al., 2008b) have revealed that NH_2-PS nanoparticles are indeed internalised into cells, and reach the lysosomes. Although detailed study of the route of entry into the cell was not pursued in this work, largely due to the fact that fluorescently-labelled 50 nm NH_2-PS nanoparticles were not available, clearly this is an important question to address. A variety of methods to probe cellular internalisation events are available, including the use of pharmacological inhibitors of endocytosis, and colocalisation studies with markers of the different endocytic mechanisms. However, perhaps the most specific approach would be to again employ an RNAi strategy targeting the endocytic machinery and then assessing the effect on nanoparticle internalisation. In this regard, either flow cytometry or automated high content screening microscopy would seem to be appropriate visualisation and quantification methods through which to do this. Imaging-based techniques are particularly relevant, as this work has also established that nanoparticle accumulation in lysosomes seems to occur during the cell death response. Indeed, analysis of cells containing nanoparticles revealed that lysosomal membranes were often damaged, potentially allowing their contents to be released into the cytosol. Among the potential contents being released in this scenario would be the proteolytic enzyme CTSL, which together with other members of the cathepsin family, has been reported to mediate the crosstalk that occurs during apoptosis between the lysosome and mitochondria (Droga-Mazovec et al., 2008; Stoka et al., 2007). Preliminary fluorescence-based studies carried out in this work indicated that lysosomal contents did indeed change their localisation profile from distinct punctate structures to a more diffuse

appearance, suggesting membrane rupture and cytosolic accumulation. The precise role of lysosomal contents, and in particular of the cathepsin family of proteins, in the mechanism of cell death should also be further investigated by means of pharmacological inhibition or RNAi experiments. However, the existence of numerous highly homologous family members may make such studies challenging. (Conus and Simon, 2008).

Two additional findings that are described in this work are the involvement of two cellular adaptive responses to stress, namely autophagy and the ER stress response. Both events occur when a cell is under stress and are the mechanisms by which the cell attempts to resolve the stressing event in order to survive. However, if the insult is too intense, then the cell may not be able to overcome it and the cell will be driven into apoptosis. Cells exposed to nanoparticles displayed a high degree of vacuolation, with increased LC3 levels. RNAi studies demonstrated that by preventing autophagy through knockdown of ATG5, the levels of caspase activation decreased. ATG5 has been suggested to play a pro-apoptotic role (Yousefi et al., 2006) and it has been shown that in BAX- and BAK-deficient cells, the depletion of ATG5 promotes cell survival (Shimizu et al., 2004). In order to clarify the scenario in 1321N1 cells exposed to NH_2-PS nanoparticles, it would be interesting to analyse how cells depleted of BAX, BAK and ATG5 react to the presence of NH_2-PS nanoparticles. It would also be interesting to evaluate whether ATG5 has a role in mitochondrial morphology, as this organelle was still observed to undergo fragmentation in a BAX- and BAK-independent manner upon treatment with NH_2-PS nanoparticles.

The other adaptive response that was observed in the cells treated with nanoparticles was the ER stress response. Upregulation of several ER stress related genes such as CHOP and HERPUD1 was detected. CHOP is a transcription factor that induces expression of several pro-apoptotic genes such as PUMA and NOXA (Galehdar et al., 2010; Szegezdi et al.,

2006). Indeed, upregulation of PUMA was detected with similar kinetics to that of CHOP expression. These results, together with those employing RNAi of PUMA, highlight the importance of this protein to the mechanism of cell death. However, as PUMA expression is also upregulated in response to other transcription factors, such as p53 (Nakano and Vousden, 2001; Yu and Zhang, 2008), the precise role of this protein in the context of nanoparticle-induced toxicity also remains unclear. Nevertheless, a more in-depth study of how ER stress is induced by NH_2-PS nanoparticles, and how this contributes to the induction of apoptosis, is necessary and its execution is currently underway.

If nanoparticles are to be safely used in human applications, such as in medicine, further extensive research into their cellular interactions is still required. However, in order for this to occur, there also needs to be development and standardisation of their synthesis and dispersion. In addition, it may also be valuable to expand these experiments to other positively-charged nanoparticles, both with different charges and with different surface modifications, in order to clarify if the observed cellular and molecular responses are caused by the general charge or by the specific NH_2- modification. In this respect, bio-compatible nanoparticles also need to be developed and studied if nanotechnology is to become an extensively applied tool in a therapeutic context in humans. Similar experiments should also be carried out in different cellular models to clarify if the observed mechanisms are cell-type specific or if they are universal. Published results (Xia et al., 2008b), as well as research performed by others in the Dawson laboratory, indicate that the former might be true, as incubation with the same nanoparticles in a different cell line induces cell cycle arrest rather than cell death (Kim et al., unpublished). Clearly therefore, there is still much to discover about this critical area of cell-nanoparticle interaction.

In summary, the results presented in this work indicate that 50 nm NH_2-PS nanoparticles can enter 1321N1 cells and can be routed to lysosomes. There, and in accordance with the proton sponge hypothesis (Nel et al., 2009), the positive charge on the particles likely leads to the destabilisation of the lysosomal membrane, thereby instigating the release of both nanoparticles and proteolytic enzymes, such as cathepsins, into the cytoplasm. This in turn results in damage to the mitochondria and BAX- and BAK-dependent activation of CASP9, CASP3 and CASP7, with consequent cleavage of PARP1. ER stress and autophagy are also elicited upon incubation with NH_2-PS nanoparticles. The ultimate consequence of these events is that the cell is driven into apoptosis.

The first molecular account of cationic nanoparticle-induced cell death in a model cell line is therefore presented in this work. These experiments not only identify critical molecular machinery associated with these cellular events, but also correlate this with dramatic morphological effects on internal membrane organelles. An additional novel aspect developed in this work was the establishment of RNAi in the study of the interactions of nanoparticles in general, and NH_2-PS nanoparticles in particular, with cells.

The results presented here only begin to provide a basic understanding of the biology of nanoparticle-cell interaction, and therefore they help pave the way for future deeper understanding of the critical relationship between nano structures and the human body.

APPENDIX I

NANOPARTICLE CHARACTERISATION

DLS and ζ-potential measurements and image analyses were performed by Juan A. Varela. TEM imaging was performed by Federico Fenaroli and Filippo Bertoli.

AI.1. Introduction

With the increase in manufacture and use of engineered nanoparticles, there is an ever growing demand by both scientists, regulatory authorities and also the public to fully understand the properties of nanoparticles and how they influence the way they interact with living systems.

As the size of a nanoparticle decreases, its relative surface area increases, leading to a complete change in the characteristics of the nanoparticle when compared to the bulk material (Nel et al., 2009). Another aspect to consider is that for nanoparticles smaller than 100 nm, this size makes them increasingly biologically active, being able to reach distant parts of an organism and indeed able to interact with single cells. Another important concern is the accidental release of the nanoparticles into the environment and therefore their potential impact on it.

Despite the existence of several reports describing the toxicity of nanoparticles at the cellular level, including ROS formation (Bexiga et al., 2010; Xia et al., 2008a; Xia et al., 2008b) and genotoxicity (Barnes et al., 2008; Park et al., 2011) among others, this is still an area at its infancy. Most of the methods used to study toxicity have been developed to study bulk materials, but due to the specific physicochemical characteristics of nanoparticles, they pose many obstacles to the use of the conventional toxicity tests. Therefore, one of the requirements when one is developing a toxicity assay is to fully characterise the nanoparticles.

Currently different laboratories use a variety of techniques to assess different characteristics of the nanoparticles, with often only a single characteristic being investigated (Dhawan and Sharma, 2010). As would be expected, this causes difficulties in comparing the data obtained by different researchers. In 2010, during a workshop of the European Network on the

Health and Impact of Nanomaterials, a cohort of academic and non-academic researchers worked on reaching a consensus on the minimal characteristics that should be studied to assess more precisely the characteristics of nanoparticles relevant for their toxicity (Bouwmeester et al., 2011). According to the report that was issued, the essential characteristics that should be described include the size distribution and structure (whether it presents aggregates or not), the chemical composition, and characteristics of the nanoparticle surface such as surface charge and area (Bouwmeester et al., 2011).

Here, dynamic light scattering (DLS) and TEM were employed to analyse the size, distribution and state of aggregation of the different commercial nanoparticles used in this study. The nanoparticles were observed to have a typical size of approximately 50 nm and they were also shown not to be aggregated in PBS. ζ-potential was also investigated as a measurement of the surface charge of the nanoparticles and performed a pH titration with the NH_2-PS nanoparticles, which were the principal particles of our study. These nanoparticles were found to have a positive ζ-potential that increased with a decrease in pH, whereas the unmodified and COOH-PS nanoparticles presented a negative ζ-potential.

AI.2. Materials and Methods

AI.2.1. Nanoparticle physicochemical characterisation

50 nm NH_2-PS nanoparticles (Sigma Aldrich) and 50 nm unmodified and COOH-PS unlabelled polystyrene nanoparticles (Polysciences) were used without further modification. Size and ζ-potential were determined using a Malvern Zetasizer Nano Series. Polystyrene

nanoparticles were diluted to 50 μg/ml in PBS before measurement. Measurements were conducted at pH 7.0 and 25 °C.

AI.2.2. Transmission electron microscopy

Nanoparticles were diluted to 25 μg/ml in distilled water and were deposited on a formvar-coated TEM copper grid and were then analysed by TEM. The average particle size and standard deviation were determined after measuring more than 160 individual nanoparticles using Image J 1.34e software (National Institutes of Health) and the results were analysed using MATLAB R2007a software (The MathWorks).

AI.3. Results

In this work, polystyrene nanoparticles with a NH_2- surface modification were used as a model for cationic nanoparticles, and the effects of their addition to cells were compared with the effects of addition of unmodified and COOH-PS nanoparticles.

The nanoparticles were carefully characterised for their hydrodynamic size by DLS and also for their ζ-potential (as an indication of the surface charge). DLS measurements indicated that when dispersed in PBS unmodified and NH_2-PS nanoparticles had a size of 55 nm and 55.1 nm respectively, and the COOH-PS nanoparticles measured 41.8 nm (Table AI.I), which was consistent with that reported by the manufacturers. These measurements also revealed that the particles had a low polydispersity index (PDI), indicating that they were well dispersed in PBS.

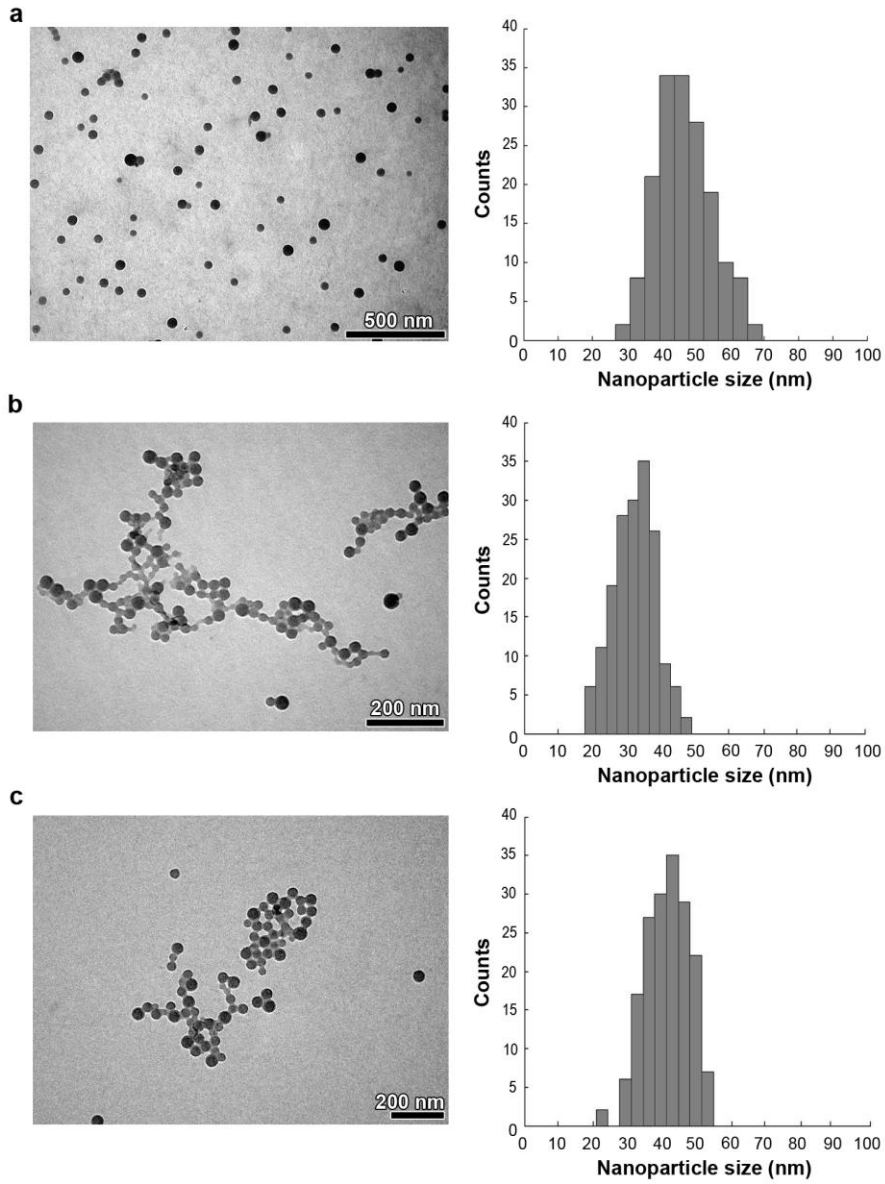

Figure AI.1. *Transmission electron microscopy of the polystyrene nanoparticles used.* An aqueous solution of 25 μg/ml nanoparticles was applied to a TEM grid and was analysed by TEM. Nanoparticle size distribution obtained from TEM is represented by a histogram. **a.** NH_2-PS nanoparticles with mean diameter of 46.7 nm **b.** COOH-PS nanoparticles with mean diameter of 33.0 nm and **c.** unmodified nanoparticles with mean diameter of 41.5 nm. More than 160 nanoparticles were measured in each case.

Measurement of NH_2-PS nanoparticle size and distribution using TEM images corroborated the results obtained by DLS (Figure AI.1). For the unmodified and the COOH-PS nanoparticles, the mean size obtained was smaller than that obtained for the NH_2-PS nanoparticles and in the TEM images, the particles were observed to be aggregated. However, it is more important to understand what happens when the particles are in solution, and in that respect the DLS measurements indicated that all three particles tested were well dispersed (Table AI.I).

As expected from the chemistry of the nanoparticles, both the unmodified and the COOH-PS nanoparticles presented a negative ζ-potential (Table AI.I), indicating that these nanoparticles have a negative surface charge. By contrast, the nanoparticles with the NH_2 modification displayed a positive ζ-potential, indicating a positive surface charge.

As the presence of a positive charge is likely to be a critical parameter in cellular toxicity, we performed measurements of the ζ-potential of these particles across a wide pH range. These studies indicated the ζ-potential was higher at lower pH values, reflecting the increase in the degree of protonation on the surface of the particles. Across the pH range tested, the hydrodynamic size was also measured and found to be relatively invariable indicating no particle aggregation (Figure AI.2).

Table AI.I. Physicochemical characterisation of the nanoparticles used in this study. All particles were characterised in PBS at pH 7.0 and 25 °C.

Nanoparticle	Hydrodynamic size (nm)	PDI *	ζ-Potential (mV)	Standard Deviation ζ-Potential (mV)
NH_2-modified	55.1 ± 0.1	0.105	+25.8	0.7
COOH-modified	41.8 ± 0.2	0.132	-40.7	2.4
Unmodified	55.0 ± 0.1	0.072	-38.3	1.8

* PDI- polydispersity index

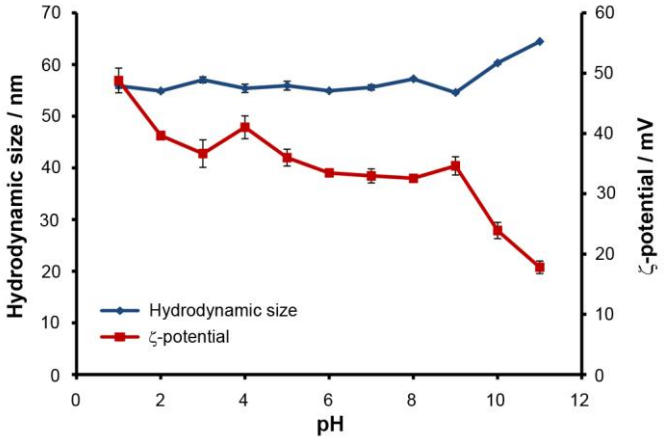

Figure AI.2. *Characterisation of 50 nm NH_2-PS nanoparticles.* Using DLS, the hydrodynamic size and ζ-potential of the particles were measured in water using NaOH and HCl to calibrate pH. The PDI for the size measurements ranged between 0.03 and 0.14. Graphs show means and standard deviations from two independent experiments. Each data point was obtained from 30 measurements.

APPENDIX II

siRNA TRANSFECTION OPTIMISATION

AII.1. Introduction

As described in Chapter 1, RNAi is a highly specific mechanism of down-regulating gene expression. siRNAs can be inserted into cells via a variety of techniques including microinjection (Hu et al., 2008; Sun et al., 2011) and electroporation (Prechtel et al., 2006), but the most widely used is lipofection (Gilmore et al., 2006).

In this work the method used was lipofection, using Oligofectamine as the transfection reagent. To optimise the transfection conditions, we used a siRNA targeting the inner centromere protein (INCENP), which is part of the chromosomal passenger complex together with Aurora-B kinase, survivin and borealin (Ruchaud et al., 2007). These proteins are involved in cell division and the absence of any of these components disrupts mitosis and the stability of the other members of the complex (Ruchaud et al., 2007). INCENP was the first member of this complex to be discovered (Cooke et al., 1987) and its localisation in the cell is very dynamic during mitosis (Figure AII.1) (Earnshaw and Cooke, 1991; Ruchaud et al., 2007).

At the early stages of mitosis, INCENP has a diffuse localisation along the chromosomes, but gradually converges into the centromeres as the cell cycle progresses to mid-metaphase (Cooke et al., 1987; Earnshaw and Cooke, 1991). From late-metaphase to anaphase, INCENP delocalises from the centrosomes to the spindle at the equatorial cortex until finally concentrating in the midbody during telophase and cytokinesis (Cooke et al., 1987; Earnshaw and Cooke, 1991). INCENP concentrates at the cleavage furrow very early in the formation of this structure and interacts very strongly with the inner surface of the plasma membrane at the cleavage furrow site (Earnshaw and Cooke, 1991; Eckley et al., 1997). This event occurs before recruitment of cytoplasmic myosin II, which, together with

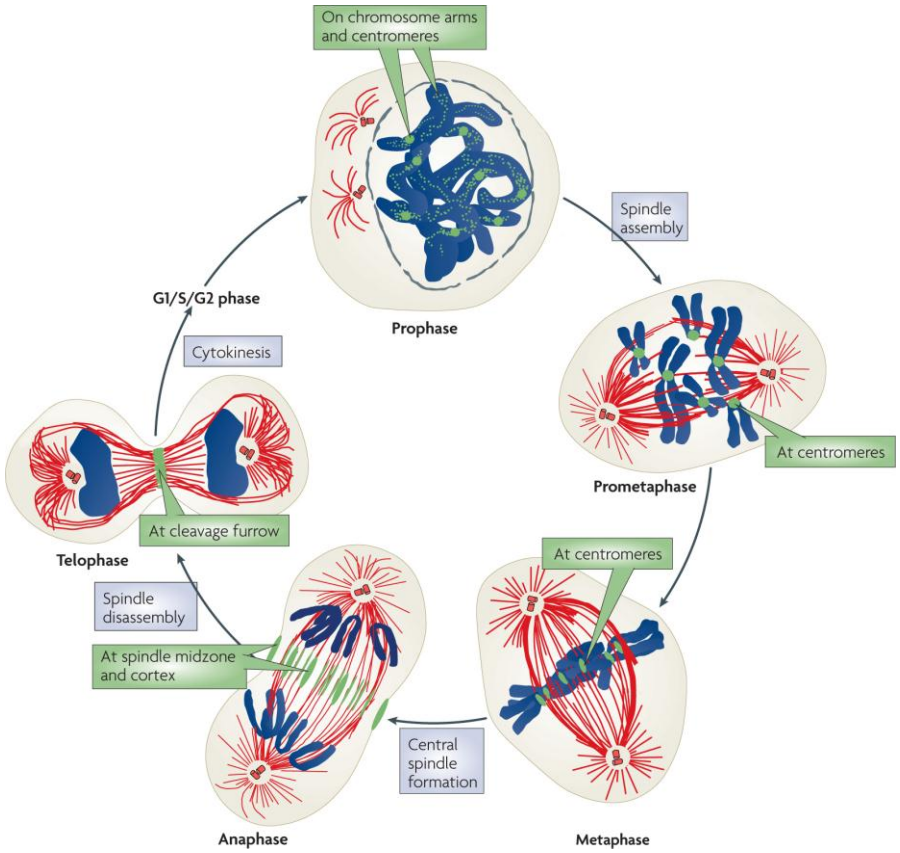

Figure AII.1. *INCENP localisation during mitosis.* Schematic representation of INCENP localisation (green) correlated with its multiple functions (blue boxes) during the different phases of mitosis relative to tubulin (red) and chromosome (blue) dynamics. In prophase, INCENP is found on chromosome arms and starts to accumulate at the centromeres where the maturation of kinetochores begins and continues through prometaphase. In metaphase, it localises at centromeres and in anaphase translocates to the spindle midzone and appears at the cortex. In telophase, INCENP concentrates at the cleavage furrow and, subsequently, at the midbody, where it is required for completion of cytokinesis. Adapted from Ruchaud et al., 2007.

actin, forms the contractile ring responsible for cytokinesis (Earnshaw and Cooke, 1991; Eckley et al., 1997).

From the sub-cellular localisation dynamics of INCENP, one would expect that when this protein is not present in the cell or when it is rendered inactive, the effect on mitosis would be significant. Studies carried out in cultured cells and in transgenic animals show that when INCENP function is impaired there is the formation of very large multi-nucleated cells (Cutts et al., 1999; Eckley et al., 1997).

These phenotypic effects make INCENP a very appealing target for siRNA transfection optimisation studies, as one can very easily differentiate, by florescence microscopy, single from large multinucleated cells. Here, different ratios of siRNA:Oligofectamine were tested, followed by analysis for the presence of multinucleated cells in the different samples by fluorescence microscopy. The optimal conditions were found to be when 30 pmol of siRNA were transfected using 2 μl of Oligofectamine per well of a 12-well plate.

AII.2. Materials and Methods

AII.2.1. siRNA transfection

Cells (25×10^3 cells/cm^2) were seeded in 12-well plates containing coverslips previously coated with collagen as described in section 2.9. and left overnight to adhere. Cells were then transfected with different amounts (10, 20, 30 and 50 pmol) of Silencer Select siRNA targeting INCENP (siRNA ID: s7423; sense sequence: GCUUGUACCUCAUAUCAGAtt) (Ambion) for each, using either 1 of 2 μl of Oligofectamine (Invitrogen). Briefly, siRNA and Oligofectamine were diluted separately in OptiMEM (Gibco) and

incubated for 7 minutes at room temperature. After this, diluted siRNA and Oligofectamine were mixed together and incubated for further 20 minutes at room temperature to allow the formation of the transfection complexes. Transfection complexes were added to the cells, previously washed with serum-free DMEM, in a dropwise manner and cells were then incubated at 37 °C for 4 hours. DMEM containing 30 % FBS was added to the cells and incubation proceeded for a further 44 hours.

AII.2.2. Fluorescent staining and microscopy

Cells were fixed with 3 % PFA in PBS for 20 minutes at room temperature. PFA was quenched with 30 mM glycine in PBS, pH 7.5, for 5 minutes at room temperature, after which the cells were washed 3 times in PBS, each for 3 minutes. Cells were permeabilised with 0.1 % Triton-X100 in PBS, for 5 minutes at room temperature, after which they were washed 3 times for 3 minutes each. Filamentous actin (F-actin) was stained using fluorescein-phalloidin (Molecular Probes) diluted 1:40 in 1 % bovine serum albumin diluted in PBS, for 20 minutes at room temperature, after which cells were washed twice with PBS, each for 5 minutes. Nuclei were stained using 0.2 μg/ml Hoechst 33342 for 5 minutes at room temperature. Cells were then washed 3 times with PBS, each for 5 minutes and coverslips were mounted using Mowiol and left to dry overnight at room temperature. Slides were analysed using a Leica DMI6000B epifluorescence microscope equipped with a Leica DFC340 FX Digital CCD camera. Images were acquired using a PL APO 40x/1.25 oil immersion objective. At least 3 randomly chosen fields of view were imaged and the number of multi- or single-nucleated cells was counted. Mitotic cells and spherical cells were also taken into account.

AII.3. Results

A critical step in every experiment is to have the experimental conditions optimised. In a siRNA experiment it is crucial that the amounts of siRNA and transfection reagent used are optimal in order to achieve a maximal reduction in the amount of gene expression, but at the same time reducing to a minimum the toxicity that the transfection procedure might cause the cells.

To optimise the transfection conditions for the 1321N1 cell line in which this work was performed, 4 different amounts of siRNA (10, 20, 30 and 50 pmol) combined with either 1 or 2 μl of Oligofectamine, a lipid-based transfection reagent, were tested. After 48 hours of siRNA transfection, the cells were fixed and the number of multi- and single-nucleated cells was counted (Figure AII.2). Spherical cells and mitotic cells were counted separately, as the type of nucleus present in these cells could

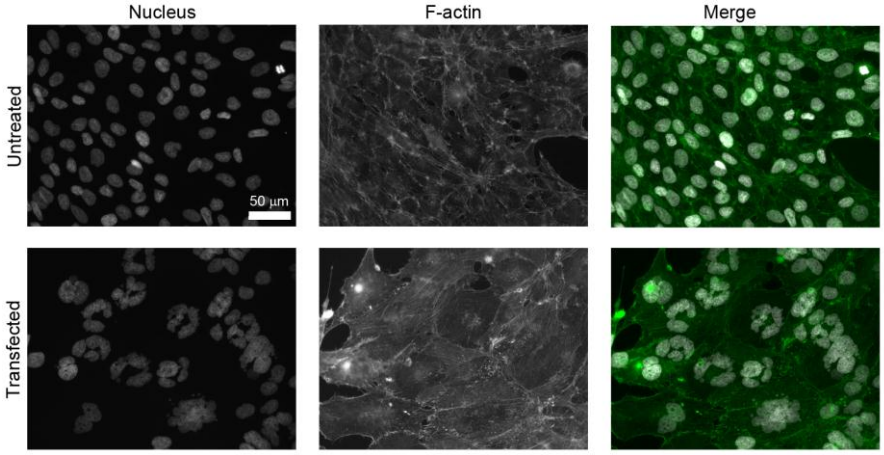

Figure AII.2. *Transfection with INCENP siRNA induces the formation of multi-nucleated cells.* 1321N1 cells were left untreated or transfected with a combination of 2 μl Oligofectamine and 30 pmol of siRNA targeting INCENP for 48 hours. Cells were then fixed and the nuclei and F-actin were stained and analysed as described in section AII.2.2. Scale bar represents 50 μm.

not be determined, and also because the presence of spherical cells could be indicative of cell death, and hence toxicity.

As can be seen in Table AII.I, in cells that were not treated with siRNA or Oligofectamine, no multi-nucleated cells were detected in all 4 fields of view analysed. It was also observed that the number of mitotic cells was slightly higher than in the other conditions studied. As expected, the number of multi-nucleated cells increased as the concentration of siRNA increased, which also led to a decrease in the total number of cells counted. Another observation from these optimisation experiments was that there was an increase in transfection efficiency when higher concentrations of Oligofectamine were used (2 μl compared to 1 μl) (Table AII.I). This was illustrated by a higher number of multi-nucleated cells and a lower number of single-nucleated cells with all siRNA amounts used. The best transfection conditions were determined to be when 30 and 50 pmol of siRNA were used in combination with 2 μl of Oligofectamine. Although the results for both conditions were quite similar, when 50 pmol of siRNA were used there was an increase in the number of spherical cells, indicating that there might be a higher toxicity when using this combination of reagents. This, together with the desire to use less siRNA, led to the choice of the combination of 30 pmol and 2 μl of Oligofectamine as the optimal transfection conditions for the 1321N1 cell line. When other formats of wells were used, these values were adjusted accordingly based on the surface area of the wells.

Table AII.I. Optimisation of the transfection conditions for 1321N1 cells using INCENP siRNA as a reporter. The total number of cells displaying single or multi nuclei is shown. Mitotic and spherical cells were also accounted for.

	siRNA	0 pmol	10 pmol	20 pmol	30 pmol	50 pmol
0 µl Oligofectamine	Single Nucleus	314	Not determined	Not determined	Not determined	Not determined
	Multi-Nuclei	0				
	Mitotic	11				
	Spherical	0				
1 µl Oligofectamine	Single Nucleus	210*	40	93	42	106
	Multi-Nuclei	0*	59	52	62	61
	Mitotic	3*	0	0	1	0
	Spherical	0*	1	0	1	0
2 µl Oligofectamine	Single Nucleus	238	34	27*	18	22
	Multi-Nuclei	2	62	44*	74	68
	Mitotic	2	1	0*	0	0
	Spherical	0	2	2*	0	9

* – only 3 fields of view were taken into account in the counting.

REFERENCE LIST

Aillon, K.L., Xie, Y., El-Gendy, N., Berkland, C.J., and Forrest, M.L. (2009). Effects of nanomaterial physicochemical properties on in vivo toxicity. *Adv Drug Deliv Rev* 61: 457-466.

Alnemri, E.S., Livingston, D.J., Nicholson, D.W., Salvesen, G., Thornberry, N.A., Wong, W.W., and Yuan, J. (1996). Human ICE/CED-3 protease nomenclature. *Cell* 87: 171.

Ambros, V. (2001). microRNAs: tiny regulators with great potential. *Cell* 107: 823-826.

Aramaki, Y., Takano, S., and Tsuchiya, S. (2001). Cationic liposomes induce macrophage apoptosis through mitochondrial pathway. *Arch Biochem Biophys* 392: 245-250.

AshaRani, P.V., Low Kah Mun, G., Hande, M.P., and Valiyaveettil, S. (2009). Cytotoxicity and genotoxicity of silver nanoparticles in human cells. *ACS Nano* 3: 279-290.

Auffan, M., Rose, J., Bottero, J.Y., Lowry, G.V., Jolivet, J.P., and Wiesner, M.R. (2009). Towards a definition of inorganic nanoparticles from an environmental, health and safety perspective. *Nat Nanotechnol* 4: 634-641.

Aza-Blanc, P., Cooper, C.L., Wagner, K., Batalov, S., Deveraux, Q.L., and Cooke, M.P. (2003). Identification of modulators of TRAIL-induced apoptosis via RNAi-based phenotypic screening. *Mol Cell* 12: 627-637.

Bakhshi, A., Jensen, J.P., Goldman, P., Wright, J.J., McBride, O.W., Epstein, A.L., and Korsmeyer, S.J. (1985). Cloning the chromosomal breakpoint of t(14;18) human lymphomas: clustering around JH on chromosome 14 and near a transcriptional unit on 18. *Cell* 41: 899-906.

Bao, Q., and Shi, Y. (2007). Apoptosome: a platform for the activation of initiator caspases. *Cell Death Differ* 14: 56-65.

Barnes, C.A., Elsaesser, A., Arkusz, J., Smok, A., Palus, J., Lesniak, A., Salvati, A., Hanrahan, J.P., Jong, W.H., Dziubaltowska, E.*, et al.* (2008). Reproducible

comet assay of amorphous silica nanoparticles detects no genotoxicity. *Nano Lett* 8: 3069-3074.

Bass, D.A., Parce, J.W., Dechatelet, L.R., Szejda, P., Seeds, M.C., and Thomas, M. (1983). Flow cytometric studies of oxidative product formation by neutrophils: a graded response to membrane stimulation. *J Immunol* 130: 1910-1917.

Bernstein, E., Caudy, A.A., Hammond, S.M., and Hannon, G.J. (2001). Role for a bidentate ribonuclease in the initiation step of RNA interference. *Nature* 409: 363-366.

Bexiga, M.G., Varela, J.A., Wang, F., Fenaroli, F., Salvati, A., Lynch, I., Simpson, J.C., and Dawson, K.A. (2010). Cationic nanoparticles induce caspase 3-, 7- and 9-mediated cytotoxicity in a human astrocytoma cell line. *Nanotoxicology*.

Bidere, N., Lorenzo, H.K., Carmona, S., Laforge, M., Harper, F., Dumont, C., and Senik, A. (2003). Cathepsin D triggers Bax activation, resulting in selective apoptosis-inducing factor (AIF) relocation in T lymphocytes entering the early commitment phase to apoptosis. *J Biol Chem* 278: 31401-31411.

Boatright, K.M., and Salvesen, G.S. (2003). Mechanisms of caspase activation. *Curr Opin Cell Biol* 15: 725-731.

Boldin, M.P., Goncharov, T.M., Goltsev, Y.V., and Wallach, D. (1996). Involvement of MACH, a novel MORT1/FADD-interacting protease, in Fas/APO-1- and TNF receptor-induced cell death. *Cell* 85: 803-815.

Bouchier-Hayes, L., Munoz-Pinedo, C., Connell, S., and Green, D.R. (2008). Measuring apoptosis at the single cell level. *Methods* 44: 222-228.

Boulares, A.H., Yakovlev, A.G., Ivanova, V., Stoica, B.A., Wang, G., Iyer, S., and Smulson, M. (1999). Role of poly(ADP-ribose) polymerase (PARP) cleavage in apoptosis. Caspase 3-resistant PARP mutant increases rates of apoptosis in transfected cells. *J Biol Chem* 274: 22932-22940.

Bouwmeester, H., Lynch, I., Marvin, H.J., Dawson, K.A., Berges, M., Braguer, D., Byrne, H.J., Casey, A., Chambers, G., Clift, M.J., *et al.* (2011). Minimal

analytical characterization of engineered nanomaterials needed for hazard assessment in biological matrices. *Nanotoxicology* 5: 1-11.

Boya, P., Andreau, K., Poncet, D., Zamzami, N., Perfettini, J.L., Metivier, D., Ojcius, D.M., Jaattela, M., and Kroemer, G. (2003). Lysosomal membrane permeabilization induces cell death in a mitochondrion-dependent fashion. *J Exp Med* 197: 1323-1334.

Boya, P., Gonzalez-Polo, R.A., Casares, N., Perfettini, J.L., Dessen, P., Larochette, N., Metivier, D., Meley, D., Souquere, S., Yoshimori, T.*, et al.* (2005). Inhibition of macroautophagy triggers apoptosis. *Mol Cell Biol* 25: 1025-1040.

Bradbury, D.A., Simmons, T.D., Slater, K.J., and Crouch, S.P. (2000). Measurement of the ADP:ATP ratio in human leukaemic cell lines can be used as an indicator of cell viability, necrosis and apoptosis. *J Immunol Methods* 240: 79-92.

Brown, D.M., Wilson, M.R., MacNee, W., Stone, V., and Donaldson, K. (2001). Size-dependent proinflammatory effects of ultrafine polystyrene particles: a role for surface area and oxidative stress in the enhanced activity of ultrafines. *Toxicol Appl Pharmacol* 175: 191-199.

Cabaleiro-Lago, C., Quinlan-Pluck, F., Lynch, I., Lindman, S., Minogue, A.M., Thulin, E., Walsh, D.M., Dawson, K.A., and Linse, S. (2008). Inhibition of amyloid beta protein fibrillation by polymeric nanoparticles. *Journal of the American Chemical Society* 130: 15437-15443.

Calderon-Garciduenas, L., Solt, A.C., Henriquez-Roldan, C., Torres-Jardon, R., Nuse, B., Herritt, L., Villarreal-Calderon, R., Osnaya, N., Stone, I., Garcia, R.*, et al.* (2008). Long-term air pollution exposure is associated with neuroinflammation, an altered innate immune response, disruption of the blood-brain barrier, ultrafine particulate deposition, and accumulation of amyloid beta-42 and alpha-synuclein in children and young adults. *Toxicol Pathol* 36: 289-310.

Calfon, M., Zeng, H., Urano, F., Till, J.H., Hubbard, S.R., Harding, H.P., Clark, S.G., and Ron, D. (2002). IRE1 couples endoplasmic reticulum load to secretory capacity by processing the XBP-1 mRNA. *Nature* 415: 92-96.

Caplen, N.J., Parrish, S., Imani, F., Fire, A., and Morgan, R.A. (2001). Specific inhibition of gene expression by small double-stranded RNAs in invertebrate and vertebrate systems. *Proc Natl Acad Sci U S A* 98: 9742-9747.

Casey, J.R., Grinstein, S., and Orlowski, J. (2010). Sensors and regulators of intracellular pH. *Nat Rev Mol Cell Biol* 11: 50-61.

Cauwels, A., Janssen, B., Waeytens, A., Cuvelier, C., and Brouckaert, P. (2003). Caspase inhibition causes hyperacute tumor necrosis factor-induced shock via oxidative stress and phospholipase A2. *Nat Immunol* 4: 387-393.

Cedervall, T., Lynch, I., Lindman, S., Berggard, T., Thulin, E., Nilsson, H., Dawson, K.A., and Linse, S. (2007). Understanding the nanoparticle-protein corona using methods to quantify exchange rates and affinities of proteins for nanoparticles. *Proc Natl Acad Sci U S A* 104: 2050-2055.

Cereghetti, G.M., and Scorrano, L. (2006). The many shapes of mitochondrial death. *Oncogene* 25: 4717-4724.

Chen, H., Detmer, S.A., Ewald, A.J., Griffin, E.E., Fraser, S.E., and Chan, D.C. (2003). Mitofusins Mfn1 and Mfn2 coordinately regulate mitochondrial fusion and are essential for embryonic development. *J Cell Biol* 160: 189-200.

Chiarugi, A. (2005). "Simple but not simpler": toward a unified picture of energy requirements in cell death. *Faseb J* 19: 1783-1788.

Chipuk, J.E., and Green, D.R. (2008). How do BCL-2 proteins induce mitochondrial outer membrane permeabilization? *Trends Cell Biol* 18: 157-164.

Chipuk, J.E., Moldoveanu, T., Llambi, F., Parsons, M.J., and Green, D.R. (2010). The BCL-2 family reunion. *Mol Cell* 37: 299-310.

Choi, H.S., Ashitate, Y., Lee, J.H., Kim, S.H., Matsui, A., Insin, N., Bawendi, M.G., Semmler-Behnke, M., Frangioni, J.V., and Tsuda, A. (2010). Rapid translocation of nanoparticles from the lung airspaces to the body. *Nat Biotechnol* 28: 1300-1303.

Christensen, K.A., Myers, J.T., and Swanson, J.A. (2002). pH-dependent regulation of lysosomal calcium in macrophages. *J Cell Sci* 115: 599-607.

Chwieralski, C.E., Welte, T., and Buhling, F. (2006). Cathepsin-regulated apoptosis. *Apoptosis* 11: 143-149.

Cipolat, S., Martins de Brito, O., Dal Zilio, B., and Scorrano, L. (2004). OPA1 requires mitofusin 1 to promote mitochondrial fusion. *Proc Natl Acad Sci U S A* 101: 15927-15932.

Cirman, T., Oresic, K., Mazovec, G.D., Turk, V., Reed, J.C., Myers, R.M., Salvesen, G.S., and Turk, B. (2004). Selective disruption of lysosomes in HeLa cells triggers apoptosis mediated by cleavage of Bid by multiple papain-like lysosomal cathepsins. *J Biol Chem* 279: 3578-3587.

Cohen, G.M. (1997). Caspases: the executioners of apoptosis. *Biochem J* 326 (Pt 1): 1-16.

Colell, A., Ricci, J.E., Tait, S., Milasta, S., Maurer, U., Bouchier-Hayes, L., Fitzgerald, P., Guio-Carrion, A., Waterhouse, N.J., Li, C.W., *et al.* (2007). GAPDH and autophagy preserve survival after apoptotic cytochrome c release in the absence of caspase activation. *Cell* 129: 983-997.

Conus, S., and Simon, H.U. (2008). Cathepsins: key modulators of cell death and inflammatory responses. *Biochem Pharmacol* 76: 1374-1382.

Cooke, C.A., Heck, M.M., and Earnshaw, W.C. (1987). The inner centromere protein (INCENP) antigens: movement from inner centromere to midbody during mitosis. *J Cell Biol* 105: 2053-2067.

Cutts, S.M., Fowler, K.J., Kile, B.T., Hii, L.L., O'Dowd, R.A., Hudson, D.F., Saffery, R., Kalitsis, P., Earle, E., and Choo, K.H. (1999). Defective chromosome segregation, microtubule bundling and nuclear bridging in inner centromere protein gene (Incenp)-disrupted mice. *Hum Mol Genet* 8: 1145-1155.

Danial, N.N. (2007). BCL-2 family proteins: critical checkpoints of apoptotic cell death. *Clin Cancer Res* 13: 7254-7263.

de La Motte Rouge, T., Galluzzi, L., Olaussen, K.A., Zermati, Y., Tasdemir, E., Robert, T., Ripoche, H., Lazar, V., Dessen, P., Harper, F., *et al.* (2007). A novel epidermal growth factor receptor inhibitor promotes apoptosis in

non-small cell lung cancer cells resistant to erlotinib. *Cancer Res* 67: 6253-6262.

Degterev, A., Boyce, M., and Yuan, J. (2001). The channel of death. *J Cell Biol* 155: 695-698.

Degterev, A., Boyce, M., and Yuan, J. (2003). A decade of caspases. *Oncogene* 22: 8543-8567.

Degterev, A., Huang, Z., Boyce, M., Li, Y., Jagtap, P., Mizushima, N., Cuny, G.D., Mitchison, T.J., Moskowitz, M.A., and Yuan, J. (2005). Chemical inhibitor of nonapoptotic cell death with therapeutic potential for ischemic brain injury. *Nat Chem Biol* 1: 112-119.

Degterev, A., and Yuan, J. (2008). Expansion and evolution of cell death programmes. *Nat Rev Mol Cell Biol* 9: 378-390.

Dekkers, S., Krystek, P., Peters, R.J., Lankveld, D.X., Bokkers, B.G., van Hoeven-Arentzen, P.H., Bouwmeester, H., and Oomen, A.G. (2010). Presence and risks of nanosilica in food products. *Nanotoxicology*.

Desagher, S., Osen-Sand, A., Montessuit, S., Magnenat, E., Vilbois, F., Hochmann, A., Journot, L., Antonsson, B., and Martinou, J.C. (2001). Phosphorylation of bid by casein kinases I and II regulates its cleavage by caspase 8. *Mol Cell* 8: 601-611.

Deter, R.L., and De Duve, C. (1967). Influence of glucagon, an inducer of cellular autophagy, on some physical properties of rat liver lysosomes. *J Cell Biol* 33: 437-449.

Dhawan, A., and Sharma, V. (2010). Toxicity assessment of nanomaterials: methods and challenges. *Anal Bioanal Chem* 398: 589-605.

Dong, M., Bridges, J.P., Apsley, K., Xu, Y., and Weaver, T.E. (2008). ERdj4 and ERdj5 are required for endoplasmic reticulum-associated protein degradation of misfolded surfactant protein C. *Mol Biol Cell* 19: 2620-2630.

Droga-Mazovec, G., Bojic, L., Petelin, A., Ivanova, S., Romih, R., Repnik, U., Salvesen, G.S., Stoka, V., Turk, V., and Turk, B. (2008). Cysteine cathepsins

trigger caspase-dependent cell death through cleavage of bid and antiapoptotic Bcl-2 homologues. *J Biol Chem* 283: 19140-19150.

Du, C., Fang, M., Li, Y., Li, L., and Wang, X. (2000). Smac, a mitochondrial protein that promotes cytochrome c-dependent caspase activation by eliminating IAP inhibition. *Cell* 102: 33-42.

Du, H., Wolf, J., Schafer, B., Moldoveanu, T., Chipuk, J.E., and Kuwana, T. (2011). BH3 domains other than Bim and Bid can directly activate Bax/Bak. *J Biol Chem* 286: 491-501.

Dykxhoom, D.M., Novina, C.D., and Sharp, P.A. (2003). Killing the messenger: short RNAs that silence gene expression. *Nat Rev Mol Cell Biol* 4: 457-467.

Earnshaw, W.C., and Cooke, C.A. (1991). Analysis of the distribution of the INCENPs throughout mitosis reveals the existence of a pathway of structural changes in the chromosomes during metaphase and early events in cleavage furrow formation. *J Cell Sci* 98 (Pt 4): 443-461.

Ebbesen, T.W., and Ajayan, P.M. (1992). Large-Scale Synthesis of Carbon Nanotubes. *Nature* 358: 220-222.

Eckley, D.M., Ainsztein, A.M., Mackay, A.M., Goldberg, I.G., and Earnshaw, W.C. (1997). Chromosomal proteins and cytokinesis: patterns of cleavage furrow formation and inner centromere protein positioning in mitotic heterokaryons and mid-anaphase cells. *J Cell Biol* 136: 1169-1183.

Elbashir, S.M., Harborth, J., Lendeckel, W., Yalcin, A., Weber, K., and Tuschl, T. (2001). Duplexes of 21-nucleotide RNAs mediate RNA interference in cultured mammalian cells. *Nature* 411: 494-498.

Farokhzad, O.C., and Langer, R. (2009). Impact of nanotechnology on drug delivery. *ACS Nano* 3: 16-20.

Ferri, K.F., and Kroemer, G. (2001). Organelle-specific initiation of cell death pathways. *Nat Cell Biol* 3: E255-263.

Fire, A., Xu, S., Montgomery, M.K., Kostas, S.A., Driver, S.E., and Mello, C.C. (1998). Potent and specific genetic interference by double-stranded RNA in Caenorhabditis elegans. *Nature* 391: 806-811.

Frank, S., Gaume, B., Bergmann-Leitner, E.S., Leitner, W.W., Robert, E.G., Catez, F., Smith, C.L., and Youle, R.J. (2001). The role of dynamin-related protein 1, a mediator of mitochondrial fission, in apoptosis. *Dev Cell* 1: 515-525.

Freundt, E.C., Czapiga, M., and Lenardo, M.J. (2007). Photoconversion of Lysotracker Red to a green fluorescent molecule. *Cell Res* 17: 956-958.

Frey, T.G., and Mannella, C.A. (2000). The internal structure of mitochondria. *Trends Biochem Sci* 25: 319-324.

Fribley, A., Zhang, K., and Kaufman, R.J. (2009). Regulation of apoptosis by the unfolded protein response. *Methods Mol Biol* 559: 191-204.

Frohlich, E., Samberger, C., Kueznik, T., Absenger, M., Roblegg, E., Zimmer, A., and Pieber, T.R. (2009). Cytotoxicity of nanoparticles independent from oxidative stress. *J Toxicol Sci* 34: 363-375.

Furuya, N., Yu, J., Byfield, M., Pattingre, S., and Levine, B. (2005). The evolutionarily conserved domain of Beclin 1 is required for Vps34 binding, autophagy and tumor suppressor function. *Autophagy* 1: 46-52.

Galehdar, Z., Swan, P., Fuerth, B., Callaghan, S.M., Park, D.S., and Cregan, S.P. (2010). Neuronal apoptosis induced by endoplasmic reticulum stress is regulated by ATF4-CHOP-mediated induction of the Bcl-2 homology 3-only member PUMA. *J Neurosci* 30: 16938-16948.

Gallenne, T., Gautier, F., Oliver, L., Hervouet, E., Noel, B., Hickman, J.A., Geneste, O., Cartron, P.F., Vallette, F.M., Manon, S.*, et al.* (2009). Bax activation by the BH3-only protein Puma promotes cell dependence on antiapoptotic Bcl-2 family members. *J Cell Biol* 185: 279-290.

Galluzzi, L., Aaronson, S.A., Abrams, J., Alnemri, E.S., Andrews, D.W., Baehrecke, E.H., Bazan, N.G., Blagosklonny, M.V., Blomgren, K., Borner, C.*, et al.* (2009a). Guidelines for the use and interpretation of assays for monitoring cell death in higher eukaryotes. *Cell Death Differ* 16: 1093-1107.

Galluzzi, L., Blomgren, K., and Kroemer, G. (2009b). Mitochondrial membrane permeabilization in neuronal injury. *Nat Rev Neurosci* 10: 481-494.

Galluzzi, L., and Kroemer, G. (2008). Necroptosis: a specialized pathway of programmed necrosis. *Cell* 135: 1161-1163.

Galluzzi, L., Maiuri, M.C., Vitale, I., Zischka, H., Castedo, M., Zitvogel, L., and Kroemer, G. (2007). Cell death modalities: classification and pathophysiological implications. *Cell Death Differ* 14: 1237-1243.

Galluzzi, L., Morselli, E., Kepp, O., and Kroemer, G. (2009c). Targeting post-mitochondrial effectors of apoptosis for neuroprotection. *Biochim Biophys Acta* 1787: 402-413.

Galonek, H.L., and Hardwick, J.M. (2006). Upgrading the BCL-2 network. *Nat Cell Biol* 8: 1317-1319.

Gavathiotis, E., Suzuki, M., Davis, M.L., Pitter, K., Bird, G.H., Katz, S.G., Tu, H.C., Kim, H., Cheng, E.H., Tjandra, N., *et al.* (2008). BAX activation is initiated at a novel interaction site. *Nature* 455: 1076-1081.

Germain, M., Mathai, J.P., McBride, H.M., and Shore, G.C. (2005). Endoplasmic reticulum BIK initiates DRP1-regulated remodelling of mitochondrial cristae during apoptosis. *Embo J* 24: 1546-1556.

Giaume, C., Kirchhoff, F., Matute, C., Reichenbach, A., and Verkhratsky, A. (2007). Glia: the fulcrum of brain diseases. *Cell Death Differ* 14: 1324-1335.

Gilmore, I.R., Fox, S.P., Hollins, A.J., and Akhtar, S. (2006). Delivery strategies for siRNA-mediated gene silencing. *Curr Drug Deliv* 3: 147-155.

Goldstein, J.C., Waterhouse, N.J., Juin, P., Evan, G.I., and Green, D.R. (2000). The coordinate release of cytochrome c during apoptosis is rapid, complete and kinetically invariant. *Nat Cell Biol* 2: 156-162.

Golstein, P., and Kroemer, G. (2005). Redundant cell death mechanisms as relics and backups. *Cell Death Differ* 12 Suppl 2: 1490-1496.

Golstein, P., and Kroemer, G. (2007). A multiplicity of cell death pathways. Symposium on apoptotic and non-apoptotic cell death pathways. *EMBO Rep* 8: 829-833.

Gratton, S.E., Ropp, P.A., Pohlhaus, P.D., Luft, J.C., Madden, V.J., Napier, M.E., and DeSimone, J.M. (2008). The effect of particle design on cellular internalization pathways. *Proc Natl Acad Sci U S A* 105: 11613-11618.

Grishchuk, Y., Ginet, V., Truttmann, A.C., Clarke, P.G., and Puyal, J. (2011). Beclin 1-independent autophagy contributes to apoptosis in cortical neurons. *Autophagy* 7.

Hannon, G.J. (2002). RNA interference. *Nature* 418: 244-251.

Harding, H.P., Zhang, Y., and Ron, D. (1999). Protein translation and folding are coupled by an endoplasmic-reticulum-resident kinase. *Nature* 397: 271-274.

Hitomi, J., Christofferson, D.E., Ng, A., Yao, J., Degterev, A., Xavier, R.J., and Yuan, J. (2008). Identification of a molecular signaling network that regulates a cellular necrotic cell death pathway. *Cell* 135: 1311-1323.

Hollien, J., Lin, J.H., Li, H., Stevens, N., Walter, P., and Weissman, J.S. (2009). Regulated Ire1-dependent decay of messenger RNAs in mammalian cells. *J Cell Biol* 186: 323-331.

Hollien, J., and Weissman, J.S. (2006). Decay of endoplasmic reticulum-localized mRNAs during the unfolded protein response. *Science* 313: 104-107.

Hotchkiss, R.S., Strasser, A., McDunn, J.E., and Swanson, P.E. (2009). Cell death. *N Engl J Med* 361: 1570-1583.

Hu, Q., Kwon, Y.S., Nunez, E., Cardamone, M.D., Hutt, K.R., Ohgi, K.A., Garcia-Bassets, I., Rose, D.W., Glass, C.K., Rosenfeld, M.G., *et al.* (2008). Enhancing nuclear receptor-induced transcription requires nuclear motor and LSD1-dependent gene networking in interchromatin granules. *Proc Natl Acad Sci U S A* 105: 19199-19204.

Ichimura, Y., Kirisako, T., Takao, T., Satomi, Y., Shimonishi, Y., Ishihara, N., Mizushima, N., Tanida, I., Kominami, E., Ohsumi, M., *et al.* (2000). A ubiquitin-like system mediates protein lipidation. *Nature* 408: 488-492.

Iijima, S. (1991). Helical Microtubules of Graphitic Carbon. *Nature* 354: 56-58.

Indo, H.P., Davidson, M., Yen, H.C., Suenaga, S., Tomita, K., Nishii, T., Higuchi, M., Koga, Y., Ozawa, T., and Majima, H.J. (2007). Evidence of ROS generation by mitochondria in cells with impaired electron transport chain and mitochondrial DNA damage. *Mitochondrion* 7: 106-118.

Iwaoka, S., Nakamura, T., Takano, S., Tsuchiya, S., and Aramaki, Y. (2006). Cationic liposomes induce apoptosis through p38 MAP kinase-caspase-8-Bid pathway in macrophage-like RAW264.7 cells. *J Leukoc Biol* 79: 184-191.

Jaattela, M. (2004). Multiple cell death pathways as regulators of tumour initiation and progression. *Oncogene* 23: 2746-2756.

Jabbour, A.M., Heraud, J.E., Daunt, C.P., Kaufmann, T., Sandow, J., O'Reilly, L.A., Callus, B.A., Lopez, A., Strasser, A., Vaux, D.L., *et al.* (2009). Puma indirectly activates Bax to cause apoptosis in the absence of Bid or Bim. *Cell Death Differ* 16: 555-563.

Jagtap, P., and Szabo, C. (2005). Poly(ADP-ribose) polymerase and the therapeutic effects of its inhibitors. *Nat Rev Drug Discov* 4: 421-440.

James, D.I., Parone, P.A., Mattenberger, Y., and Martinou, J.C. (2003). hFis1, a novel component of the mammalian mitochondrial fission machinery. *J Biol Chem* 278: 36373-36379.

Jellinger, K.A. (2009). Recent advances in our understanding of neurodegeneration. *J Neural Transm* 116: 1111-1162.

Kabeya, Y., Mizushima, N., Ueno, T., Yamamoto, A., Kirisako, T., Noda, T., Kominami, E., Ohsumi, Y., and Yoshimori, T. (2000). LC3, a mammalian homologue of yeast Apg8p, is localized in autophagosome membranes after processing. *Embo J* 19: 5720-5728.

Karbowski, M., Lee, Y.J., Gaume, B., Jeong, S.Y., Frank, S., Nechushtan, A., Santel, A., Fuller, M., Smith, C.L., and Youle, R.J. (2002). Spatial and temporal association of Bax with mitochondrial fission sites, Drp1, and Mfn2 during apoptosis. *J Cell Biol* 159: 931-938.

Karbowski, M., Norris, K.L., Cleland, M.M., Jeong, S.Y., and Youle, R.J. (2006). Role of Bax and Bak in mitochondrial morphogenesis. *Nature* 443: 658-662.

Kaushik, S., Singh, R., and Cuervo, A.M. (2010). Autophagic pathways and metabolic stress. *Diabetes Obes Metab* 12 Suppl 2: 4-14.

Kerr, J.F., Wyllie, A.H., and Currie, A.R. (1972). Apoptosis: a basic biological phenomenon with wide-ranging implications in tissue kinetics. *Br J Cancer* 26: 239-257.

Ketting, R.F., Fischer, S.E., Bernstein, E., Sijen, T., Hannon, G.J., and Plasterk, R.H. (2001). Dicer functions in RNA interference and in synthesis of small RNA involved in developmental timing in C. elegans. *Genes Dev* 15: 2654-2659.

Khanal, B.P., and Zubarev, E.R. (2008). Purification of high aspect ratio gold nanorods: complete removal of platelets. *Journal of the American Chemical Society* 130: 12634-12635.

Kim, D.H., and Rossi, J.J. (2007). Strategies for silencing human disease using RNA interference. *Nat Rev Genet* 8: 173-184.

Kirisako, T., Ichimura, Y., Okada, H., Kabeya, Y., Mizushima, N., Yoshimori, T., Ohsumi, M., Takao, T., Noda, T., and Ohsumi, Y. (2000). The reversible modification regulates the membrane-binding state of Apg8/Aut7 essential for autophagy and the cytoplasm to vacuole targeting pathway. *J Cell Biol* 151: 263-276.

Klionsky, D.J. (2007). Autophagy: from phenomenology to molecular understanding in less than a decade. *Nat Rev Mol Cell Biol* 8: 931-937.

Klionsky, D.J., Abeliovich, H., Agostinis, P., Agrawal, D.K., Aliev, G., Askew, D.S., Baba, M., Baehrecke, E.H., Bahr, B.A., Ballabio, A.*, et al.* (2008). Guidelines for the use and interpretation of assays for monitoring autophagy in higher eukaryotes. *Autophagy* 4: 151-175.

Kobayashi, S., Kojidani, T., Osakada, H., Yamamoto, A., Yoshimori, T., Hiraoka, Y., and Haraguchi, T. (2010). Artificial induction of autophagy around polystyrene beads in nonphagocytic cells. *Autophagy* 6: 36-45.

Kroemer, G., El-Deiry, W.S., Golstein, P., Peter, M.E., Vaux, D., Vandenabeele, P., Zhivotovsky, B., Blagosklonny, M.V., Malorni, W., Knight, R.A., *et al.* (2005). Classification of cell death: recommendations of the Nomenclature Committee on Cell Death. *Cell Death Differ* 12 Suppl 2: 1463-1467.

Kroemer, G., Galluzzi, L., Vandenabeele, P., Abrams, J., Alnemri, E.S., Baehrecke, E.H., Blagosklonny, M.V., El-Deiry, W.S., Golstein, P., Green, D.R., *et al.* (2009). Classification of cell death: recommendations of the Nomenclature Committee on Cell Death 2009. *Cell Death Differ* 16: 3-11.

Kroemer, G., and Jaattela, M. (2005). Lysosomes and autophagy in cell death control. *Nat Rev Cancer* 5: 886-897.

Kroemer, G., and Levine, B. (2008). Autophagic cell death: the story of a misnomer. *Nat Rev Mol Cell Biol* 9: 1004-1010.

Kroto, H.W., Heath, J.R., Obrien, S.C., Curl, R.F., and Smalley, R.E. (1985). C-60 - Buckminsterfullerene. *Nature* 318: 162-163.

Krysko, D.V., Vanden Berghe, T., D'Herde, K., and Vandenabeele, P. (2008). Apoptosis and necrosis: detection, discrimination and phagocytosis. *Methods* 44: 205-221.

Kuma, A., Hatano, M., Matsui, M., Yamamoto, A., Nakaya, H., Yoshimori, T., Ohsumi, Y., Tokuhisa, T., and Mizushima, N. (2004). The role of autophagy during the early neonatal starvation period. *Nature* 432: 1032-1036.

Kumar, S. (2007). Caspase function in programmed cell death. *Cell Death Differ* 14: 32-43.

Kuwana, T., Bouchier-Hayes, L., Chipuk, J.E., Bonzon, C., Sullivan, B.A., Green, D.R., and Newmeyer, D.D. (2005). BH3 domains of BH3-only proteins differentially regulate Bax-mediated mitochondrial membrane permeabilization both directly and indirectly. *Mol Cell* 17: 525-535.

Leber, B., Lin, J., and Andrews, D.W. (2007). Embedded together: the life and death consequences of interaction of the Bcl-2 family with membranes. *Apoptosis* 12: 897-911.

Lee, R.C., Feinbaum, R.L., and Ambros, V. (1993). The C. elegans heterochronic gene lin-4 encodes small RNAs with antisense complementarity to lin-14. *Cell* 75: 843-854.

Lee, Y.J., Jeong, S.Y., Karbowski, M., Smith, C.L., and Youle, R.J. (2004). Roles of the mammalian mitochondrial fission and fusion mediators Fis1, Drp1, and Opa1 in apoptosis. *Mol Biol Cell* 15: 5001-5011.

Leist, M., Single, B., Castoldi, A.F., Kuhnle, S., and Nicotera, P. (1997). Intracellular adenosine triphosphate (ATP) concentration: a switch in the decision between apoptosis and necrosis. *J Exp Med* 185: 1481-1486.

Levine, B., and Yuan, J. (2005). Autophagy in cell death: an innocent convict? *J Clin Invest* 115: 2679-2688.

Lewinski, N., Colvin, V., and Drezek, R. (2008). Cytotoxicity of nanoparticles. *Small* 4: 26-49.

Li, C., Liu, H., Sun, Y., Wang, H., Guo, F., Rao, S., Deng, J., Zhang, Y., Miao, Y., Guo, C.*, et al.* (2009). PAMAM nanoparticles promote acute lung injury by inducing autophagic cell death through the Akt-TSC2-mTOR signaling pathway. *J Mol Cell Biol* 1: 37-45.

Li, H., Zhu, H., Xu, C.J., and Yuan, J. (1998). Cleavage of BID by caspase 8 mediates the mitochondrial damage in the Fas pathway of apoptosis. *Cell* 94: 491-501.

Li, J., Lee, B., and Lee, A.S. (2006). Endoplasmic reticulum stress-induced apoptosis: multiple pathways and activation of p53-up-regulated modulator of apoptosis (PUMA) and NOXA by p53. *J Biol Chem* 281: 7260-7270.

Li, P., Nijhawan, D., Budihardjo, I., Srinivasula, S.M., Ahmad, M., Alnemri, E.S., and Wang, X. (1997). Cytochrome c and dATP-dependent formation of Apaf-1/caspase-9 complex initiates an apoptotic protease cascade. *Cell* 91: 479-489.

Li, S.D., and Huang, L. (2008). Pharmacokinetics and biodistribution of nanoparticles. *Mol Pharm* 5: 496-504.

Lin, J.H., Li, H., Yasumura, D., Cohen, H.R., Zhang, C., Panning, B., Shokat, K.M., Lavail, M.M., and Walter, P. (2007). IRE1 signaling affects cell fate during the unfolded protein response. *Science* 318: 944-949.

Linse, S., Cabaleiro-Lago, C., Xue, W.F., Lynch, I., Lindman, S., Thulin, E., Radford, S.E., and Dawson, K.A. (2007). Nucleation of protein fibrillation by nanoparticles. *Proc Natl Acad Sci U S A* 104: 8691-8696.

Liu, H.L., Zhang, Y.L., Yang, N., Zhang, Y.X., Liu, X.Q., Li, C.G., Zhao, Y., Wang, Y.G., Zhang, G.G., Yang, P.*, et al.* (2011). A functionalized single-walled carbon nanotube-induced autophagic cell death in human lung cells through Akt-TSC2-mTOR signaling. *Cell Death Dis* 2: e159.

Liu, J., Carmell, M.A., Rivas, F.V., Marsden, C.G., Thomson, J.M., Song, J.J., Hammond, S.M., Joshua-Tor, L., and Hannon, G.J. (2004). Argonaute2 is the catalytic engine of mammalian RNAi. *Science* 305: 1437-1441.

Liu, Y., and Ye, Y. (2011). Proteostasis regulation at the endoplasmic reticulum: a new perturbation site for targeted cancer therapy. *Cell Res* 21: 867-883.

Lovell, J.F., Billen, L.P., Bindner, S., Shamas-Din, A., Fradin, C., Leber, B., and Andrews, D.W. (2008). Membrane binding by tBid initiates an ordered series of events culminating in membrane permeabilization by Bax. *Cell* 135: 1074-1084.

Lundqvist, M., Stigler, J., Elia, G., Lynch, I., Cedervall, T., and Dawson, K.A. (2008). Nanoparticle size and surface properties determine the protein corona with possible implications for biological impacts. *Proc Natl Acad Sci U S A* 105: 14265-14270.

Luo, X., Budihardjo, I., Zou, H., Slaughter, C., and Wang, X. (1998). Bid, a Bcl2 interacting protein, mediates cytochrome c release from mitochondria in response to activation of cell surface death receptors. *Cell* 94: 481-490.

Luzio, J.P., Pryor, P.R., and Bright, N.A. (2007). Lysosomes: fusion and function. *Nat Rev Mol Cell Biol* 8: 622-632.

Lv, H., Zhang, S., Wang, B., Cui, S., and Yan, J. (2006). Toxicity of cationic lipids and cationic polymers in gene delivery. *J Control Release* 114: 100-109.

Mace, P.D., and Riedl, S.J. (2010). Molecular cell death platforms and assemblies. *Curr Opin Cell Biol* 22: 828-836.

Mahmoudi, M., Lynch, I., Ejtehadi, M.R., Monopoli, M.P., Bombelli, F.B., and Laurent, S. (2011). Protein-Nanoparticle Interactions: Opportunities and Challenges. *Chem Rev.*

Mailander, V., and Landfester, K. (2009). Interaction of nanoparticles with cells. *Biomacromolecules* 10: 2379-2400.

Maiuri, M.C., Criollo, A., Tasdemir, E., Vicencio, J.M., Tajeddine, N., Hickman, J.A., Geneste, O., and Kroemer, G. (2007a). BH3-only proteins and BH3 mimetics induce autophagy by competitively disrupting the interaction between Beclin 1 and Bcl-2/Bcl-X(L). *Autophagy* 3: 374-376.

Maiuri, M.C., Zalckvar, E., Kimchi, A., and Kroemer, G. (2007b). Self-eating and self-killing: crosstalk between autophagy and apoptosis. *Nat Rev Mol Cell Biol* 8: 741-752.

Martinez, J., Patkaniowska, A., Urlaub, H., Luhrmann, R., and Tuschl, T. (2002). Single-stranded antisense siRNAs guide target RNA cleavage in RNAi. *Cell* 110: 563-574.

Matranga, C., Tomari, Y., Shin, C., Bartel, D.P., and Zamore, P.D. (2005). Passenger-strand cleavage facilitates assembly of siRNA into Ago2-containing RNAi enzyme complexes. *Cell* 123: 607-620.

Mayor, S., and Pagano, R.E. (2007). Pathways of clathrin-independent endocytosis. *Nat Rev Mol Cell Biol* 8: 603-612.

McCullough, K.D., Martindale, J.L., Klotz, L.O., Aw, T.Y., and Holbrook, N.J. (2001). Gadd153 sensitizes cells to endoplasmic reticulum stress by down-regulating Bcl2 and perturbing the cellular redox state. *Mol Cell Biol* 21: 1249-1259.

McStay, G.P., Salvesen, G.S., and Green, D.R. (2008). Overlapping cleavage motif selectivity of caspases: implications for analysis of apoptotic pathways. *Cell Death Differ* 15: 322-331.

Mizushima, N., and Levine, B. (2010). Autophagy in mammalian development and differentiation. *Nat Cell Biol* 12: 823-830.

Moquin, D., and Chan, F.K. (2010). The molecular regulation of programmed necrotic cell injury. *Trends Biochem Sci* 35: 434-441.

Muchmore, S.W., Sattler, M., Liang, H., Meadows, R.P., Harlan, J.E., Yoon, H.S., Nettesheim, D., Chang, B.S., Thompson, C.B., Wong, S.L.*, et al.* (1996). X-ray and NMR structure of human Bcl-xL, an inhibitor of programmed cell death. *Nature* 381: 335-341.

Munoz-Pinedo, C., Guio-Carrion, A., Goldstein, J.C., Fitzgerald, P., Newmeyer, D.D., and Green, D.R. (2006). Different mitochondrial intermembrane space proteins are released during apoptosis in a manner that is coordinately initiated but can vary in duration. *Proc Natl Acad Sci U S A* 103: 11573-11578.

Muzio, M., Chinnaiyan, A.M., Kischkel, F.C., O'Rourke, K., Shevchenko, A., Ni, J., Scaffidi, C., Bretz, J.D., Zhang, M., Gentz, R.*, et al.* (1996). FLICE, a novel FADD-homologous ICE/CED-3-like protease, is recruited to the CD95 (Fas/APO-1) death--inducing signaling complex. *Cell* 85: 817-827.

Nakano, K., and Vousden, K.H. (2001). PUMA, a novel proapoptotic gene, is induced by p53. *Mol Cell* 7: 683-694.

Nechushtan, A., Smith, C.L., Hsu, Y.T., and Youle, R.J. (1999). Conformation of the Bax C-terminus regulates subcellular location and cell death. *Embo J* 18: 2330-2341.

Nechushtan, A., Smith, C.L., Lamensdorf, I., Yoon, S.H., and Youle, R.J. (2001). Bax and Bak coalesce into novel mitochondria-associated clusters during apoptosis. *J Cell Biol* 153: 1265-1276.

Nel, A., Xia, T., Madler, L., and Li, N. (2006). Toxic potential of materials at the nanolevel. *Science* 311: 622-627.

Nel, A.E., Madler, L., Velegol, D., Xia, T., Hoek, E.M., Somasundaran, P., Klaessig, F., Castranova, V., and Thompson, M. (2009). Understanding biophysicochemical interactions at the nano-bio interface. *Nat Mater* 8: 543-557.

Neumann, B., Walter, T., Heriche, J.K., Bulkescher, J., Erfle, H., Conrad, C., Rogers, P., Poser, I., Held, M., Liebel, U., *et al.* (2010). Phenotypic profiling of the human genome by time-lapse microscopy reveals cell division genes. *Nature* 464: 721-727.

Oberdorster, G. (2010). Safety assessment for nanotechnology and nanomedicine: concepts of nanotoxicology. *Journal of Internal Medicine* 267: 89-105.

Oberdorster, G., Sharp, Z., Atudorei, V., Elder, A., Gelein, R., Kreyling, W., and Cox, C. (2004). Translocation of inhaled ultrafine particles to the brain. *Inhal Toxicol* 16: 437-445.

Oberdorster, G., Stone, V., and Donaldson, K. (2007). Toxicology of nanoparticles: A historical perspective. *Nanotoxicology* 1: 2-25.

Oberdörster, G., Stone, V., and Donaldson, K. (2007). Toxicology of nanoparticles: A historical perspective. *Nanotoxicology* 1: 2-25.

Oberle, C., Huai, J., Reinheckel, T., Tacke, M., Rassner, M., Ekert, P.G., Buellesbach, J., and Borner, C. (2010). Lysosomal membrane permeabilization and cathepsin release is a Bax/Bak-dependent, amplifying event of apoptosis in fibroblasts and monocytes. *Cell Death Differ* 17: 1167-1178.

Oda, E., Ohki, R., Murasawa, H., Nemoto, J., Shibue, T., Yamashita, T., Tokino, T., Taniguchi, T., and Tanaka, N. (2000). Noxa, a BH3-only member of the Bcl-2 family and candidate mediator of p53-induced apoptosis. *Science* 288: 1053-1058.

Olichon, A., Baricault, L., Gas, N., Guillou, E., Valette, A., Belenguer, P., and Lenaers, G. (2003). Loss of OPA1 perturbates the mitochondrial inner membrane structure and integrity, leading to cytochrome c release and apoptosis. *J Biol Chem* 278: 7743-7746.

Olivari, S., Cali, T., Salo, K.E., Paganetti, P., Ruddock, L.W., and Molinari, M. (2006). EDEM1 regulates ER-associated degradation by accelerating de-mannosylation of folding-defective polypeptides and by inhibiting their covalent aggregation. *Biochem Biophys Res Commun* 349: 1278-1284.

Orban, T.I., and Izaurralde, E. (2005). Decay of mRNAs targeted by RISC requires XRN1, the Ski complex, and the exosome. *RNA* 11: 459-469.

Osmond, M.J., and McCall, M.J. (2010). Zinc oxide nanoparticles in modern sunscreens: an analysis of potential exposure and hazard. *Nanotoxicology* 4: 15-41.

Pack, D.W., Hoffman, A.S., Pun, S., and Stayton, P.S. (2005). Design and development of polymers for gene delivery. *Nat Rev Drug Discov* 4: 581-593.

Palade, G.E. (1952). The fine structure of mitochondria. *Anat Rec* 114: 427-451.

Pardridge, W.M. (2007). Drug targeting to the brain. *Pharm Res* 24: 1733-1744.

Park, M.V., Verharen, H.W., Zwart, E., Hernandez, L.G., van Benthem, J., Elsaesser, A., Barnes, C., McKerr, G., Howard, C.V., Salvati, A.*, et al.* (2011). Genotoxicity evaluation of amorphous silica nanoparticles of different sizes using the micronucleus and the plasmid lacZ gene mutation assay. *Nanotoxicology*.

Paroo, Z., Liu, Q., and Wang, X. (2007). Biochemical mechanisms of the RNA-induced silencing complex. *Cell Res* 17: 187-194.

Peer, D., Karp, J.M., Hong, S., Farokhzad, O.C., Margalit, R., and Langer, R. (2007). Nanocarriers as an emerging platform for cancer therapy. *Nat Nanotechnol* 2: 751-760.

Petros, A.M., Olejniczak, E.T., and Fesik, S.W. (2004). Structural biology of the Bcl-2 family of proteins. *Biochim Biophys Acta* 1644: 83-94.

Plantin-Carrenard, E., Bringuier, A., Derappe, C., Pichon, J., Guillot, R., Bernard, M., Foglietti, M.J., Feldmann, G., Aubery, M., and Braut-Boucher, F.

(2003). A fluorescence microplate assay using yopro-1 to measure apoptosis: application to HL60 cells subjected to oxidative stress. *Cell Biol Toxicol* 19: 121-133.

Prechtel, A.T., Turza, N.M., Theodoridis, A.A., Kummer, M., and Steinkasserer, A. (2006). Small interfering RNA (siRNA) delivery into monocyte-derived dendritic cells by electroporation. *J Immunol Methods* 311: 139-152.

Puthalakath, H., O'Reilly, L.A., Gunn, P., Lee, L., Kelly, P.N., Huntington, N.D., Hughes, P.D., Michalak, E.M., McKimm-Breschkin, J., Motoyama, N.*, et al.* (2007). ER stress triggers apoptosis by activating BH3-only protein Bim. *Cell* 129: 1337-1349.

Rabolli, V., Thomassen, L.C., Princen, C., Napierska, D., Gonzalez, L., Kirsch-Volders, M., Hoet, P.H., Huaux, F., Kirschhock, C.E., Martens, J.A.*, et al.* (2010). Influence of size, surface area and microporosity on the in vitro cytotoxic activity of amorphous silica nanoparticles in different cell types. *Nanotoxicology* 4: 307-318.

Rana, T.M. (2007). Illuminating the silence: understanding the structure and function of small RNAs. *Nat Rev Mol Cell Biol* 8: 23-36.

Rand, T.A., Petersen, S., Du, F., and Wang, X. (2005). Argonaute2 cleaves the anti-guide strand of siRNA during RISC activation. *Cell* 123: 621-629.

Ren, D., Tu, H.C., Kim, H., Wang, G.X., Bean, G.R., Takeuchi, O., Jeffers, J.R., Zambetti, G.P., Hsieh, J.J., and Cheng, E.H. (2010). BID, BIM, and PUMA are essential for activation of the BAX- and BAK-dependent cell death program. *Science* 330: 1390-1393.

Riedl, S.J., and Salvesen, G.S. (2007). The apoptosome: signalling platform of cell death. *Nat Rev Mol Cell Biol* 8: 405-413.

Riedl, S.J., and Shi, Y. (2004). Molecular mechanisms of caspase regulation during apoptosis. *Nat Rev Mol Cell Biol* 5: 897-907.

Rodriguez, D., Rojas-Rivera, D., and Hetz, C. (2011). Integrating stress signals at the endoplasmic reticulum: The BCL-2 protein family rheostat. *Biochim Biophys Acta* 1813: 564-574.

Rual, J.F., Hirozane-Kishikawa, T., Hao, T., Bertin, N., Li, S., Dricot, A., Li, N., Rosenberg, J., Lamesch, P., Vidalain, P.O., *et al.* (2004). Human ORFeome version 1.1: a platform for reverse proteomics. *Genome Res* 14: 2128-2135.

Ruchaud, S., Carmena, M., and Earnshaw, W.C. (2007). Chromosomal passengers: conducting cell division. *Nat Rev Mol Cell Biol* 8: 798-812.

Saito, M., Korsmeyer, S.J., and Schlesinger, P.H. (2000). BAX-dependent transport of cytochrome c reconstituted in pure liposomes. *Nat Cell Biol* 2: 553-555.

Salvati, A., Aberg, C., Dos Santos, T., Varela, J., Pinto, P., Lynch, I., and Dawson, K.A. (2011). Experimental and theoretical comparison of intracellular import of polymeric nanoparticles and small molecules: toward models of uptake kinetics. *Nanomedicine*.

Santel, A., and Fuller, M.T. (2001). Control of mitochondrial morphology by a human mitofusin. *J Cell Sci* 114: 867-874.

Sato, N., Urano, F., Yoon Leem, J., Kim, S.H., Li, M., Donoviel, D., Bernstein, A., Lee, A.S., Ron, D., Veselits, M.L., *et al.* (2000). Upregulation of BiP and CHOP by the unfolded-protein response is independent of presenilin expression. *Nat Cell Biol* 2: 863-870.

Schendel, S.L., Xie, Z., Montal, M.O., Matsuyama, S., Montal, M., and Reed, J.C. (1997). Channel formation by antiapoptotic protein Bcl-2. *Proc Natl Acad Sci U S A* 94: 5113-5118.

Scorrano, L., Ashiya, M., Buttle, K., Weiler, S., Oakes, S.A., Mannella, C.A., and Korsmeyer, S.J. (2002). A distinct pathway remodels mitochondrial cristae and mobilizes cytochrome c during apoptosis. *Dev Cell* 2: 55-67.

Seglen, P.O., and Gordon, P.B. (1982). 3-Methyladenine: specific inhibitor of autophagic/lysosomal protein degradation in isolated rat hepatocytes. *Proc Natl Acad Sci U S A* 79: 1889-1892.

Shimizu, S., Kanaseki, T., Mizushima, N., Mizuta, T., Arakawa-Kobayashi, S., Thompson, C.B., and Tsujimoto, Y. (2004). Role of Bcl-2 family proteins in a non-apoptotic programmed cell death dependent on autophagy genes. *Nat Cell Biol* 6: 1221-1228.

Shintani, T., and Klionsky, D.J. (2004). Autophagy in health and disease: a double-edged sword. *Science* 306: 990-995.

Simpson, J.C., Cetin, C., Erfle, H., Joggerst, B., Liebel, U., Ellenberg, J., and Pepperkok, R. (2007). An RNAi screening platform to identify secretion machinery in mammalian cells. *J Biotechnol* 129: 352-365.

Sjostrand, F.S. (1953). Electron microscopy of mitochondria and cytoplasmic double membranes. *Nature* 171: 30-32.

Smirnova, E., Griparic, L., Shurland, D.L., and van der Bliek, A.M. (2001). Dynamin-related protein Drp1 is required for mitochondrial division in mammalian cells. *Mol Biol Cell* 12: 2245-2256.

Sorensen, C.E., and Novak, I. (2001). Visualization of ATP release in pancreatic acini in response to cholinergic stimulus. Use of fluorescent probes and confocal microscopy. *J Biol Chem* 276: 32925-32932.

Soriano, M.E., and Scorrano, L. (2010). The interplay between BCL-2 family proteins and mitochondrial morphology in the regulation of apoptosis. *Adv Exp Med Biol* 687: 97-114.

Spencer, B.J., and Verma, I.M. (2007). Targeted delivery of proteins across the blood-brain barrier. *Proc Natl Acad Sci U S A* 104: 7594-7599.

Stern, S.T., Zolnik, B.S., McLeland, C.B., Clogston, J., Zheng, J., and McNeil, S.E. (2008). Induction of autophagy in porcine kidney cells by quantum dots: a common cellular response to nanomaterials? *Toxicol Sci* 106: 140-152.

Stoka, V., Turk, V., and Turk, B. (2007). Lysosomal cysteine cathepsins: signaling pathways in apoptosis. *Biol Chem* 388: 555-560.

Sugioka, R., Shimizu, S., and Tsujimoto, Y. (2004). Fzo1, a protein involved in mitochondrial fusion, inhibits apoptosis. *J Biol Chem* 279: 52726-52734.

Sun, S.C., Wang, Z.B., Xu, Y.N., Lee, S.E., Cui, X.S., and Kim, N.H. (2011). Arp2/3 complex regulates asymmetric division and cytokinesis in mouse oocytes. *PLoS One* 6: e18392.

Szegezdi, E., Logue, S.E., Gorman, A.M., and Samali, A. (2006). Mediators of endoplasmic reticulum stress-induced apoptosis. *EMBO Rep* 7: 880-885.

Tait, S.W., and Green, D.R. (2010). Mitochondria and cell death: outer membrane permeabilization and beyond. *Nat Rev Mol Cell Biol* 11: 621-632.

Todde, V., Veenhuis, M., and van der Klei, I.J. (2009). Autophagy: principles and significance in health and disease. *Biochim Biophys Acta* 1792: 3-13.

Tooze, S.A., and Yoshimori, T. (2010). The origin of the autophagosomal membrane. *Nat Cell Biol* 12: 831-835.

Tschopp, J. (2011). Mitochondria: Sovereign of inflammation? *Eur J Immunol* 41: 1196-1202.

Tsujimoto, Y., Cossman, J., Jaffe, E., and Croce, C.M. (1985). Involvement of the bcl-2 gene in human follicular lymphoma. *Science* 228: 1440-1443.

Vandenabeele, P., Galluzzi, L., Vanden Berghe, T., and Kroemer, G. (2010). Molecular mechanisms of necroptosis: an ordered cellular explosion. *Nat Rev Mol Cell Biol* 11: 700-714.

Vaux, D.L., Cory, S., and Adams, J.M. (1988). Bcl-2 gene promotes haemopoietic cell survival and cooperates with c-myc to immortalize pre-B cells. *Nature* 335: 440-442.

Vembar, S.S., and Brodsky, J.L. (2008). One step at a time: endoplasmic reticulum-associated degradation. *Nat Rev Mol Cell Biol* 9: 944-957.

Vercammen, D., Brouckaert, G., Denecker, G., Van de Craen, M., Declercq, W., Fiers, W., and Vandenabeele, P. (1998). Dual signaling of the Fas receptor: initiation of both apoptotic and necrotic cell death pathways. *J Exp Med* 188: 919-930.

Vergoni, A.V., Tosi, G., Tacchi, R., Vandelli, M.A., Bertolini, A., and Costantino, L. (2009). Nanoparticles as drug delivery agents specific for CNS: in vivo biodistribution. *Nanomedicine* 5: 369-377.

Walczyk, D., Bombelli, F.B., Monopoli, M.P., Lynch, I., and Dawson, K.A. (2010). What the cell "sees" in bionanoscience. *Journal of the American Chemical Society* 132: 5761-5768.

Watson, P., Jones, A.T., and Stephens, D.J. (2005). Intracellular trafficking pathways and drug delivery: fluorescence imaging of living and fixed cells. *Adv Drug Deliv Rev* 57: 43-61.

Weisiger, R.A., and Fridovich, I. (1973a). Mitochondrial superoxide simutase. Site of synthesis and intramitochondrial localization. *J Biol Chem* 248: 4793-4796.

Weisiger, R.A., and Fridovich, I. (1973b). Superoxide dismutase. Organelle specificity. *J Biol Chem* 248: 3582-3592.

Willis, S.N., Fletcher, J.I., Kaufmann, T., van Delft, M.F., Chen, L., Czabotar, P.E., Ierino, H., Lee, E.F., Fairlie, W.D., Bouillet, P.*, et al.* (2007). Apoptosis initiated when BH3 ligands engage multiple Bcl-2 homologs, not Bax or Bak. *Science* 315: 856-859.

Woehlbier, U., and Hetz, C. (2011). Modulating stress responses by the UPRosome: A matter of life and death. *Trends Biochem Sci* 36: 329-337.

Wolter, K.G., Hsu, Y.T., Smith, C.L., Nechushtan, A., Xi, X.G., and Youle, R.J. (1997). Movement of Bax from the cytosol to mitochondria during apoptosis. *J Cell Biol* 139: 1281-1292.

Wu, Y.T., Tan, H.L., Shui, G., Bauvy, C., Huang, Q., Wenk, M.R., Ong, C.N., Codogno, P., and Shen, H.M. (2010). Dual role of 3-methyladenine in modulation of autophagy via different temporal patterns of inhibition on class I and III phosphoinositide 3-kinase. *J Biol Chem* 285: 10850-10861.

Xia, T., Kovochich, M., Brant, J., Hotze, M., Sempf, J., Oberley, T., Sioutas, C., Yeh, J.I., Wiesner, M.R., and Nel, A.E. (2006). Comparison of the abilities of ambient and manufactured nanoparticles to induce cellular toxicity according to an oxidative stress paradigm. *Nano Lett* 6: 1794-1807.

Xia, T., Kovochich, M., Liong, M., Madler, L., Gilbert, B., Shi, H., Yeh, J.I., Zink, J.I., and Nel, A.E. (2008a). Comparison of the mechanism of toxicity of zinc

oxide and cerium oxide nanoparticles based on dissolution and oxidative stress properties. *ACS Nano* 2: 2121-2134.

Xia, T., Kovochich, M., Liong, M., Zink, J.I., and Nel, A.E. (2008b). Cationic polystyrene nanosphere toxicity depends on cell-specific endocytic and mitochondrial injury pathways. *ACS Nano* 2: 85-96.

Xiao, A.Y., Wang, X.Q., Yang, A., and Yu, S.P. (2002). Slight impairment of Na+,K+-ATPase synergistically aggravates ceramide- and beta-amyloid-induced apoptosis in cortical neurons. *Brain Res* 955: 253-259.

Xie, Z., and Klionsky, D.J. (2007). Autophagosome formation: core machinery and adaptations. *Nat Cell Biol* 9: 1102-1109.

Yamamoto, K., Sato, T., Matsui, T., Sato, M., Okada, T., Yoshida, H., Harada, A., and Mori, K. (2007). Transcriptional induction of mammalian ER quality control proteins is mediated by single or combined action of ATF6alpha and XBP1. *Dev Cell* 13: 365-376.

Yang, Z., and Klionsky, D.J. (2009). An overview of the molecular mechanism of autophagy. *Curr Top Microbiol Immunol* 335: 1-32.

Yang, Z., and Klionsky, D.J. (2010a). Eaten alive: a history of macroautophagy. *Nat Cell Biol* 12: 814-822.

Yang, Z., and Klionsky, D.J. (2010b). Mammalian autophagy: core molecular machinery and signaling regulation. *Curr Opin Cell Biol* 22: 124-131.

Yoon, Y., Krueger, E.W., Oswald, B.J., and McNiven, M.A. (2003). The mitochondrial protein hFis1 regulates mitochondrial fission in mammalian cells through an interaction with the dynamin-like protein DLP1. *Mol Cell Biol* 23: 5409-5420.

Yoshida, H., Matsui, T., Yamamoto, A., Okada, T., and Mori, K. (2001). XBP1 mRNA is induced by ATF6 and spliced by IRE1 in response to ER stress to produce a highly active transcription factor. *Cell* 107: 881-891.

Yoshimori, T., Yamamoto, A., Moriyama, Y., Futai, M., and Tashiro, Y. (1991). Bafilomycin A1, a specific inhibitor of vacuolar-type H(+)-ATPase, inhibits

acidification and protein degradation in lysosomes of cultured cells. *J Biol Chem* 266: 17707-17712.

Youle, R.J., and Karbowski, M. (2005). Mitochondrial fission in apoptosis. *Nat Rev Mol Cell Biol* 6: 657-663.

Youle, R.J., and Strasser, A. (2008). The BCL-2 protein family: opposing activities that mediate cell death. *Nat Rev Mol Cell Biol* 9: 47-59.

Yousefi, S., Perozzo, R., Schmid, I., Ziemiecki, A., Schaffner, T., Scapozza, L., Brunner, T., and Simon, H.U. (2006). Calpain-mediated cleavage of Atg5 switches autophagy to apoptosis. *Nat Cell Biol* 8: 1124-1132.

Yu, J., and Zhang, L. (2008). PUMA, a potent killer with or without p53. *Oncogene* 27 Suppl 1: S71-83.

Yuan, X., Naguib, S., and Wu, Z. (2011). Recent advances of siRNA delivery by nanoparticles. *Expert Opin Drug Deliv* 8: 521-536.

Zamaraeva, M.V., Sabirov, R.Z., Maeno, E., Ando-Akatsuka, Y., Bessonova, S.V., and Okada, Y. (2005). Cells die with increased cytosolic ATP during apoptosis: a bioluminescence study with intracellular luciferase. *Cell Death Differ* 12: 1390-1397.

Zamore, P.D., Tuschl, T., Sharp, P.A., and Bartel, D.P. (2000). RNAi: double-stranded RNA directs the ATP-dependent cleavage of mRNA at 21 to 23 nucleotide intervals. *Cell* 101: 25-33.

Zhao, M., Antunes, F., Eaton, J.W., and Brunk, U.T. (2003). Lysosomal enzymes promote mitochondrial oxidant production, cytochrome c release and apoptosis. *Eur J Biochem* 270: 3778-3786.

Zong, W.X., Ditsworth, D., Bauer, D.E., Wang, Z.Q., and Thompson, C.B. (2004). Alkylating DNA damage stimulates a regulated form of necrotic cell death. *Genes Dev* 18: 1272-1282.